ornl

OAK RIDGE NATIONAL LABORATORY

MARTIN MARIETTA

ORNL-6629/P1



# Evaluation of Advanced Austenitic Alloys Relative to Alloy Design Criteria for Steam Service: Part 1 — Lean Stainless Steels

R. W. Swindeman
P. J. Maziasz
E. Bolling
J. F. King



Fossil Energy Program

OPERATED BY
MARTIN MARIETTA ENERGY SYSTEMS, INC.
FOR THE UNITED STATES
DEPARTMENT OF ENERGY

ORNL-6629/P1

Metals and Ceramics Division

# EVALUATION OF ADVANCED AUSTENITIC ALLOYS RELATIVE TO ALLOY DESIGN CRITERIA FOR STEAM SERVICE: PART 1 — LEAN STAINLESS STEELS*

R. W. Swindeman, P. J. Maziasz, E. Bolling, and J. F. King

Date Published: May 1990

Prepared for the
U.S. DOE Fossil Energy AR&TD Materials Program
AA 15 10 10 0

NOTICE This document contains information of a preliminary nature. It is subject to revision or correction and therefore does not represent a final report.

Prepared by the
OAK RIDGE NATIONAL LABORATORY
Oak Ridge, Tennessee 37831-6285
operated by
MARTIN MARIETTA ENERGY SYSTEMS, INC.
for the
U.S. DEPARTMENT OF ENERGY
under Contract DE-AC05-84OR21400

ACKNOWLEDGMENTS

This activity was initiated under the guidance of R. A. Bradley, R. R. Judkins, and D. N. Braski of the Fossil Energy AR&TD Materials Program, and E. E. Hoffman of DOE-ORO. G. M. Goodwin participated in the development of welding procedures, Sigmajig testing, and the selection of the CRE 16-8-2 filler metal for the HT-UPS alloys. The metallography was performed by S. Eatherly. The report was reviewed by B. G. Gieseke and D. N. Braski and prepared by D. L. Balltrip.

## CONTENTS

## LIST OF TABLES

## LIST OF FIGURES

# EVALUATION OF ADVANCED AUSTENITIC ALLOYS RELATIVE TO ALLOY DESIGN CRITERIA FOR STEAM SERVICE: PART 1 — LEAN STAINLESS STEELS*

R. W. Swindeman, P. J. Maziasz, E. Bolling, and J. F. King

## ABSTRACT

The results are summarized for a 6-year activity on advanced austenitic stainless steels for heat recovery systems. Commercial, near-commercial, and developmental alloys were evaluated relative to criteria for metallurgical stability, fabricability, weldability, and mechanical strength. Fireside and steamside corrosion were also considered, but no test data were collected. Lean stainless steel alloys that were given special attention in the study were type 316 stainless steel, fine-grained type 347 stainless steel, 17-14CuMo stainless steel, Esshete 1250, Sumitomo ST3Cu® stainless steel, and a group of alloys identified as HT-UPS (high-temperature, ultrafine-precipitation strengthened) steels that were basically 14Cr-16Ni-Mo steels modified by various additions of MC-forming elements. It was found that, by solution treating the MC-forming alloys to temperatures above 1150°C and subsequently cold or warm working, excellent metallurgical stability and creep strength could be achieved. Test data to beyond 35,000 h were collected. The ability to clad the steels for improved fireside corrosion resistance was demonstrated. Weldability of the alloys was of concern, and hot cracking was found to be a problem in the HT-UPS alloys. By reducing the phosphorous content and selecting either CRE 16-8-2 stainless steel or alloy 556 filler metal, weldments were produced that had excellent strength and ductility. The major issues related to the development of the advanced alloys were identified and ways to resolve the issues suggested.

---

## 1. INTRODUCTION

An assessment by Rittenhouse et al. (1985) of the materials needs related to the development of advanced steam cycle coal-fired power plants identified several materials selection issues that could be addressed by research supported by the U.S. Department of Energy Fossil Energy Advanced Research and Technology Development Materials Program. One issue was the choice of an alloy for the superheater/reheater where high-strength, corrosion-resistant tubing is required. The alloy design and evaluation methods for this application

*Research sponsored by the U.S. Department of Energy, Fossil Energy AR&TD Materials Program [DOE/FE AA 15 10 10 0, Work Breakdown Structure Element ORNL-2(B)] under contract No. DE-AC05-84OR21400 with Martin Marietta Energy Systems, Inc.

were then developed by Swindeman et al. (1986), and a 6-year program was started to examine the potential of commercial, near-commercial, and developmental alloys. The alloys were separated into four categories: lean stainless steels containing less than 20% chromium, high-chromium iron base alloys containing 20 to 30% chromium, nickel base alloys, and aluminum-bearing alloys. Because of their strength potential and relatively low cost, emphasis was placed on the performance of lean stainless steels. Two previous reports described the procurement of candidate alloys and summarized the results of screening tests performed at the Oak Ridge National Laboratory (ORNL) (Swindeman et al. 1987, 1988). Several university and industrial subcontractors were involved in the work, and their results have reached a stage where the information may be folded into the data produced at ORNL to form a fairly comprehensive picture of the strengths and weaknesses of this group of alloys. The information provided in this report addresses the evaluation of the lean stainless steels relative to the alloy design criteria specified in ORNL-6274 (Swindeman et al. 1987). The criteria were divided into five categories: metallurgical stability, fabrication and joining, mechanical properties, fireside corrosion, and steamside corrosion. There exists an overlap between these categories, but an attempt is made in the information that follows to retain the framework identified in the alloy design criteria report.

## 2. MATERIALS

Several lean stainless steels are viable candidates for superheater/reheater tubing in an advanced steam cycle, and some will be described briefly before going into the details of the evaluation relative to the design criteria. Compositions to be discussed in this report are listed in Table 1. Included in the first group of alloys are those that are used on a commercial basis in the United States and identified in Sect. I of the American Society of Mechanical Engineers (ASME) Boiler and Pressure Vessel (BPV) Code. These are types 316 and 347 stainless steels. Data produced on several heats of type 316 stainless steel have been examined. These include nine heats of boiler tubing examined by the National Research Institute for Metals (1978), two heats of type 316 stainless steel main steam line tubing from the Eddystone Unit #1 plant, and a reference heat of type 316 stainless steel that has a long history of testing at ORNL. The chemistry listed is for the ORNL heat (80432297). The chemistry listed for type 347 stainless steel is representative of the chemistry of several heats of type 347 stainless steel tubing examined by Teranishi (1989). This fine-grained material was found to be much superior to standard 347 stainless steel and is a serious contender for tubing in an advanced steam cycle.

Table 1. Chemical compositions of several lean austenitic stainless steels (wt %)

| Alloy | C | Si | Mn | Ni | Cr | Ti | Nb | V | Mo | P | B | S | N | Cu |
|---|---|---|---|---|---|---|---|---|---|---|---|---|---|---|
| 316 SS | 0.057 | 0.58 | 1.86 | 13.50 | 17.2 | 0.02 | | | 2.34 | 0.024 | | 0.019 | 0.030 | 0.10 |
| 347 SS | 0.070 | 0.60 | 1.60 | 12.00 | 18.0 | | 0.70 | | | | | | | |
| TEMPALOY A2 | 0.090 | 0.50 | 1.50 | 14.00 | 18.0 | 0.16 | 0.23 | | 1.50 | | 0.003 | | | |
| 17-14CuMo | 0.098 | 0.95 | 0.83 | 13.80 | 16.5 | 0.21 | 0.45 | 0.07 | 1.96 | 0.014 | | 0.005 | 0.025 | 3.34 |
| Esshete 1250 | 0.100 | 0.50 | 6.00 | 10.00 | 15.5 | | 1.00 | 0.25 | 1.00 | 0.025 | 0.006 | 0.014 | | |
| TEMPALOY 17-14 | 0.120 | 0.56 | 0.77 | 14.50 | 15.4 | 0.23 | 0.43 | | 2.42 | 0.018 | | 0.001 | | 2.97 |
| ST3Cu | 0.110 | 0.19 | 0.80 | 09.20 | 18.0 | | 0.39 | | | 0.021 | | 0.001 | 0.086 | 2.88 |
| PCA | 0.048 | 0.52 | 1.83 | 16.63 | 14.3 | 0.31 | 0.02 | 0.02 | 1.95 | 0.014 | 0.001 | 0.002 | 0.008 | 0.01 |
| HT-UTS CE0 | 0.072 | 0.41 | 1.80 | 16.00 | 14.2 | 0.24 | 0.10 | 0.57 | 2.45 | 0.071 | 0.005 | 0.007 | 0.015 | |
| HT-UTS CE1 | 0.085 | 0.21 | 1.64 | 16.20 | 13.1 | 0.21 | 0.12 | 0.52 | 2.30 | 0.076 | 0.005 | 0.008 | 0.016 | 0.04 |
| HT-UTS CE2 | 0.079 | 0.26 | 1.89 | 16.00 | 16.1 | 0.31 | 0.11 | 0.58 | 2.26 | 0.069 | 0.007 | 0.008 | 0.017 | |
| HT-UTS CE3 | 0.086 | 0.21 | 1.75 | 16.20 | 14.5 | 0.27 | 0.12 | 0.56 | 2.41 | 0.071 | 0.005 | 0.008 | 0.012 | 1.96 |
| HT-UTS AX5 | 0.076 | 0.12 | 2.04 | 16.20 | 13.9 | 0.27 | 0.15 | 0.52 | 2.46 | 0.024 | 0.005 | 0.015 | 0.021 | |
| HT-UTS AX6 | 0.074 | 0.12 | 1.96 | 16.00 | 14.3 | 0.28 | 0.15 | 0.51 | 2.48 | 0.041 | 0.005 | 0.015 | 0.020 | |
| HT-UTS AX7 | 0.073 | 0.11 | 2.00 | 16.00 | 14.2 | 0.18 | 0.15 | 0.53 | 2.48 | 0.073 | 0.005 | 0.014 | 0.024 | 1.50 |
| HT-UTS AX8 | 0.074 | 0.12 | 2.05 | 15.90 | 13.9 | 0.24 | 0.08 | 0.15 | 2.48 | 0.043 | 0.005 | 0.015 | 0.022 | |
| HT-UTS MS1 | 0.097 | 0.64 | 1.76 | 16.07 | 14.1 | 0.11 | 0.09 | 0.5 | 2.52 | 0.043 | 0.001 | 0.006 | 0.016 | |
| HT-UTS MS4 | 0.100 | 0.49 | 1.91 | 16.00 | 14.2 | 0.22 | 0.08 | 0.49 | 2.52 | 0.037 | 0.001 | 0.006 | 0.022 | |
| HT-UTS MS5 | 0.110 | 0.57 | 1.89 | 15.99 | 14.1 | 0.16 | 0.20 | 0.48 | 2.53 | 0.044 | 0.001 | 0.006 | 0.011 | |
| HT-UTS MS6 | 0.097 | 0.53 | 1.89 | 15.88 | 14.0 | 0.19 | 0.09 | 0.99 | 2.54 | 0.043 | 0.001 | 0.006 | 0.017 | |
| HT-UTS CET1 | 0.078 | 0.25 | 1.79 | 16.85 | 14.3 | 0.21 | 0.10 | 0.52 | 2.26 | 0.039 | 0.006 | 0.025 | 0.011 | |
| HT-UTS BWT4 | 0.088 | 0.10 | 1.79 | 15.04 | 13.7 | 0.10 | 0.17 | 0.44 | 2.19 | 0.016 | 0.004 | 0.002 | 0.008 | |

A second group of alloys in Table 1 includes near-commercial alloys. Alloys in the near-commercial group include Esshete 1250, 17-14CuMo stainless steel, and TEMPALOY A2® and TEMPALOY 17-14CuMo® stainless steel. TEMPALOY A2 had a very limited data base and will not be considered in this report. TEMPALOY 17-14CuMo stainless steel is essentially the same as 17-14CuMo stainless steel, and the two alloys will often be treated as the same. The near-commercial alloys have been used on a somewhat restricted basis within the United States, but some have experienced extensive use overseas. They may appear in BPV Code cases. A third group of alloys are new materials that are very much in the research stage. Alloys include Sumitomo ST3Cu® stainless steel, PCA stainless steel developed for fusion energy applications (Maziasz and McHargue 1987), and variations within an alloy family identified as HT-UTS (high-temperature, ultrafine-precipitation strengthened) steels by Maziasz (1989). The PCA alloys were found to offer no attractive advantages over the near-commercial alloys for fossil applications, and its properties will not be discussed in this report. Some of the HT-UTS steels fall within a compositional range patented by Maziasz, Braski, and Rowcliffe (1989), and this report reviews the commercial potential of these HT-UTS alloys. The chemistries of all alloys listed in Table 1 should be regarded as typical and do not provide the range specified for the specific alloy designation. Alloys evaluated experimentally in this work include type 316 stainless steel, 17-14CuMo stainless steel, and the HT-UTS group. The fabrication procedures, heat treatments, and other important processing variables are provided in the appropriate sections included below and in the appendices.

## 3. METALLURGICAL STABILITY

The alloy design criteria in ORNL-6274 specified that stability would be assured by the suppression of intermetallic and other embrittling phases by the addition of elements that promote austenitic stabilization. Means of accomplishing this objective have been reviewed by Maziasz and McHargue (1987) and Maziasz (1989) and will not be discussed here in any detail. Addressing the specific alloy design criteria listed in ORNL-6274, the findings below are pertinent.

<u>I-A. The alloys will fall within or near the austenite field of the iron-nickel-chromium ternary diagram at temperatures in the range 500 to 750°C.</u>

To meet this Criterion for a temperature of 650°C, the alloys need to have equivalent chromium levels less than 18% and equivalent nickel levels greater than 10%. In their reviews, Harries (1981) and Marshall (1984) plotted the iron-nickel-chromium ternary phase diagram for several temperatures and included the 300 series stainless steels. They used the following formulas for the nickel and chromium equivalents:

$$Ni_{eq}(A) = Ni + Co + 0.5Mn + 30C + 0.3Cu + 25N \quad , \tag{1}$$

$$Cr_{eq}(A) = Cr + 2Si + 1.5Mo + 5V + 5.5Al + 1.75Nb + 1.5Ti + 0.75W \quad , \tag{2}$$

where the weight percent of each of the indicated elements is used in the formulae. Some of the data provided in Table 1 were used in combination with the equations above to determine the locations of several alloys within the ternary diagram shown in Fig. 1. Virtually all alloys

ORNL-DWG 90-8145

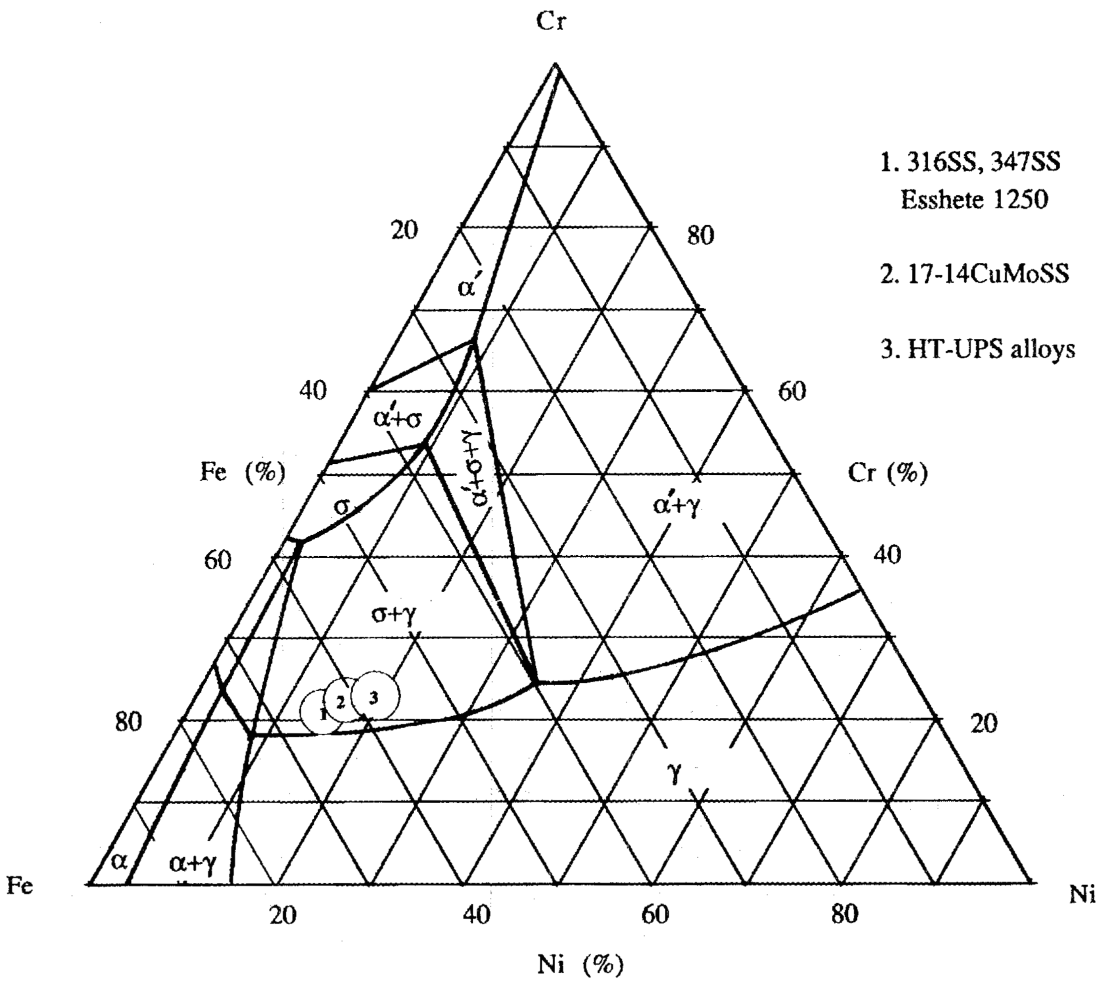


**Fig. 1. Location of several alloys in the iron-nickel-chromium ternary phase diagram at 650°C.**

fell into the austenite plus sigma field which occurs at 650°C when the $Cr_{eq}(A)$ is near 18%. However, the use of Eqs. (1) and (2) to locate alloys in the ternary diagram does not take into consideration the fact that carbide precipitates will deplete the matrix of elements that stabilize austenite (such as carbon and nitrogen) or promote sigma (such as molybdenum). Further, an incomplete picture is obtained in the sense that other intermetallic phase fields, such as chi and Laves, could be present and are not included in the ternary diagram. Nevertheless, all of the developmental alloys listed in Table 1 were judged to be sufficiently close to the austenite field at 650°C to meet Criterion I-A.

<u>I-B. The chromium and nickel equivalents will be maintained to balance the matrix composition on the high nickel equivalent side.</u>

Several empirical equations have been developed that use the terms "nickel equivalent" and "chromium equivalent." Equations (1) and (2) were provided above in connection with the ternary phase diagram. Similar terms are used in connection with fabricability, weldability, and long-term metallurgical stability, and these terms were reviewed by Ellis et al. (1988) and Domian and LeBeau (1989). In specifying Criterion I-B, the equations used for $Ni_{eq}(B)$ and $Cr_{eq}(B)$ were based on the DeLong equations used by Ellis et al. (1988) and were written as

$$Ni_{eq}(B) = Ni + 0.5Mn + 30(C+N)\ , \tag{3}$$

$$Cr_{eq}(B) = Cr + Mo + 1.5Si + 0.5Nb\ . \tag{4}$$

On the basis of these two equations, all commercial and near-commercial alloys listed in Table 1 were balanced on the high $Cr_{eq}(B)$ side, with the exception of TEMPALOY 17-14CuMo stainless steel, as may be seen in Table 2. Of the developmental alloys, only ST3Cu was balanced on the high $Cr_{eq}(B)$ side. In a later section of this report, the problems with weldability introduced by high $Ni_{eq}(B)$ are discussed. Reference was made in ORNL-6274 to other indices for estimating the tendency toward sigma formation. These indices include Phacomp (Woodyatt et al. 1966), Sigma Safe (Machlin and Shao 1978), CALPHAD (Kaufman and Nesor 1974), and Nibal (McGaugh et al. 1985). These and other indices were considered by Domian and LeBeau (1989) in examining the workability of the HT-UPS alloys. They found the materials to be heavily balanced toward austenite. Because of its simplicity and relevance to the Eddystone Unit #1 advanced steam cycle plant

**Table 2. Calculated phase stability parameters and UTS for several steels**

| Alloy | $Ni_{eq}(A)$ | $Cr_{eq}(A)$ | $Ni_{eq}(B)$ | $Cr_{eq}(B)$ | Nibal | UTS calc | UTS meas | $Ni_{eq}(C)$ | $Cr_{eq}(C)$ | Ratio |
|---|---|---|---|---|---|---|---|---|---|---|
| 316 SS | 16.90 | 21.90 | 17.00 | 20.40 | 0.88 | 595 | 570 | 15.9 | 21.3 | 1.34 |
| 347 SS | 15.60 | 20.00 | 15.80 | 19.30 | 1.22 | 610 | 750 | 14.5 | 20.3 | 1.40 |
| TEMPALOY A2 | 18.10 | 21.90 | 18.40 | 20.40 | 2.25 | 620 | | 16.9 | 21.7 | 1.29 |
| 17-14CuMo | 18.80 | 22.80 | 17.90 | 20.10 | 2.15 | 665 | 540 | 19.9 | 22.4 | 1.11 |
| Esshete 1250 | 16.75 | 21.00 | 16.90 | 17.75 | 4.36 | 660 | 590 | 14.5 | 19.6 | 1.35 |
| TEMPALOY 17-14 | 20.10 | 21.20 | 19.40 | 18.90 | 5.32 | 675 | 560 | 20.8 | 21.1 | 1.02 |
| ST3Cu | 15.90 | 19.10 | 15.20 | 18.50 | 1.65 | 635 | 630 | 16.0 | 19.7 | 1.19 |
| PCA | 19.20 | 19.00 | 19.20 | 17.00 | 7.68 | 580 | 540 | 18.4 | 18.7 | 1.01 |
| HT-UTS CE1 | 20.00 | 20.10 | 20.00 | 15.80 | 10.20 | 625 | 565 | 18.9 | 17.4 | 0.93 |
| HT-UTS CE3 | 20.50 | 22.00 | 20.00 | 17.30 | 8.10 | 640 | 565 | 20.8 | 19.2 | 0.92 |
| HT-UTS AX5 | 20.00 | 21.10 | 20.10 | 16.60 | 9.13 | 635 | | 18.8 | 18.6 | 0.99 |
| HT-UTS MS6 | 20.20 | 24.30 | 20.20 | 17.40 | 8.21 | 670 | | 18.8 | 19.0 | 1.01 |
| HT-UTS CET1 | 20.40 | 21.30 | 20.40 | 17.00 | 8.91 | 620 | 605 | 19.3 | 18.6 | 0.96 |
| HT-UTS BWT4 | 18.80 | 19.80 | 18.80 | 16.10 | 8.48 | 610 | 490 | 17.6 | 17.5 | 0.99 |

(Masuyama et al. 1987), the Nibal number deserves attention here. From Eqs. (2) and (3), the Nibal number is calculated from the expression

$$\text{Nibal} = \text{Ni}_{eq}(\text{B}) - 1.36\text{Cr}_{eq}(\text{B}) + 11.6\,. \qquad (5)$$

Criterion I-B called for a Nibal number greater than 4. Esshete 1250, TEMPALOY 17-14CuMo, PCA, and all of the HT-UPS compositions meet this Criterion. Data are provided in Table 2.

<u>I-C. Local chemical changes associated with the depletion of austenite stabilizing elements will not produce sigma, Laves, and chi phases.</u>

The phases present in several of the alloys listed in Table 1 have been identified and reported in the literature. Some information has been provided in Table 3, and time-temperature-precipitation (TTP) diagrams have been plotted in Fig. 2 for type 316 stainless steel (Maziasz and McHargue 1987) and in Fig. 3 for type 347 stainless steel (from Minami et al. 1986), Esshete 1250 (from Murray et al. 1967), 17-14CuMo stainless steel (from Kimura and Minami 1986), and two HT-UPS stainless steels (from Todd and Ren 1989).

**Table 3. Phases identified in several lean austenitic stainless steels**

| Alloy | $M_{23}C_6$ | MC | $M_6C$ | Sigma | Laves | Chi | Other | TTP? diagram? |
|---|---|---|---|---|---|---|---|---|
| 316 SS | Y | N | Y | Y | Y | Y | | Y |
| 347 SS | Y | Y | Y | Y | Y | | | Y |
| TEMPALOY A2 | Y | Y | | | | | | |
| 17-14CuMo | Y | Y | | N | Y | N | Cu | Y |
| Esshete 1250 | Y | Y | N | Y | N | N | | Y |
| ST3Cu | Y | Y | | | | | Cu | |
| PCA | Y | Y | | | | | | |
| HT-UTS CE0 | Y | Y | Y | N | Y | | MP | |
| HT-UTS CE1 | Y | Y | Y | N | Y | N | MP | Y |
| HT-UTS CE2 | Y | Y | Y | N | Y | | MP | |
| HT-UTS CE3 | Y | Y | Y | N | Y | | MP, Cu | |
| HT-UTS AX5 | Y | Y | Y | N | Y | Y | MP | Y |
| HT-UTS AX8 | Y | Y | Y | N | Y | | MP | |

ORNL-DWG 90-8146

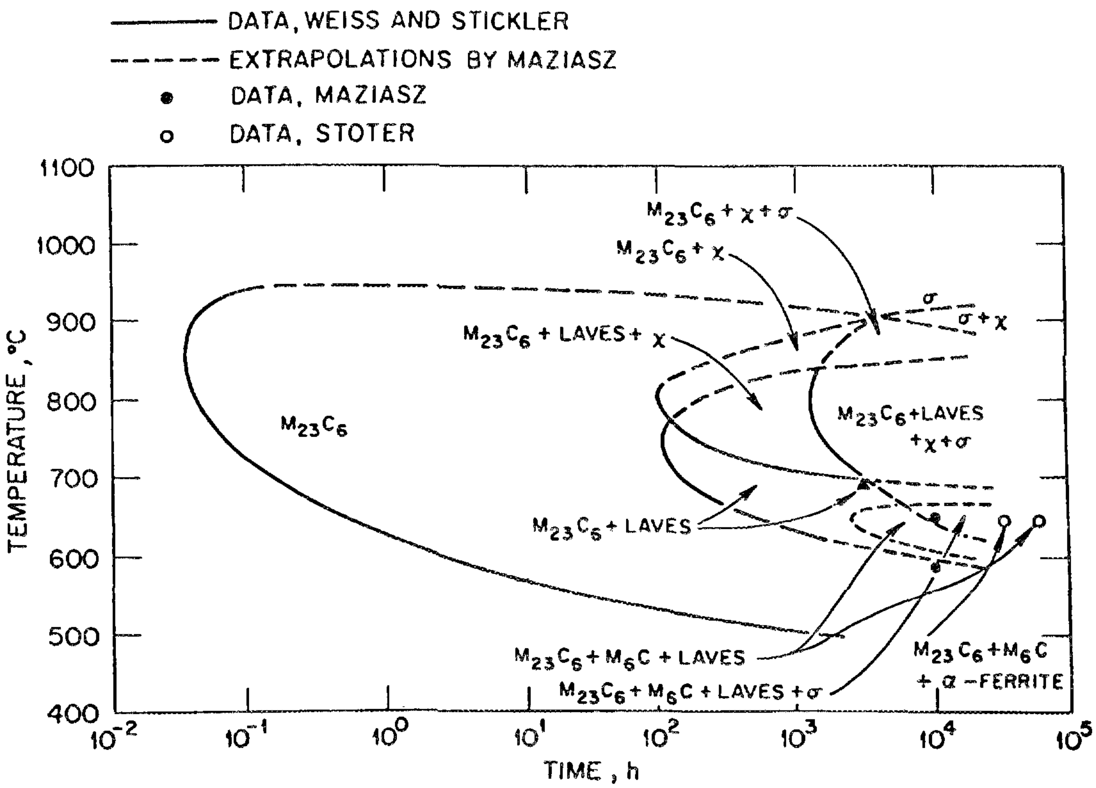


**Fig. 2. Typical time-temperature-precipitation diagram for type 316 stainless steel (after Maziasz and McHargue 1987).**

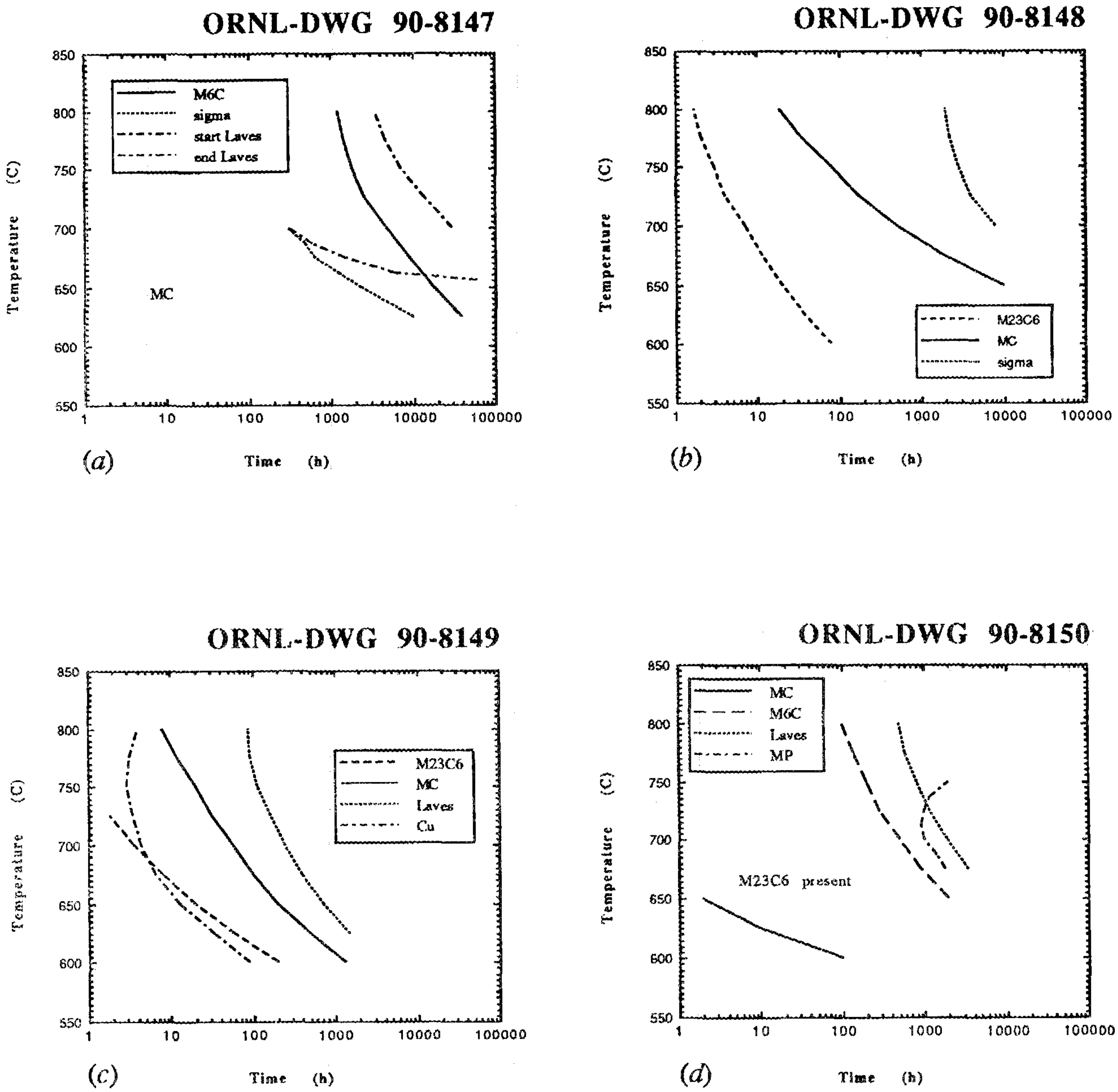


**Fig. 3. Time-temperature-precipitation diagrams for several boiler alloys: (*a*) type 347 stainless steel (Minami et al. 1985); (*b*) Esshete 1250 stainless steel (Murray et al. 1967); (*c*) 17-14CuMo stainless steel (Kimura and Minami 1986); and (*d*) HT-UPS alloys (Todd and Ren 1989).**

First, minor compositional differences, thermal-mechanical condition, and time-temperature-stress conditions influence the kinetics and location of sigma, Laves, and chi phases. Figures 2 and 3 do not provide this type of information. Not all intermetallic phases are present at the same time, occur in the same location within the microstructure, or produce the same embrittlement. Sigma and Laves are undesirable, however, and the Nibal number required to produce sigma phase embrittlement in type 316 stainless steel has been found to be 2.5 or less (McGaugh et al. 1985). Sigma phase has also been observed in type 347 stainless steel, as shown in Fig. 3(*a*), and in Esshete 1250, as shown in Fig. 3(*b*). The Nibal number for Esshete 1250 is high, near 4.4. No sigma has been reported in 17-14CuMo or ST3Cu stainless steels, which have Nibal numbers below 2.5, but the extent to which these alloys have been studied is uncertain. Laves has been found in type 316 stainless steel, as may be seen in Fig. 2. Laves has also been observed in 17-14CuMo stainless steel, as indicated in Fig. 3(*c*). The HT-UPS alloys that have been examined revealed Laves phase, as shown in Fig. 3(*d*). The amount of Laves phase observed by Maziasz (1989) was less in the HT-UPS alloys, relative to 17-14CuMo stainless steel, and the particle size was smaller in the HT-UPS alloys. A comparison of the microstructures developed under creep conditions for these two materials is shown in Fig. 4. Here, the large, blocky Laves phase particles in the grain boundaries of 17-14CuMo stainless steel may be seen in contrast to the finer, less dense dispersion of Laves phase in one of the HT-UPS alloys (CE0) tested for a long time at the same temperature. In type 347 stainless steel, the Laves-phase was observed to precipitate about the same time as sigma phase at 700°C but eventually dissolved leaving only sigma as an intermetallic phase. This trend is shown in Fig. 3(*a*). Todd and Ren (1989) found chi phase in one of two HT-UPS alloys which they examined, but the amount was relatively small and has not been indicated in Fig. 3(*d*). Finally, a gamma prime phase and a copper-rich precipitate have been observed in 17-14CuMo stainless steel, the copper-bearing HT-UPS alloys, and ST3Cu stainless steel. These phases are initially coherent and may contribute significantly to strengthening in some regimes of time and temperature. The copper phase is indicated in the TTP diagram for 17-14CuMo stainless steel shown in Fig. 3(*c*). Results gathered to date suggest that all of the alloys identified in Table 1 will have detectable amounts of intermetallic phases at some combination of time and temperature, so, in a strict sense,Criterion I-C cannot be met for any of the alloys. The degree to which intermetallic phases embrittle the alloys depends on the amount of precipitation and the testing temperature, and some data in this regard are presented in a later section of this report. With the exception of type 316 stainless steel, quantitative information is scarce concerning the amount of intermetallic phase precipitation. Ellis et al. (1988) have reviewed the kinetics of the sigma formation and included calculations of the amount of sigma in type 316 stainless steel. They used the results to specify a restricted composition range for use in procurement of main steam line piping in an advanced steam cycle plant. Marshall (1984) described unpublished research by Lai on the kinetics of Laves-phase formation in type 316 stainless steel. The assumption was that Laves phase forms after the completion of $M_{23}C_6$ precipitation, which therefore

ORNL-PHOTO 4429-87R

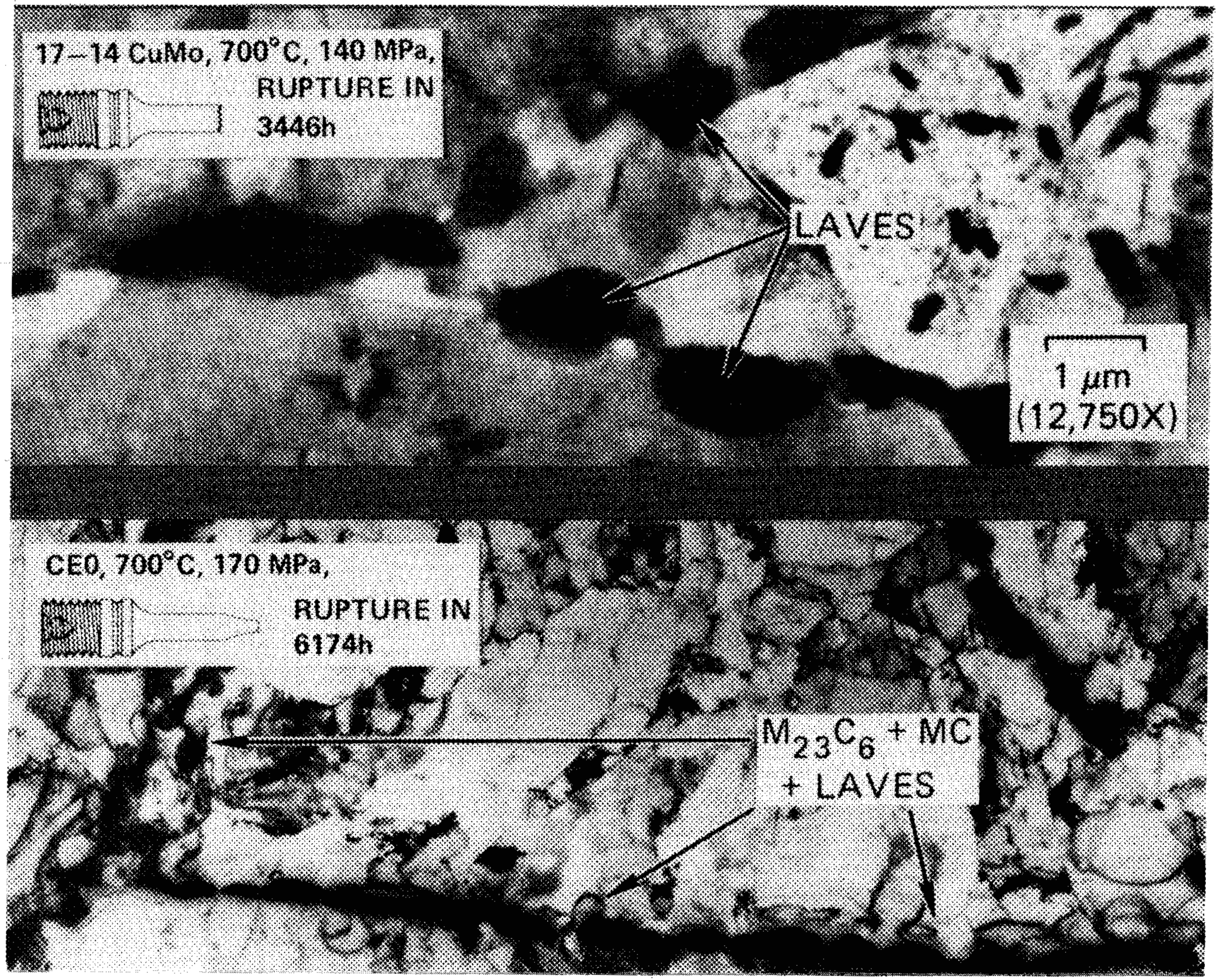


Fig. 4. Comparison of Laves phase that formed during creep testing of 17-14CuMo stainless steel and a HT-UPS alloy (CE0) at 700°C.

controls the kinetics. The amount of precipitation as a function of time has yet to be modeled. Qualitatively, information available suggests that the weight percent of intermetallic phases will vary with small differences in chemical composition and thermal-mechanical treatment. In one rare piece of work, Asbury and Willoughby (1972) measured the volume fraction of sigma phase in Esshete 1250 as a function of log of time and found that at 700°C and 10,000 h the amount of sigma precipitated ranged from approximately 3 to 12% as a function of heat treatment. Minami et al. (1986) measured approximately 5% sigma phase in type 347 stainless steel after 50,000 h at 700°C.

I-D. The alloys will be strengthened by solid solution elements and by the development of carbides and carbonitrides.

Attempts have been made by many to correlate solid solution strengthening with composition. Examples of correlations of composition with short- and long-time properties may be seen in the work of Pickering (1979), Irvine et al. (1969), Grover and Wickens (1982), and Spaeder and Defilippi (1974), to name just a few. The correlation of ultimate tensile strength (UTS) with chemistry has been given by Irvine et al. (1969) as

$$\begin{aligned} UTS = 15.4(&29 + 35C + 55N + 2.4Si + 0.11Ni + 1.2Mo + 5Nb + 3Ti \\ &+ 1.2Al + 0.14\delta + 0.82\, t^{-1/2}) , \end{aligned} \tag{7}$$

where UTS is in MPa, the elements are in weight percent, $\delta$ is percent ferrite, and t is twin spacing in millimeters. The "advanced" alloys listed in Table 1 contain important solution-hardening elements such as molybdenum, niobium, and titanium. Vanadium is not included in Eq. (7), but should increase strength as well. The calculated ultimate tensile strengths for the alloys in Table 1 are provided in Table 2, where they may be compared to experimental data reported for alloys in the annealed condition. Where data for more than one annealing temperature were reported the value chosen was that closest to 1100°C. In almost all cases, the agreement between the calculated and observed ultimate strengths was poor, indicating that factors other than the weighted solid solution strengthening elements in Eq. (7) are important in controlling the ultimate strength. The MC-forming elements, of course, are introduced for precipitation strengthening and resistance to sensitization rather than solution strengthening.

All of the alloys identified in Table 1 developed carbide precipitates during exposure at temperatures in the range of interest to advanced steam cycle applications (550 to 750°C). The types of carbides that have been observed are provided in Table 3 and included in the TTP diagrams in Figs. 2 and 3. The high-temperature creep strength is largely controlled by the size, spacing, and stability of these precipitates, both within the grains (matrix strengthening) and in the grain boundaries (grain boundary strengthening). No distinction is made in the TTP diagrams concerning the location of the precipitates. Precipitates include three types of carbides: $M_{23}C_6$, MC, and $M_6C$. A phosphide (MP) phase designed into some of the HT-UTS alloys by Maziasz, Braski, and Rowcliffe (1989) is also indicated in Fig. 3(*d*). As discussed by Maziasz and McHargue (1987), the precipitation, dissolution, and changes of the elemental composition of these precipitates is a very complex phenomenon, and it is well beyond the scope of this report to provide a comprehensive picture for even one of the alloys identified in Table 1. TheCriterion that the alloys be strengthened by precipitates was originally intended to allow this mechanism to be designed into the alloys, rather than excluded. Although none of the commercial or near-commercial alloys identified in Table 1 requires such treatments, aging to improve strength has been investigated in connection with several of the alloys, including 17-14CuMo stainless steel (Chapman and Lorentz 1960) and Esshete 1250 (Murray et al. 1967). The thermal-mechanical treatments that optimize the strength and ductility, however, were expected to vary significantly from one alloy to the next.

The $M_{23}C_6$ precipitate was expected to increase the short-time flow stress of solution-treated alloys, providing that these alloys have not been heavily cold worked. It quickly forms on grain boundaries at the temperatures of interest to the advanced steam cycle, and it may or may not form within the matrix, depending on a number of complicating factors. The TTP diagrams plotted in Fig. 3 show $M_{23}C_6$ to be present in Esshete 1250, 17-14CuMo stainless steel, and the HT-UTS steels in only a few hours at temperatures above 650°C. The formation of the MC carbide generally requires more time to develop. Figure 3 suggests that Esshete 1250 and 17-14CuMo stainless steel could require more than 10 h around 750°C to form detectable amounts of the fine MC precipitates. In contrast, the HT-UPS alloys develop MC precipitates in times less than 1 h. Cold work accelerates and improves the distribution of MC in all three alloys, as it provides nucleation sites energically favorable for the formation (Carolan et al. 1989, Todd and Ren 1989). Aging treatments to these three alloys were generally at temperatures in the range 700 to 850°C for times to 24 h (Chapman and Lorentz 1960, Murray et al. 1967). These treatments are favorable in regard to tubing production schedules. The MC, however, produces most of the long-time strengthening.

In the course of research on the HT-UPS alloys, a wide variety of thermal-mechanical treatments were examined by Carolan et al. (1987). They found that solution treating in the temperature range 1150 to 1200°C followed by 2 to 5% cold work and aging at temperatures in the range 800 to 850°C produced excellent yield and creep strengths. Additional studies were performed at ORNL on several of these alloys, and some results are summarized in Figs. 5 and 6. The room-temperature yield and ultimate strengths of the AX5 alloy were

ORNL-DWG 90-8151

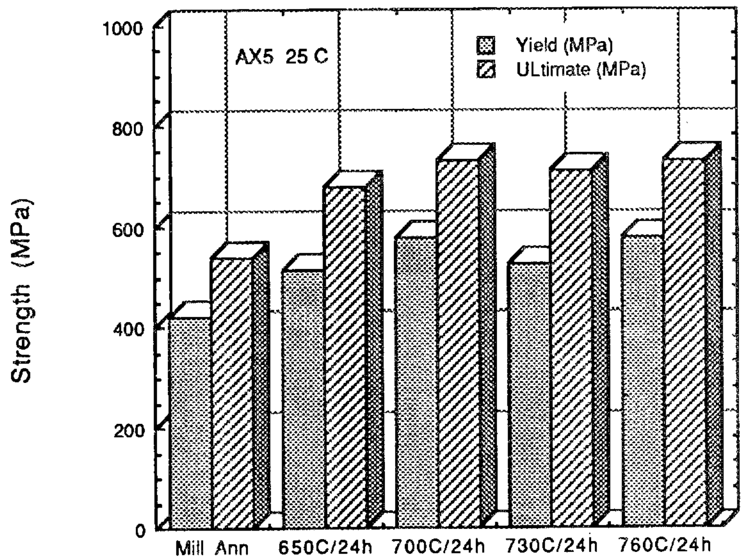


(*a*)

ORNL-DWG 90-8152

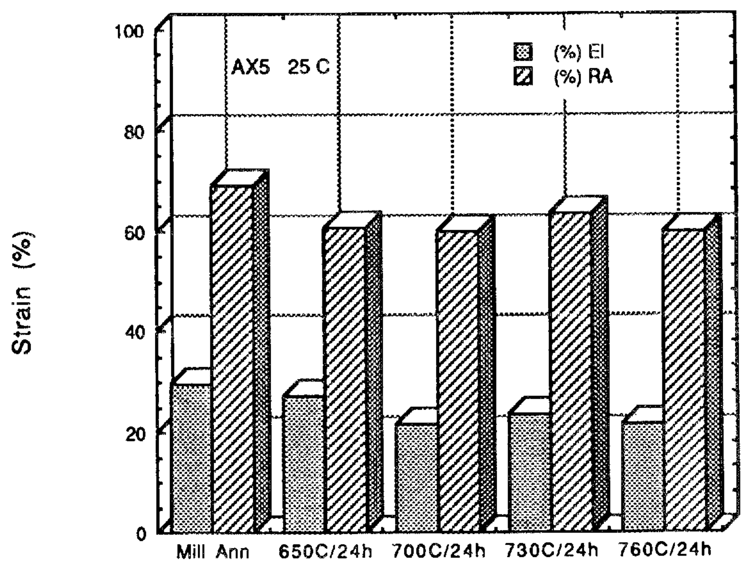


(*b*)

**Fig. 5. Effect of short-time aging on the tensile properties of cold-rolled HT-UPS alloy AX5 at 25°C: (*a*) strength and (*b*) ductility.**

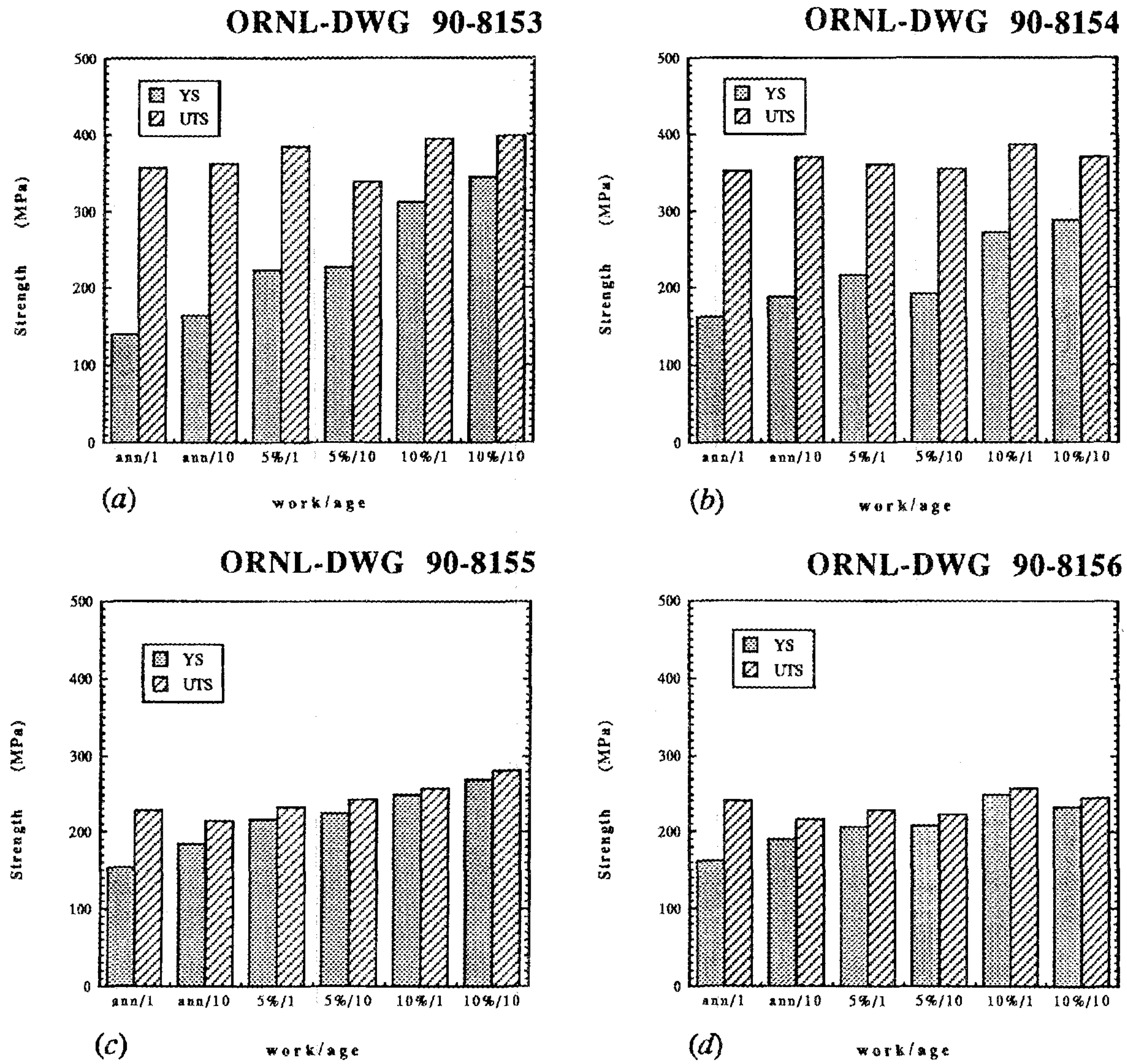


**Fig. 6. Effect of cold rolling on the yield and ultimate strengths of HT-UPS alloys CE1 and CE3 aged 1 and 10 h at 700 and 800°C and tested at the aging temperature: (*a*) alloy CE1 at 700°C; (*b*) alloy CE3 at 700°C; (*c*) alloy CE1 at 800°C; and (*d*) alloy CE3 at 800°C.**

significantly increased by short-time aging at temperatures in the range 650 to 750°C for 24 h, as may be seen in Fig. 5. This steel received a 1200°C anneal followed by 10% reduction in thickness prior to aging, whereupon the yield and ultimate strengths increased by more than 100 MPa. Small reductions in ductility accompanied the aging. More extensive aging was performed on the CE1 and CE3 alloys in connection with the studies to construct the TTP diagram in Fig. 3(*d*). Here, sheets of the two alloys were annealed at 1250°C and subsequently rolled to 0, 5, and 10% reduction in thickness. Tensile samples were machined and aged in vacuum for 1, 10, 1000, and 10,000 h. Tensile tests were performed at the aging temperature. Data are provide in Appendix B, and some of the results for the 700 and 800°C aging have been plotted in Fig. 6. It was apparent in comparing the room-temperature data in Fig. 5 with the elevated-temperature data in Fig. 6 that the high-temperature short-time strengths were not increased by aging as significantly as the room-temperature strengths. The increases in the yield and ultimate strengths between 1 and 10 h were less than 100 MPa, and in some instances decreases were noticed. The amount of cold work was related more to the strength at 700 and 800°C than aging. However, the CE1 alloy annealed at 1250°C was observed at 700°C to have a yield strength below 70 MPa and an ultimate strength below 280 MPa. Comparing these values with the strength of CE1 after the 1-h age indicated that significant strengthening occurred in the first hour of aging. This trend was consistent with the observation of rapid MC formation in the HT-UPS alloys. Thus, aging to improve the room-temperature strength of the HT-UPS alloys was practical, while aging to improve high-temperature yield and ultimate strength was unnecessary.

The effect that modest levels of cold work have on the precipitation of MC and the subsequent creep strength has been studied in considerable detail in the HT-UPS series of alloys. An example may be seen in the comparison of creep curves for the BWT4 alloy that was creep tested in the as-extruded condition, cold forged, 5% cold sunk, and 10% cold sunk conditions at 700°C and 170 MPa. Curves are shown in Fig. 7. The creep rupture life was

ORNL-DWG 90-8157

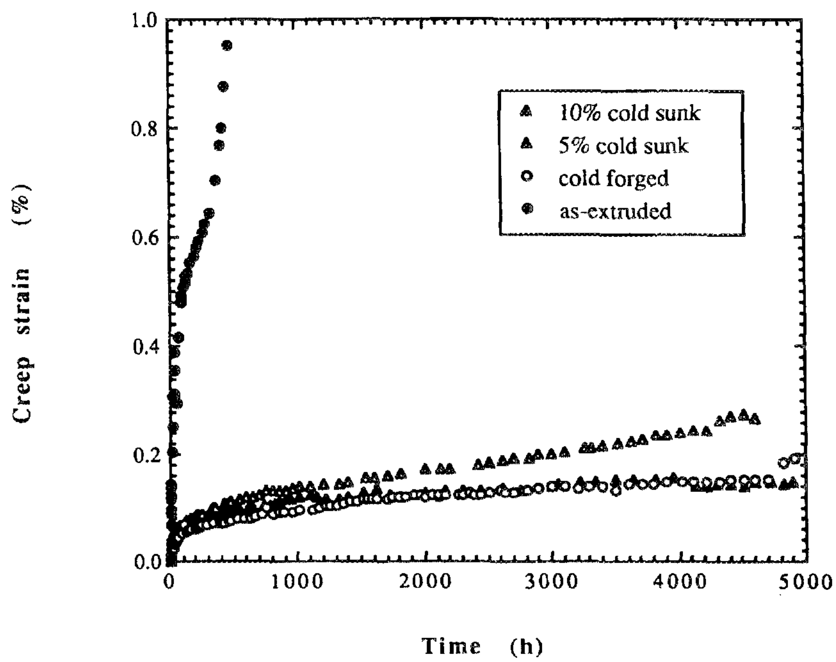


**Fig. 7. Effect of cold forging and sinking on the creep curve of HT-UPS alloy BWT at 700°C and 170 MPa.**

extended from 1315 h in the as-extruded condition to more than 10,000 h after small levels of cold work were introduced. Additional data are provided in Appendix C. All evidence collected to date suggests that Criterion I-D can be met for the near-commercial and developmental alloys in Table 1.

I-E. Aging due to Ostwald ripening will not degrade short-time strength and ductility below the minimum specified for starting material.

It was expected that some of the candidate alloys listed in Table 1 would be amenable to thermal-mechanical treatments to optimize their short- and long-time strength. By cold or warm working, for example, the yield strengths of the MC-forming alloys could be raised to levels where advantage could be taken of their extraordinary creep rupture strength at lower temperatures where the minimum yield or tensile strength would ordinarily limit the allowable design stress intensity. This was suggested by Murray et al. (1967) for Eshette 1250, Chapman and Lorentz (1960) for 17-14CuMo stainless steel, and is being considered for the HT-UPS alloys (Maziasz 1989). The purpose of Criterion I-E was to ensure that coarsening of precipitates would not result in a significant softening of an alloy whose strength depended on preservice or in-service age-hardening. Aging of lean austenitic stainless steels has been a subject of intense research for decades, and much is known about types 316 and 347 stainless steels (Marshall 1984). As a rule, the low-temperature yield and ultimate strengths of solution-treated type 316 stainless steel increases with time and ductility decreases (Sikka 1982). The high-temperature ultimate strength often diminished but the ductility improved, recognizing that sigma and other intermetallic phases could cause a reduction in creep rupture ductility. In contrast to bainitic and martensitic alloys, the yield and ultimate strengths of aged or crept stainless steels usually exceed the minimum values for the material procurement specification, although ductility and toughness may diminish to very low values as a result of the formation of both carbide and intermetallic phases (Marshall 1984). Research on Esshete 1250 by Asbury and Willoughby (1972) found that the flow stress at 3% strain and low strain rates was greatly diminished by aging for times to 10,000 h at temperatures in the range 650 to 700°C. Loss of strength was due to the formation of sigma phase which depleted the matrix of molybdenum. Aging at temperatures in the 600 to 650°C range increased the yield strength of type 347 stainless steel (Teranishi et al. 1989) and ST3Cu stainless steel (Sumitomo 1988), but at higher temperatures smaller changes in the yield strength were observed, and in some cases a loss in ultimate strength was noted. The amount of niobium precipitated from the type 347 stainless steel matrix was correlated with time and temperature on the basis of the Larson-Miller parameter. Solution-treated 17-14CuMo stainless steel generally showed increases in the yield strength with aging, as observed by Carolan et al. (1987, 1989) for 17-14CuMo stainless steel and the HT-UPS alloys. A tensile test performed on a 17-14CuMo stainless steel specimen machined from exposed Eddystone Unit #1 superheater tubing exhibited a very high room-temperature yield strength (>600 MPa) and ultimate strength (>825 MPa). Aging studies were performed by Maziasz as part of this study on two of the HT-UPS alloys (CE1 and CE3) cold rolled to 0, 5, and 10% reduction in thickness. Aging temperatures were 600, 700, and 800°C, and times were 1, 10, 1000, and 10,000 h. Tensile tests were performed at the aging temperature, and these data are provided in Appendix B. Results showed that solution-treated material gained strength with aging to 10,000 h in the range 600 to 800°C, but cold-rolled alloys lost strength at 700 and 800°C. Yield and ultimate strength data have been plotted in Fig. 8 for specimens tested after aging at 600 and 700°C for 1 and 10,000 h. The alloys experienced an increase in the yield strength between 1- and 10,000-h aging for nearly every condition. At 600°C the ultimate strength was relatively constant between 1 and 10,000 h, while at 700°C the ultimate strength decreased between 1 and 10,000 h for all levels of cold rolling.

The examination of the precipitate size as a function of time, temperature, and stress has been undertaken by many investigators. Type 316 stainless steel has been extensively examined (Marshall 1984). Coarsening of both $M_{23}C_6$ and MC in lean stainless steels was examined by Shinoda et al. (1973). They found that the $M_{23}C_6$ was more prone to coarsening than the MC at temperatures around 650°C and times to 10,000 h, and they were able to correlate much of the precipitate coarsening data on the basis of the Larson-Miller parameter. Todd and Ren (1989) examined two of the HT-UPS alloys, and their data for the MC particle size versus log time are provided in Fig. 9. The MC precipitates were found to develop quickly and stabilize at a size less than 10 nm for very long times (>3000 h) and at temperatures well above the anticipated service temperatures for the HT-UPS alloys (900°C). This particle size was significantly smaller than that observed by Shinoda et al. (1973) in Ti-Nb modified stainless steels. Todd and Ren (1989) have developed a solute exhaustion model to describe the kinetics of growth of the MC precipitation, but this model saturates without predicting further growth and coarsening. Studies by Maziasz of specimens of the HT-UPS alloys tested to times beyond 20,000 h at 700°C revealed very little particle growth beyond that shown in Fig. 9, and an example of the fine MC precipitate structure that is preserved until rupture (18,000 h at 700°C and 170 MPa) is shown in Fig. 10. Thus it would appear the Ostwald ripening of the MC precipitates at temperatures in the range 650 to 700°C may not degrade the short-time or long-time strength properties of the MC-forming HT-UTS alloys. This does not imply that aging has no significant effect on the creep properties,

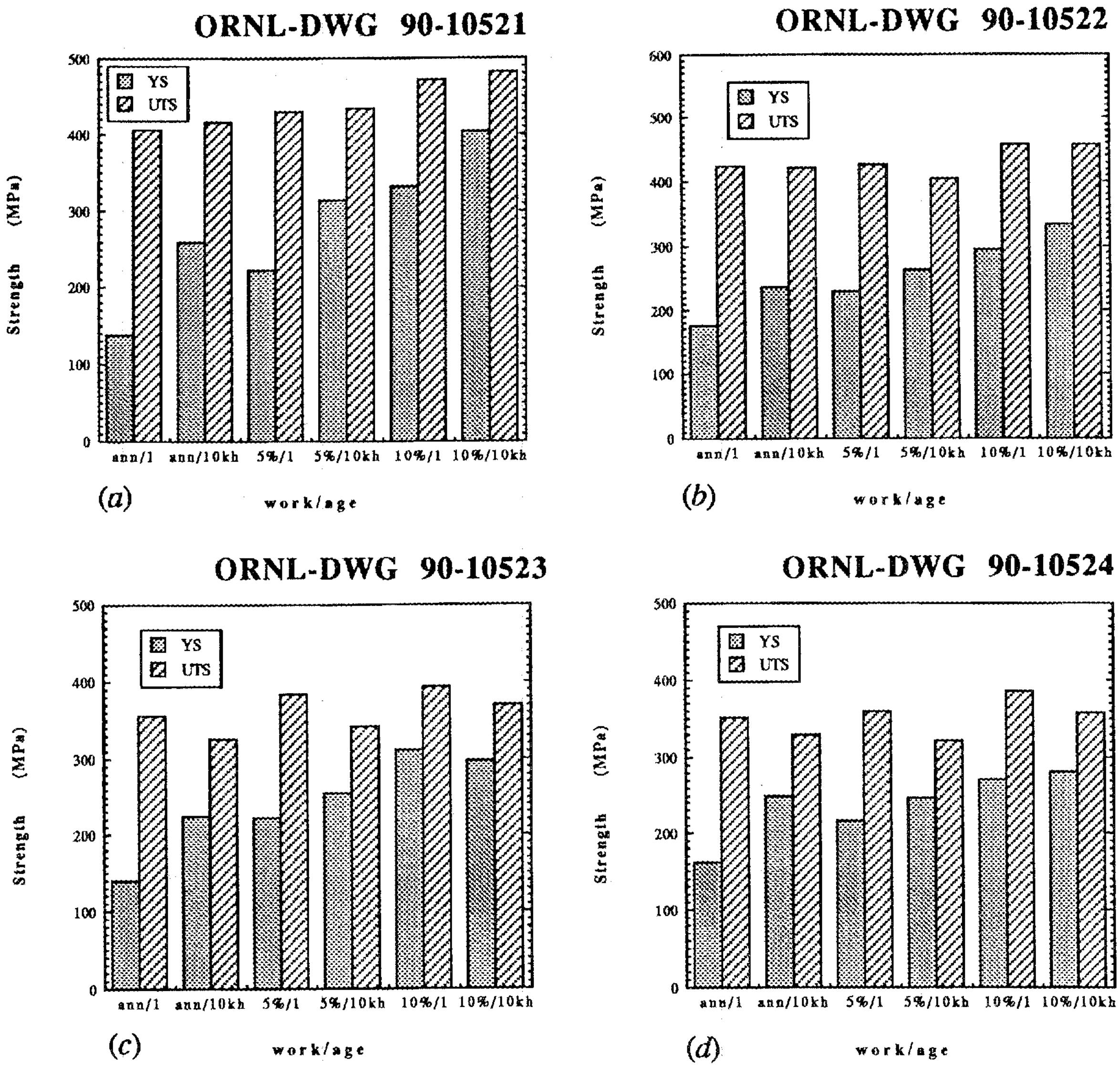


**Fig. 8. Effect of cold rolling (0, 5, or 10% work) and aging (1 or 10,000 h) on the yield and ultimate strengths of HT-UPS alloys: (*a*) alloy CE1 aged and tested at 600°C; (*b*) alloy CE3 aged and tested at 600°C; (*c*) alloy CE1 aged and tested at 700°C; and (*d*) alloy CE3 aged and tested at 700°C.**

ORNL-DWG 90-10525

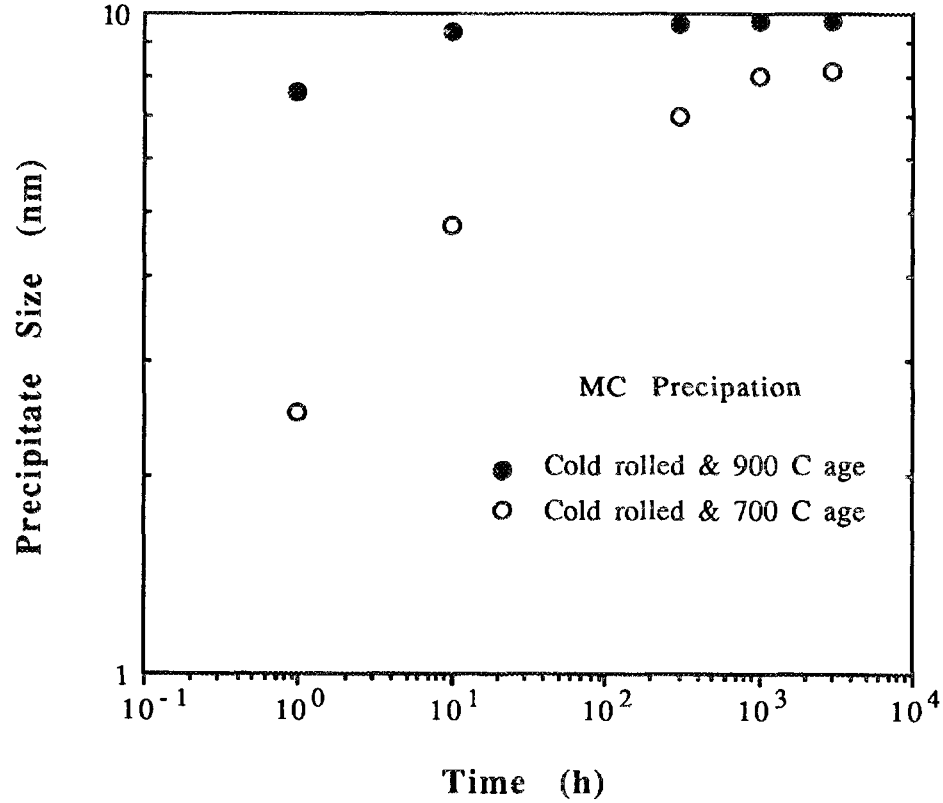


**Fig. 9. Effect of aging at 700 an 900°C on the size of MC precipitates in HT-UPS alloy AX5 cold rolled 5% prior to aging.**

however. As mentioned above, the tensile and creep response depend greatly on the initial solution temperature, warm or cold working level, and short-time aging. Much on this subject has been discussed by Maziasz (1988) and was covered in a previous report by Swindeman et al. (1987). The trends are shown for two of the HT-UPS alloys in Fig. 11, in which creep curves have been plotted for the CE2 and CE3 alloys tested at 700°C and 170 MPa. Solution treating at 1112°C followed by aging at 850°C produced a very short life relative to solution treating at 1200°C, as shown in Fig. 11(*a*). Aging at 850°C of material subjected to the high-temperature solution treatment and subsequent cold work produced only modest decreases in rupture life, as indicated in Fig. 11(*b*). An interesting result was obtained at 600°C in one of the HT-UPS alloys, however. Alloy AX5 was tested at several stresses and also aged for several times prior to stressing at 350 MPa. The specimen tested without any aging lasted considerably longer than specimens aged 4066 h prior to stressing. Thus, it would appear that the presence of a stress enhanced the strengthening process in the alloy, YE-14165

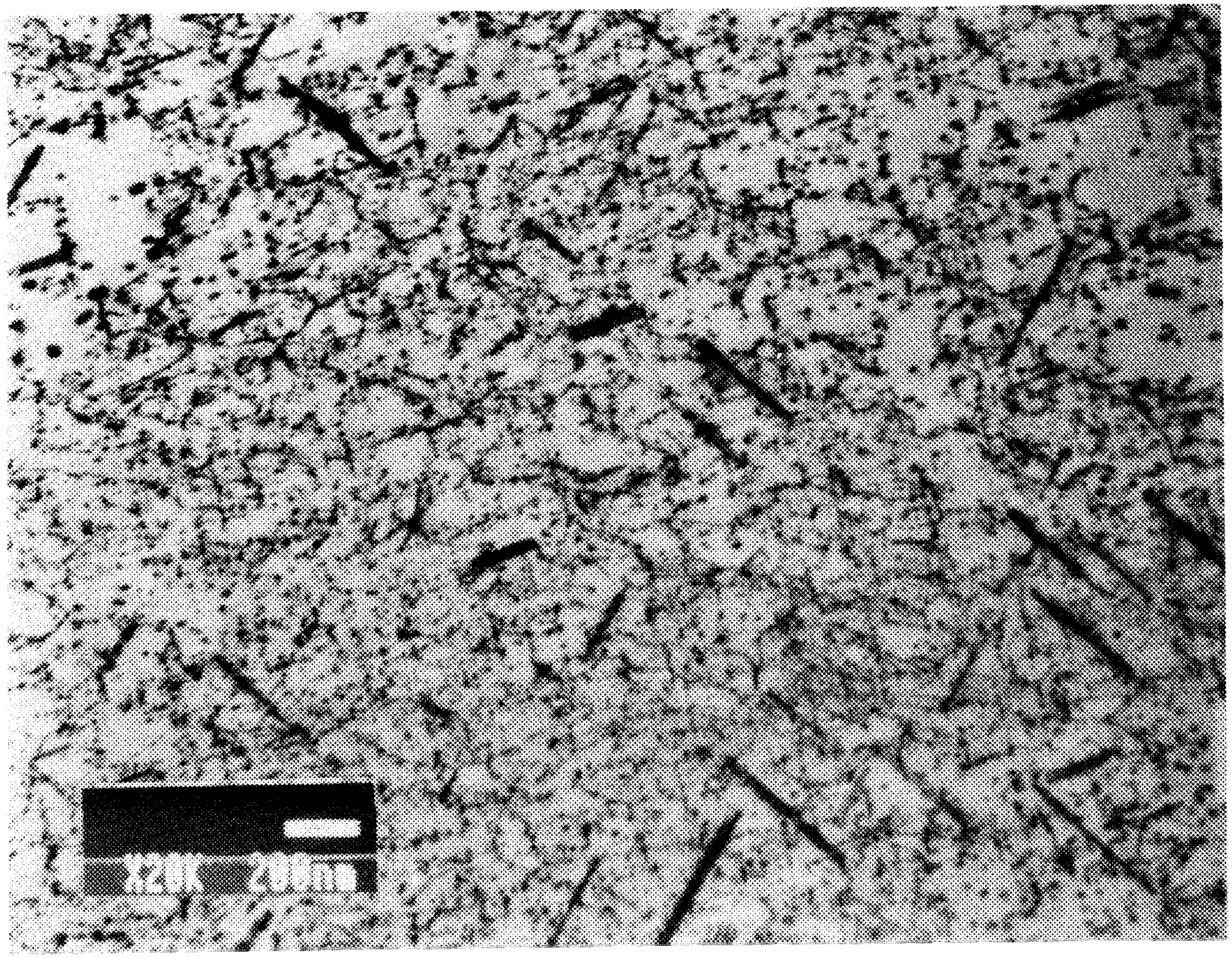


Fig. 10. Transmission electron micrograph showing the distribution and size of MC precipitates and phosphide needles in the matrix of HT-UPS alloy AX8 which ruptured after 18,745 h at 170 MPa.

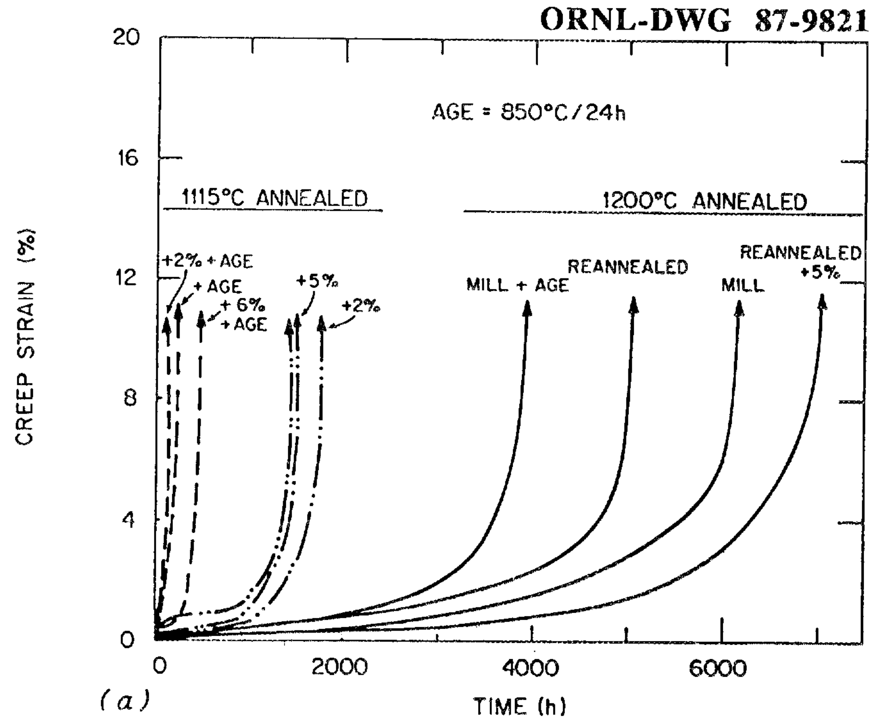


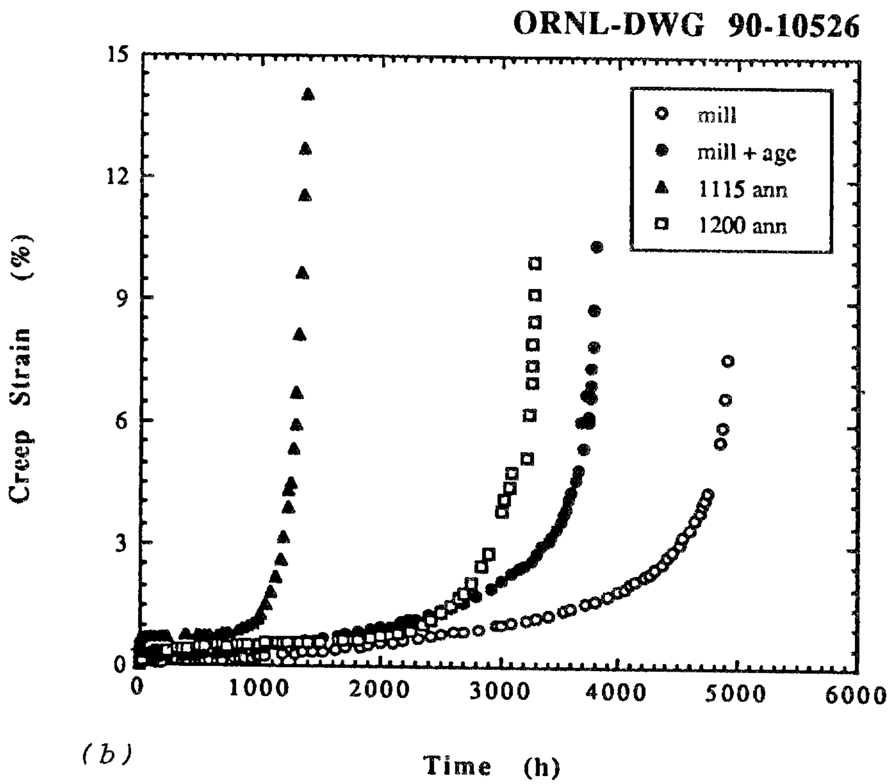


**Fig. 11. Effect of annealing temperature, cold work, and short-time aging on the creep curves for two HT-UPS alloys tested at 700°C and 170 MPa: (*a*) alloy CE0; (*b*) alloy CE3.**

perhaps by promoting the development of the fine MC precipitate. The creep curves for this series of tests are compared in Fig. 12. Many more comparisons of aging effects are possible, but it is beyond the scope of this report to discuss them in detail.

In regard to meeting Criterion I-E, however, it is necessary to consider the effects that the precipitation process has on the low-temperature strength and ductility. These effects will be discussed in a later section of this report.

I-F. The alloys will be compatible with alloy 671 cladding and not develop severely embrittled interfaces.

Esshete 1250, TEMPALOY 17-14CuMo stainless steel, and the HT-UPS BWT4 alloy have been clad with various alloys, and evaluations are in progress to determine the performance of the bimetallic tubing under boiler operating conditions. No detailed evaluations of long-time compatibility are available, with the exception of work by Asbury and Brooks (1987). They reported that Esshete 1250 was compatible with type 310 stainless steel and

ORNL-DWG 90-10527

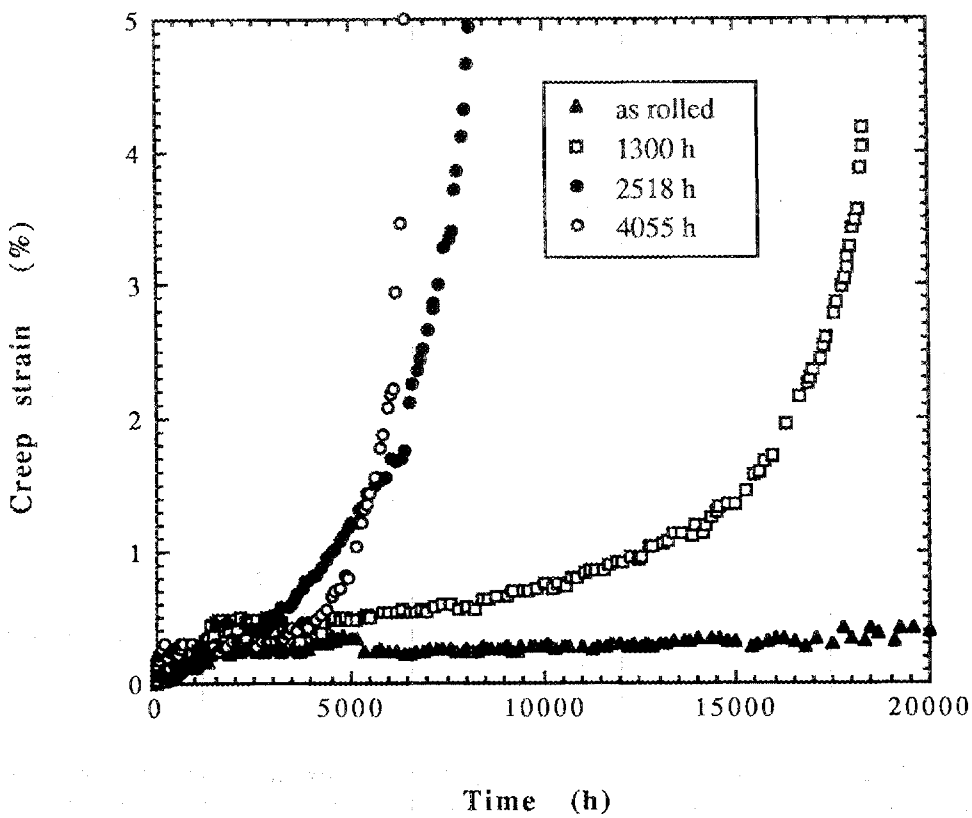


**Fig. 12. Effect of aging at 600°C on the creep curves for 10% cold-rolled HT-UPS alloy AX5 tested at 600°C and 350 MPa.**

alloy 671 for times to 50,000 h in the temperature range 600 to 625°C, athough the alloy 671 cladding was embrittled. Preliminary work on the alloy 671 cladding applied to the BWT4 tubing indicated good ductility in the side bend test after 10,000 h of exposure at 700°C.

I-G. Chromizing treatment will not degrade material strength or ductility by the formation of undesirable phases such as sigma or Laves.

It will be pointed out in the next section of this report that chromizing treatments have been applied to several of the alloys listed in Table 1, and evaluations have largely centered on corrosion resistance. In contrast, little is known about the metallurgical stability and mechanical response of the coatings and the substrates. Some exploratory tests have been performed by ORNL on chromized test specimens of 17-14CuMo stainless steel and one of the HT-UPS alloys, namely AX6. Here, 6.3-mm-diam rod specimens were creep tested in both the as-chromized and chromized-plus-solution treated conditions. Data are included in Appendix C, and results from some tests have been plotted in Fig. 13. It is clear that chromizing greatly reduced the creep rupture life and ductility for both steels. The 17-14CuMo stainless steel appeared to be more adversely affected than the AX6 alloy. The chromized layer quickly formed sigma phase, which cracked at a low creep strain. The

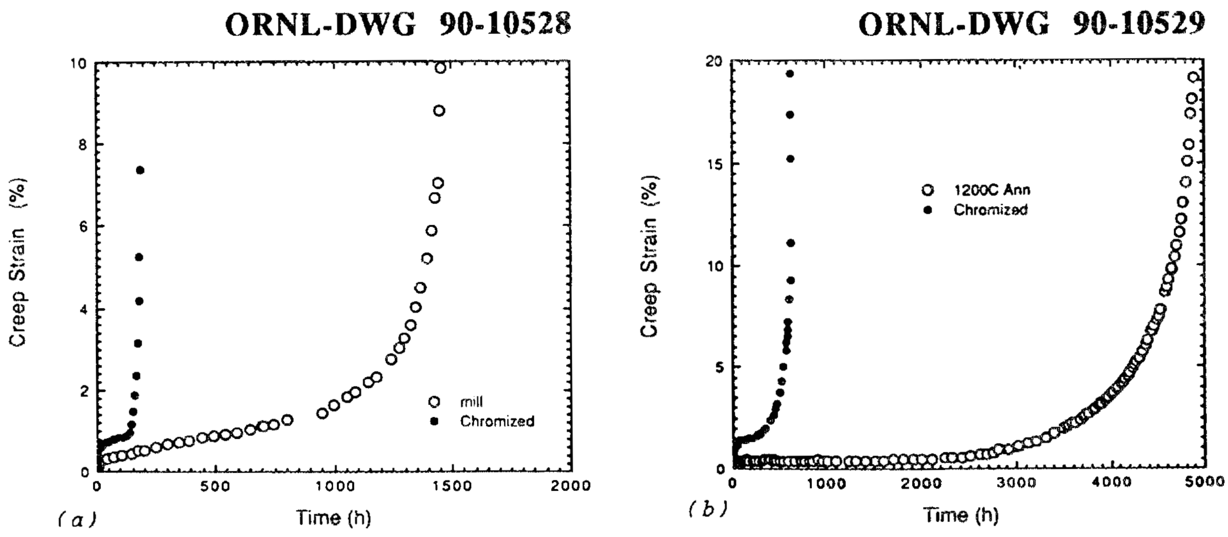


**Fig. 13. Effect of chromizing heat treatment on the creep curves at 700°C and 170 MPa for (*a*) 17-14CuMo stainless steel, and (*b*) HT-UPS alloy AX6.**

intergranular cracks continued to propagate into the substrate, as shown in the photomicrograph provided in Fig. 14(*a*). The cracking produced early tertiary creep and a significant reduction in creep life. The AX6 alloy was more creep ductile, and cracks in the coating were blunted when they reached the substrate, as shown in Fig. 14(*b*). The result was greater creep ductility and longer life in the the AX6 alloy. Unfortunately, the long time at high temperature followed by a slow cool in the chromizing bed was detrimental to the creep strength of both alloys, possibly by preventing the nucleation of the fine MC precipitate. Unless a way can be found to warm or cold work the solution-treated and chromized alloy, it appears that Criterion I-G cannot be met for the alloys that have been investigated.

I-H. The alloys will have a tolerance for at least 15% cold work introduced during boiler fabrication.

Cold-worked stainless steels have been avoided in high-temperature applications by much of the boiler and pressure vessel industry. Small levels of cold work in type 304 stainless steel were known to produce low ductility creep rupture failures (Gold et al. 1975), while high levels of cold work in type 316 stainless steel were known to promote recrystallization during service at temperatures as low as 700°C (Moen and Farwick 1978). However, the MC-forming alloys in Table 1 benefit greatly from cold work, since the dislocations produced by cold or warm work promote and stabilize the formation of the fine MC dispersion. The hardening and stability have been described in some detail by Maziasz (1988). Although less than 5% cold work is needed to promote MC formation, larger levels of cold work do not appear to be deleterious to creep rupture strength at temperatures below 700°C. However, in the tensile test cold work reduces the uniform strain and total elongation and in the creep test it lowers the creep strain at which tertiary creep starts. Considerable research has gone into the study of cold-working effects in type 316 stainless steel, the PCA alloy, and some of the HT-UPS alloys in connection with structural alloys for nuclear and fission applications (Maziasz and McHargue 1987, and Maziasz 1988). For boiler application Kinoshita et al. (1973) examined cold-working effects at the 10 and 30% levels and found no loss in rupture strength of Ti- and Nb-bearing alloys at 650°C for times to 10,000 h. At 700°C, however, strength was lost at long times in the 30% cold-worked material. Similarly, Teranishi et al. (1989) examined cold-working effects in type 347 stainless steel. They observed good stability in material cold worked 5 and 10% but a loss in strength of material worked 20 and 30%. All evidence suggests that the near-commercial and developmental alloys in Table 1 should tolerate cold work at levels to 10%. Insufficient data are available to confirm compliance to the tolerance for 15% cold work specified in Criterion I-H.

Y210995


Y210999

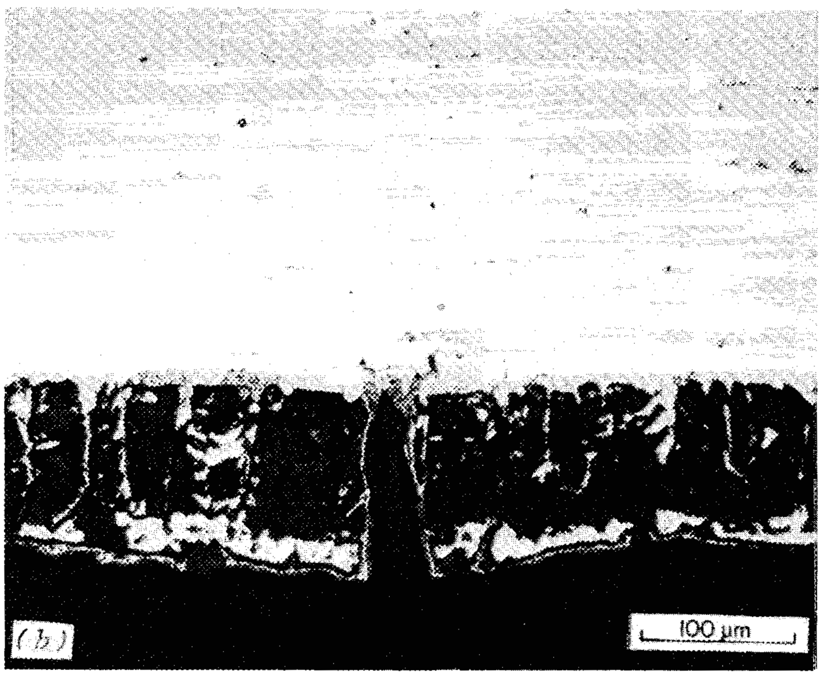


**Fig. 14. Comparison of chromized-induced cracking in two steels tested at 700°C and 170 MPa: (*a*) 17-14CuMo stainless steel that failed in 186 h with 8.2% elongation and 9.4% reduction of area; (*b*) HT-UPS alloy AX6 that failed in 630 h with 19.9% elongation and 60.3% reduction of area.**

# 4. FABRICATION AND JOINING

The general criteria that governed the fabrication and joining requirements for the advanced steam cycle alloys were that the candidate alloys be comparable to the stainless steels currently being used for superheater/reheater tubing and that production methods be typical of good fabrication practices in the boiler industry. Clearly, the near-commercial alloys listed in Table 1 have been produced as tubing; and some steels, such as Esshete 1250 and 17-14CuMo stainless steel, have had many years of boiler exposure at conditions almost as severe as what might be expected in the advanced steam cycle plant under consideration here. Of the developmental alloys, the ST3Cu stainless steel has been produced as tubing (Sumitomo 1988) and is currently undergoing evaluation. Less is known about the HT-UTS alloys; hence, they will receive most of the attention in this section of the report.

II-A. The alloys will be capable of meeting ASTM A 213 for the production of seamless tubing.

A literature review was undertaken by Domian and LeBeau (1989) to evaluate the behavior of the HT-UPS alloys regarding melting practice, workability, and phase stability. They identified several possible tube-making routes, all of which required hot working of cast and wrought structures in the temperature range 1000 to 1200°C, followed by cold working. The hot workability was assessed on the basis of the ratio of a nickel equivalent to a chromium equivalent that was proposed by Myllykosi (1983). These equivalencies are different from those previously given but involve several of the same alloying elements:

$$Ni_{eq}(C) = Ni + 0.31Mn + 22C + 14.2N + Cu \, , \tag{8}$$

$$Cr_{eq}(C) = Cr + 1.37Mo + 1.5Si + 2Nb + 3Ti \, , \tag{9}$$

where all elements are in weight percent. The optimum workability of the cast structure is achieved with the ratio $Cr_{eq}(C):Ni_{eq}(C)$ around 1.5. Lower values of the ratio represent potential cracking problems due to impurity element embrittlement on austenite grain boundaries, while higher values of the ratio portend cracking problems at austenite-ferrite interfaces. Data for the hot workability index of the alloys in Table 1 are provided in Table 2. Domian and LeBeau (1989) reached several conclusions regarding the workability of the HT-UPS alloys. They found them to be fully austenitic and prone to hot cracking in both working and welding processes. They suggested that the melting practice be selected to produce a low residual element content (Pb, As, Bi, S, Sb, and Sn). They suggested that rare earths be added to improve resistance to hot cracking. They expected the alloys to have the same cold workability as type 316 stainless steel, with no tendency toward martensite formation due to cold work.

The 14 heats of HT-UTS alloys listed in Table 1 were produced by various fabrication routes. The first group (CE0 through CE3) was produced at Combustion Engineering Metallurgical Laboratory by argon induction melting and electroslag remelting 25-kg ingots. The ingots were heated to 1200°C for 0.5 h and hot rolled with approximately 10% reduction in thickness per pass and 1200°C anneals between passes. The finished hot-rolled plate was 13 mm thick. All heats exhibited centerline delaminations in the rolled plates, starting at a location corresponding to the top of the ingot and moving toward the bottom. Approximately 40% of starting CE0 and CE2 alloy ingots was lost. The CE1 and CE3 alloys produced 90% useful material. Photomicrographs of the as-fabricated CE alloy microstructures are provided in Appendix A.

The second group of alloys (AX5 through AX8) was produced by the AMAX Company. The alloys were argon induction melted, poured as 20-kg ingots, and homogenized at 1250°C. The surfaces of the ingots were machined, and rolling was performed at 1100°C, with 10% reduction of thickness per pass and 1200°C annealing between passes. The final rollings were cold with approximately 10% reduction in thickness to produce final thicknesses of 13 mm. High yields were obtained, with nearly all of the cropped and machined ingot being usable. Photomicrographs of the as-fabricated AX alloy microstructures are provided in Appendix A.

The third group of alloys (MS series) was produced at ORNL as vacuum induction melted 10-kg slab ingots. These were homogenized at 1200°C, cropped, machined, and hot rolled at 1100°C with 10% reductions of thickness per pass. Between passes the alloys were annealed at 1150°C. Two final plate products were produced — 13 and 6.5 mm thick. High yields were obtained with nearly 80% of the cropped ingots being produced to plate. Photomicrographs of the as-fabricated MS alloy microstructures are provided in Appendix A.

The fourth melting and forming practice involved centrifugal casting and cold pilgering to fabricate tubing. This process most closely conformed to commercial boiler tube manufacturing practices and was performed by Combustion Engineering Metallurgical Laboratory. The CET1 alloy listed in Table 1 was produced. The production sequence involved argon induction melting and centrifugally casting a tube hollow 130 mm in diameter, 29 mm in wall thickness, and 3 m in length. The tube hollow was then homogenized at 1175°C for 1 h, water quenched, machined to 120-mm outside diameter by 19-mm thickness, and cold pilgered in a two-pass operation with an intermediate anneal at 1175°C. The final anneal was at 1125°C. The tubing was rotary straightened and ultrasonically inspected. Approximately 5 m of sound tubing was produced with dimensions of 63 mm in diameter and 6.9 mm in thickness. A problem was encountered in regard to the centrifugal casting of the titanium-bearing alloy. This involved the oxidation of titanium on the inside diameter of the casting, which produced the patches of oxides shown in Fig. 15. Machining of the inside

**YP10247**

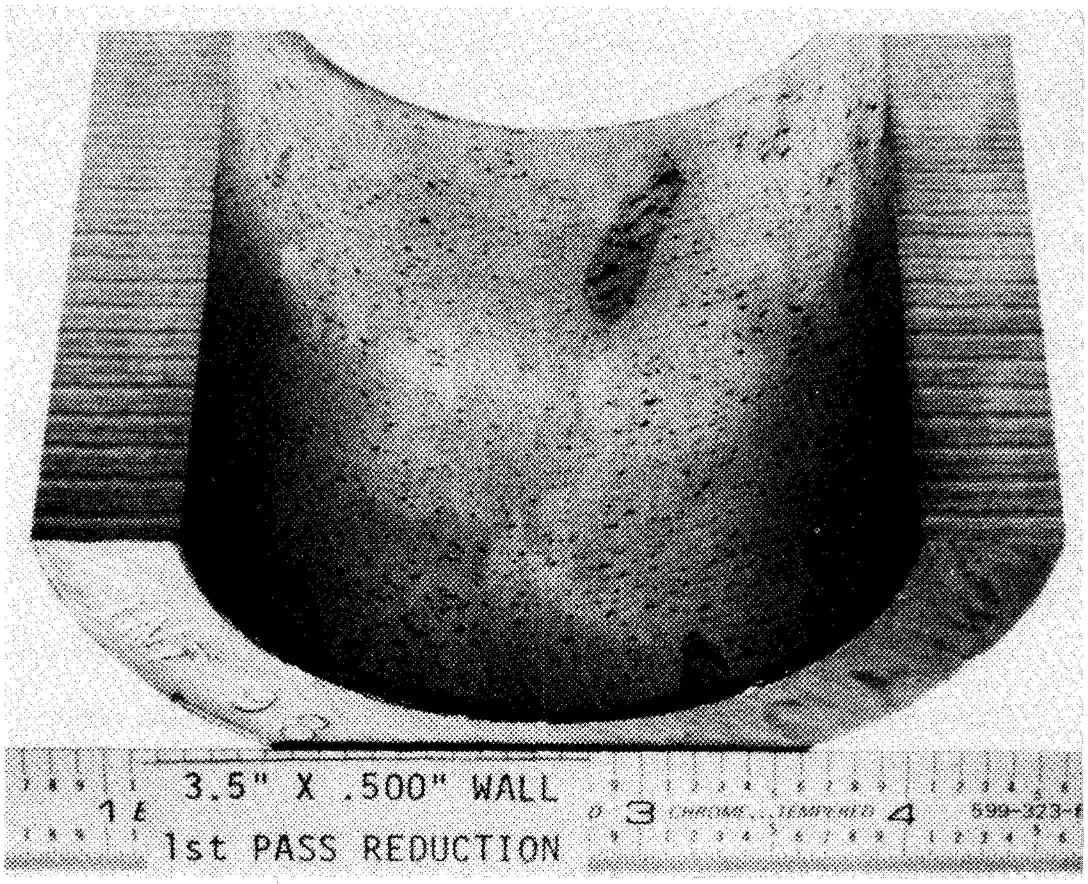


**Fig. 15. Photograph of islands of $TiO_2$ that formed on the inside diameter of centrifugally cast tubes of HT-UPS alloy CET.**

diameter of the tubing removed much of the oxide; but, to meet the target tubing dimension with the available tooling, it was necessary to leave regions which included significant oxide islands. These were carried through the subsequent fabrication processes and caused the rejection of at least 50% of the tubing on the basis of defects penetrating more than 10% of the wall thickness. A photograph of the CET1 tubing is included in Fig. 16, and the microstructure is shown in Appendix A.

The production of the BWT4 alloy listed in Table 1 was described in detail by LeBeau (1988). The alloy was vacuum induction melted and electroslag remelted at Teledyne Allvac to produce a 1270-kg, 330-mm-diam ingot. Approximately one-half of the ingot was forged to a 150-mm-diam billet, surface conditioned, drilled, and extruded by Altech Specialty Steel Corporation using standard practices for austenitic stainless steels. Two tubes were produced, each 4 m in length, 63 mm in diameter, and 13 mm in wall thickness. These were deglassed, bump straightened, and inspected. One of the two tubes exhibited a severe split on the outside diameter extending approximately 0.6 m from one end. Otherwise, no difficulties were encountered in the melting, hot forging, or extrusion of the alloy. The photograph in Fig. 16 includes a piece of the extruded BWT4 tubing, and Appendix A includes a photomicrograph of the microstructure.

Assuming that melting practices would be selected that avoided excessive oxidation of titanium, it appears that all alloys listed in Table 1 can meet Criterion II-A.

II-B. The alloys can be produced in tube diameter from 25 to 125 mm and thickness:diameter ratios from 0.15 to 0.35.

Information developed in meeting Criterion II-A assures that Criterion II-B can be met.

II-C. Tubing will be suitable for service in the mill-annealed condition after solution temperatures above 1100°C.

Criterion II-C would not be applicable to type 316 stainless steel, which is typically annealed around 1065°C. The other alloys listed in Table 1 contain MC-forming elements and are typically solution treated at 1100°C or higher. Generally speaking, the niobium-bearing alloys should be solution treated above 1150°C, with temperature increasing with niobium content (Keown and Pickering 1972, and Teranishi et al. 1989). The "mill-annealed" condition ensures that the alloy has been solution treated and is not so heavily cold worked that it would fail to meet ductility and corrosion requirements. In actual fact, warm work and modest amounts of cold work are often introduced as part of the surface finishing and straightening processes. It is this unspecified work introduced at the mill which makes it difficult to correlate composition with chemistry as might be expected when using the correlation

YP6108

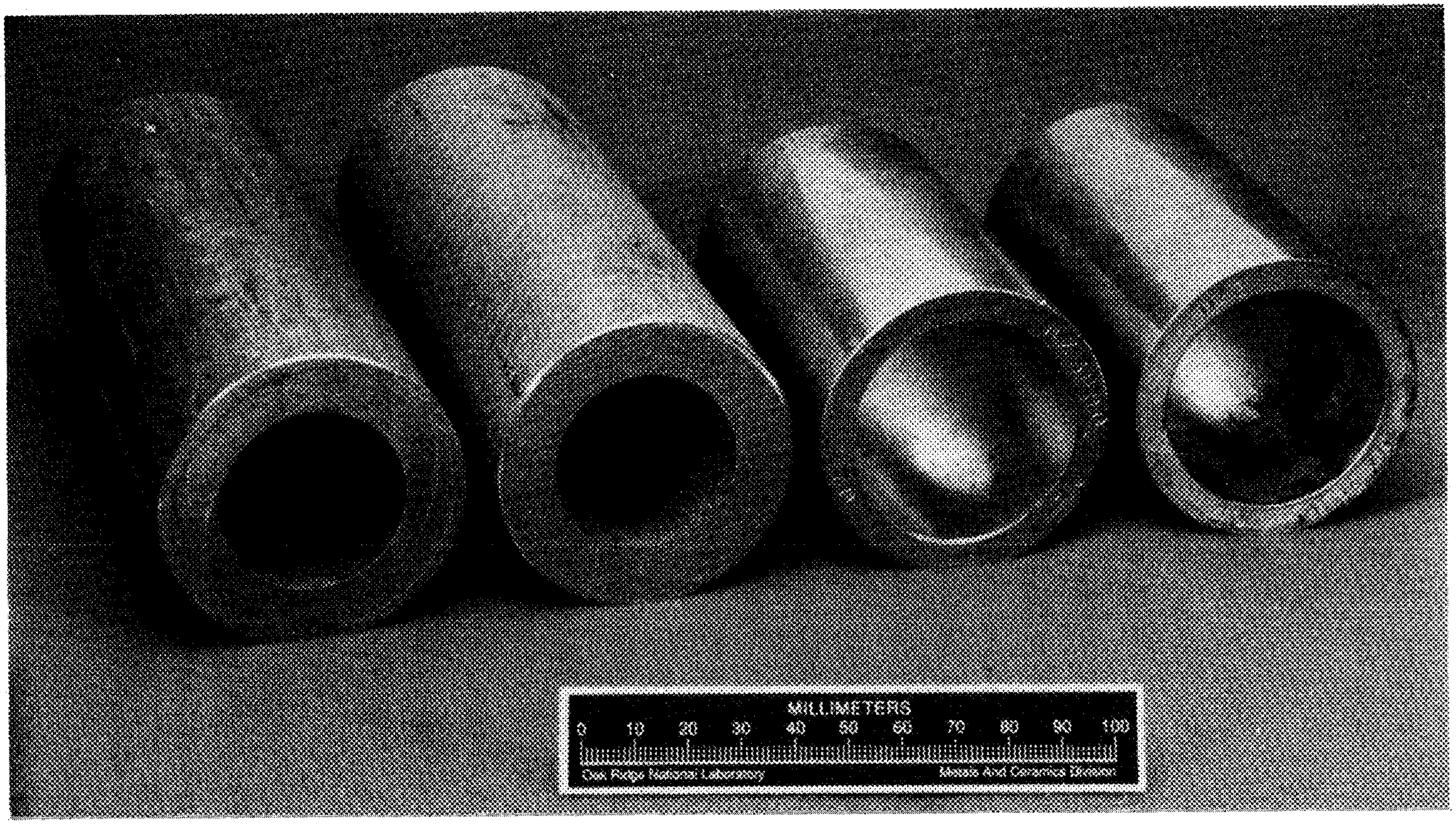


Fig. 16. Photographs of advanced alloy tubing left to right: coextruded alloy BWT clad with alloy 671; extruded BWT; cold-pilgered CET; cold-pilgered modified alloy 800.

of Irvine et al. (1969) given in Eq. (7). Because of the importance of warm or cold work to the character of the MC precipitation, small variations in the fabrication history may produce large differences in the subsequent creep rupture strength. Although the yield and tensile strength data reported for the alloys in Table 1 are represented as corresponding to solution-treated material, they often reflect this cold work. As an example, the mill-annealed 17-14CuMo stainless steel was found to have a room-temperature yield strength near 250 MPa. Other heats examined by Chapman and Lorentz (1960) exhibited yield strengths in the range 250 to 300 MPa. The laboratory anneal of 17-14CuMo stainless steel, however, produced a yield strength of only 186 MPa, well below the specified minimum strength of 207 MPa. The BWT4 alloy exhibited an even lower room-temperature yield strength (171 MPa) and would require postextrusion working to meet a 207-MPa minimum yield strength. To examine the influence of fabrication schedule, the BWT4 tubing was tested in the as-extruded, cold-forged, 5% cold-sunk, and 10% cold-sunk conditions. Curves for creep tests are presented in Fig. 7, and it was concluded in the previous section of this report that the strengthening associated with the working was due to the development of the MC precipitate. To promote the fine MC precipitation it would be necessary to specify a minimum room-temperature yield strength in excess of 300 MPa. This would require a minimum cold working strain of 5%. Additional studies are under way on the extruded tubing to establish optimum cold-working schedules.

The near-commercial alloys in Table 1 do not require cold working, although the minimum specified yield strength is probably 207 MPa; to meet this value the fabrication schedules may require an unspecified level of work. The ST3Cu alloy, however, has a minimum yield strength in the vicinity of 240 MPa, and most heats fall around 300 MPa (Sumitomo 1989). How this strength level is achieved is unknown. It should also be recognized that much of the stress rupture testing of the near-commercial alloys at temperatures below 700°C was perfomed at stresses in excess of the yield. Thus, the design stress intensities may be based on material that was hot or cold worked.

Providing that cold working of the products to levels of 5% strain is acceptable, it appears that Criterion II-C can be met for all near-commercial and developmental alloys.

II-D. Tubing alloys will be compatible with high-nickel high-chromium cladding alloys.

Several of the alloys listed in Table 1 have been clad, and summary information is provided in Table 4. Flateley et al. (1987) and Asbury and Brooks (1987) described their experience with Esshete 1250 tubing coextruded with type 310 stainless steel and alloy 671 cladding. Tamura et al. (1987) have clad 17-14CuMo stainless steel with type 310 stainless

**Table 4. List of claddings for lean stainless steel tubing**

| Base metal | Cladding | Method | Boiler exposure | Reference |
|---|---|---|---|---|
| Esshete 1250 | 310 SS | Coextrusion | Yes | Flatley et al. 1987 |
| Esshete 1250 | 50Cr-50Ni | Coextrusion | Yes | Asbury and Brooks 1987 |
| TEMPALOY 17-14CuMo | NAC Cr35A | Coextrusion | Yes | Tamura et al. 1987 |
| 17-14CuMo | 310 SS | Coextrusion | Yes | Tamura et al. 1985 |
| HT-UPS BWT | Alloy 671 | Coextrusion | No | LeBeau 1988 |
| HT-UPS BWT | Alloy 690 | Coextrusion | No | LeBeau and Domian 1990 |
| TEMPALOY A1 | NAC Cr35A | | | Flatley et al. 1987 |

steel and a nickel base alloy (CR35A®). Many hours of exposure have been accumulated regarding the performance of the claddings to coal combustion environments, but few data are available concerning the fabricability and mechanical performance.

Two of the HT-UPS alloys have been clad. LeBeau (1988) described the techniques used in extruding alloy 671 on the BWT4 alloy. Here, a machined billet, 133 mm in diameter, was encased in a mild steel can, which was subsequently filled with 50-mesh alloy 671 powder. The can was preheated, evacuated, sealed, and hot isostatically pressed (HIP) by Crucible Compaction Metals Company. The steel container was then machined from the billet, and the drilled billet subsequently extruded to tubing by Altech Specialty Steel Corporation. The clad tubing was processed in much the same way as the unclad tubing, and a photograph of the product is provided in Fig. 16. In one area of the tubing a lack of bonding was observed, but overall the clad BWT tubing presented no problems in fabrication. The microstructure of the cladding-base metal interface is shown in Fig. 17(*a*). Some evidence of the precipitation of carbides on the clad-base metal interface was observed. Possibly, this was a result of the long time and high temperature accumulated in the pressing operation. In subsequent work by LeBeau, the HIP process was omitted and the billet extruded with both alloy 671 and alloy 690 powder compacted to 70% theoretical density. The extrusion work was performed by AMAX Corporation and the cold finishing by Babcock and Wilcox. The alloy 671 cladding extruded with no problems but cracking occurred during the cold finishing. The alloy 690/BWT combination was successfully processed to cold-finished clad tubing and is currently undergoing evaluation.

Weld overlay was examined as a possible cladding method by LeBeau. Here, a piece was sawed from the BWT billet and rolled to 13-mm plate. Alloy 690 filler wire was then deposited on the plate using the gas tungsten arc (GTA) process. The clad plate was then hot rolled to produce the excellent bonding shown in Fig. 17(*b*).

Y216708

Y213328

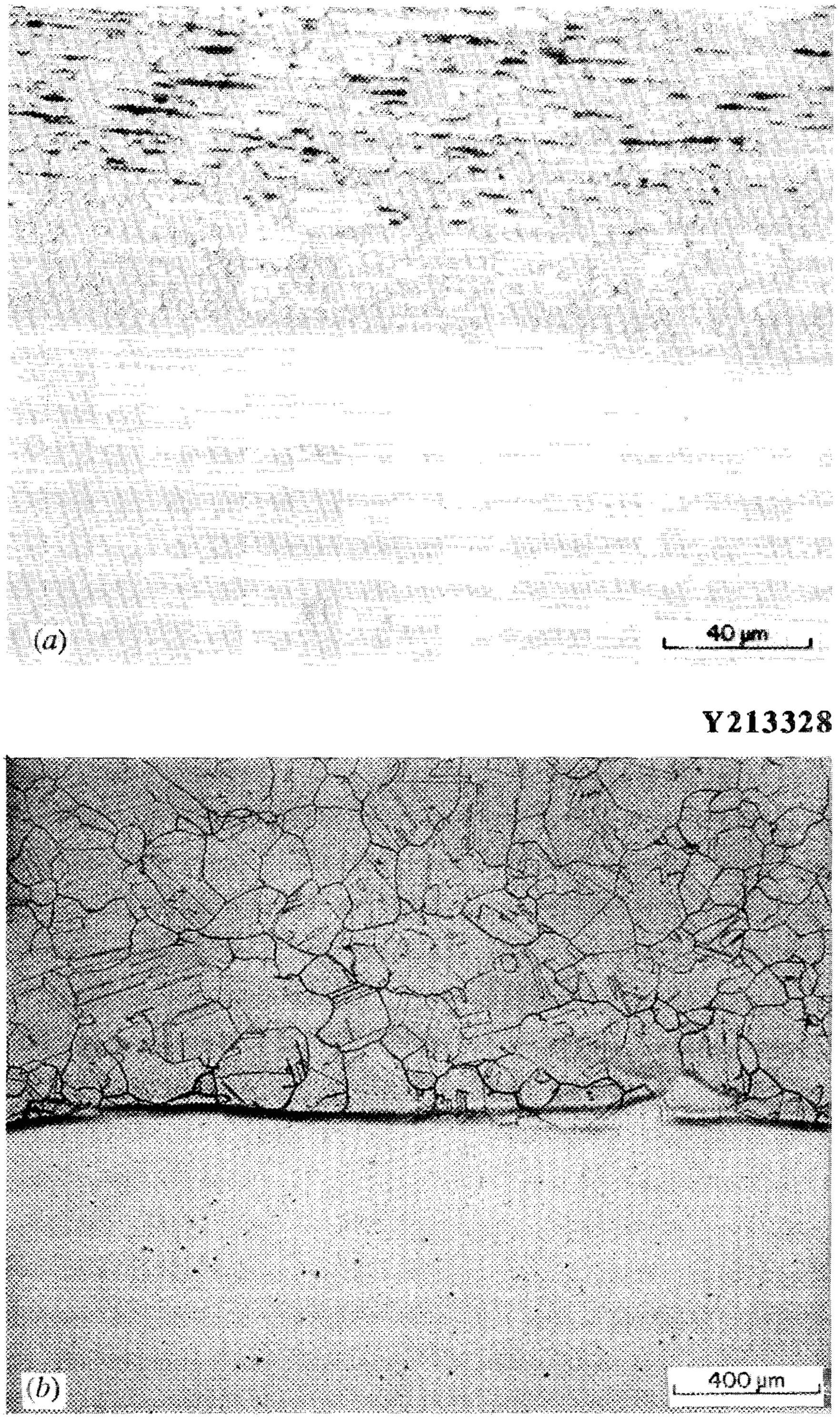


**Fig. 17. Photomicrographs of the interface between cladding and HT-UPS alloy BWT: (*a*) coextruded alloy 671 on tubing and (*b*) weld overlay alloy 692 and HT-UPS alloy BWT after hot rolling.**

It appears from the information provided above that the alloys listed in Table 1 may be clad with high-nickel high-chromium alloys, but the performance of specific claddings under the conditions imposed by advanced steam cycle operations has yet to be determined. There is some evidence from the work of Flately et al. (1987) that the 671 cladding will embrittle in service while CR35A will retain good ductility. There is reason at this time to believe that Criterion II-D can be met for most alloys in Table 1.

II-E. The alloys will be amenable to chromizing or similar surface treatments.

Chromized coatings have been produced on several alloys listed in Table 1. Tamura et al. (1987) chromized 17-14CuMo, and Turner (1987) chromized 17-14CuMo stainless steel and three of the HT-UTS alloys (CE0, CE3, and AX6). A typical chromium profile produced in a chromized sample is provided in Fig. 18. Here, a peak of 35% was produced 20 μm from the surface, while the average over the first 100 μm approached 25%. This level of chromium would be more than adequate to protect the lean stainless steels from excessive steamside corrosion. It was mentioned in the previous section, however, that the chromizing

ORNL-DWG 90-10530

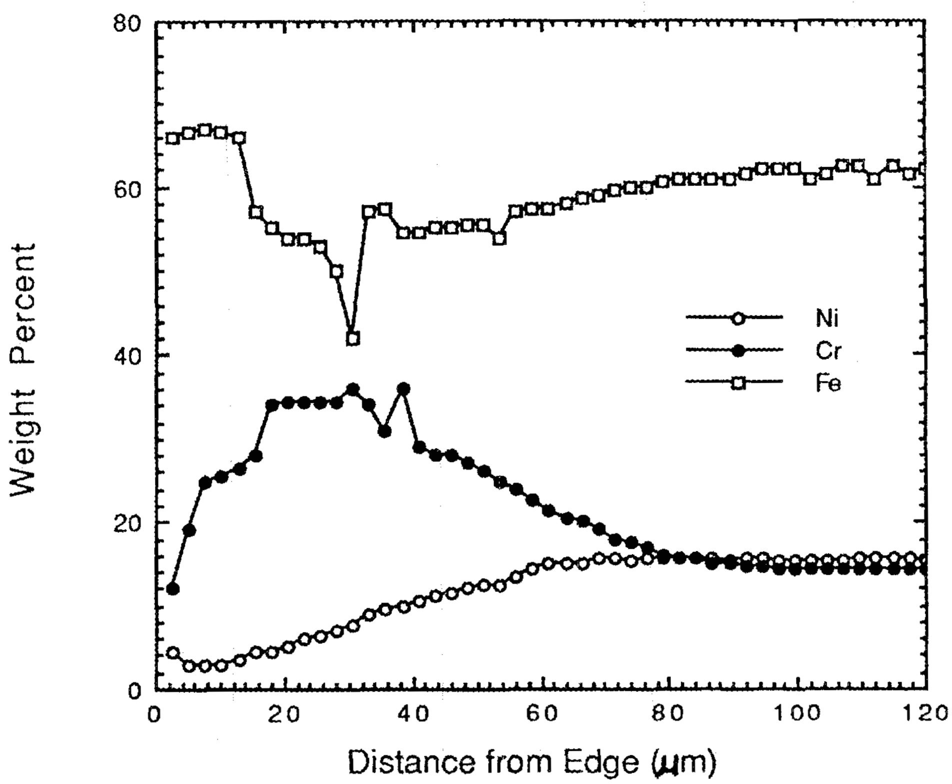


**Fig. 18. Typical Cr, Ni, and Fe contents vs depth from surface for a chromized HT-UPS alloy.**

treatment degrades the strength of the austenitic steels. In contrast to the ferritic alloys which can be heat treated after chromizing, the coarse grain size and low dislocation densities in the MC-forming alloys do not promote the formation of the strengthening precipitates.

An alternative to the chromizing that has been examined by Naylor et al. (1989) is the simultaneous chromizing/aluminizing process. Here, the aluminum combines with the nickel to form a beta-NiAl phase, and the loss of nickel promotes transformation of the austenite matrix to ferrite. The chromium diffusion is more rapid in the ferrite, which means that lower temperatures and shorter times are needed to produce coatings. The process has been used by Naylor to produce a 400-μm-thick coating on the AX7 alloy after 24 h at 1150°C. The mechanical properties of the coating have yet to be evaluated.

Although several of the near-commercial and developmental alloys identified in Table 1 have been successfully chromized or chromized/aluminized, the processes have not been demonstrated on the inside diameter of significant lengths of tubing. Further, the properties of the austenitic alloys are difficult to restore relative to the success achieved with ferritic alloys. Therefore, it appears that Criterion II-E cannot be met in the near term for those alloys which have been evaluated.

<u>II-F. The alloys will be weldable by procedures specified in the ASME Boiler and Pressure Vessel Code, Section I on Power Boilers.</u>

The American Welding Society (1989) defines weldability as "the capacity of material to be welded under the imposed fabrication conditions into a specific suitable designed structure and to perform satisfactorily in the intended use." Welds have been produced in all of the alloys identified in Table 1, but only the commercial and near-commercial alloys have been evaluated under conditions of the intended use. However, some of the alloys are more susceptible to welding problems than others. Type 316 stainless steel, for example, may be welded without great difficulty, but is subject to low ductility creep rupture failures in the weld metal and heat-affected zone (HAZ). The controlled residual element (CRE) filler metal was developed by King et al. (1976) to ameliorate this problem. The weldability of a fine-grained type 347 stainless steel was examined by Teranishi et al. (1989) who produced both gas tungsten arc (GTA) and shielded metal arc (SMA) welds in heavily restrained tubes. The SMA welds (AWS A5.4E347 filler) were sound, with very little cracking. The GTA welds exhibited cracks whose lengths summed 3% and 7% of the bead length for the GTA and SMA welds, respectively. Sumitomo (1988) observed cracking in Varestraint tests on ST3Cu stainless steel. Both the weld metal and HAZ were susceptible, but they found the alloy to have less cracking than standard type 347 stainless steel tested under similar conditions.

Lister et al. (1967) welded Esshete 1250 by the SMA process and examined the influence of minor differences in electrode chemistry. They did not report any cracking problems, possibly because of the favorable $Cr_{eq}(C):Ni_{eq}(C)$ for Esshete 1250.

A review of the potential weldability problems was undertaken by Lundin et al. (1989), with special emphasis on 17-14CuMo stainless steel and the HT-UPS alloys. One of their criteria made use of the nickel and chrome equivalencies defined in Eqs. (8) and (9). These indices were used by Kujanpää et al. (1987) to examine the tendency toward hot cracking in austenitic stainless steels. When the ratio $Cr_{eq}(C):Ni_{eq}(C)$ fell below 1.5 there was a tendency toward HAZ cracking. On the basis of thisCriterion, all of the alloys listed in Table 1 would be susceptible. The situation was found to be aggravated by the phosphorous plus sulfur content, hence the phosphorous content of some HT-UPS alloys was of particular concern. Further, they pointed out that niobium exacerbates the hot cracking problem, and it may be seen that alloys such as type 347 stainless steel and the near-commercial alloys have potential problems.

A number of experiments were performed at ORNL and by Lundin et al. (1989) to evaluate the weldability of 17-14CuMo stainless steel and the HT-UPS alloys. These experiments included, but were not limited to, Varestraint testing (Lundin et al. 1985), Sigmajig testing (Goodwin 1987), and Gleeble hot ductility testing. Correlations between the various types of tests were made, and it was concluded that the alloys had a hot cracking sensitivity equivalent to fully austenitic type 316 stainless steel and commercial type 347 stainless steel. It was determined that the alloys could not be welded with matching filler metal.

Butt welds were produced at ORNL in 17-14CuMo stainless steel and several of the HT-UPS alloys. The base metals, filler metals, and weld processes are identified in Table 5. A total of 12 alloys were welded, plus the alloy-671-clad BWT tubing. In the case of the BWT tubing, butt welds were made in the as-extruded condition; after 5, 10, and 12% cold sinking; and after creep testing for 2600 h at 700°C and 140 MPa. Five different filler metals were used — alloy 82 with the GTA process, 17-14CuMo stainless steel wire with the GTA process, 17-14CuMo stainless steel electrodes with the SMA process, CRE 16-8-2 wire with the GTA process, and alloy 556 wire with the GTA process. In all cases efforts were made to restrain the plates or tubes. The 13-mm plates were fillet welded to 19-mm-thick type 316 stainless steel strongbacks, while the as-extruded BWT tubing and cold-pilgered CET1 tubing were fillet welded to 10-mm-thick plates that were clamped in the restraining rig shown in Fig. 19. The 5, 10, and 12% sunk tubes were delivered as split tubing. The halves were longitudinally welded to form circular tubes and then butt welded. For the case of clad

Table 5. Summary of welds in lean 17-14CuMoSS and HT-UPS alloys

| Base metal | Filler metal | Process[a] | Configuration | Type | Restraint | Side bend | Metallography | Tensile | Stress rupture | Hot cracks |
|---|---|---|---|---|---|---|---|---|---|---|
| CE2 | IN82 | GTA | Plate | Butt | Full | Y | Y | Y | Y | |
| CE1 | | GTA | Plate | Butt | Full | Y | Y | Y | Y | |
| CE1 | | SMA | Plate | Butt | Full | Y | Y | Y | Y | N |
| AX5 | 17-14CuMo | SMA | Plate | Butt | Full | Y | Y | Y | Y | Y |
| AX6 | 17-14CuMo | SMA | Plate | Butt | Full | Y | Y | Y | Y | Y |
| AX7 | 17-14CuMo | SMA | Plate | Butt | Full | Y | Y | Y | Y | Y |
| AX8 | 17-14CuMo | SMA | Plate | Butt | Full | Y | Y | Y | Y | Y |
| CuMoSS | 17-14CuMo | SMA | Plate | Butt | Full | Y | Y | Y | Y | N |
| AX6 | CRE16-8-2 | GTA | Plate | Butt | Full | Y | Y | Y | Y | N |
| BWT4 | CRE16-8-2 | GTA | Tube | Butt | Full | Y | Y | Y | Y | N |
| BWT2 | CRE16-8-2 | GTA | Tube | Butt | Full | Y | Y | Y | Y | N |
| CET1 | CRE16-8-2 | GTA | Tube | Butt | Full | Y | Y | N | N | N |
| BWT | IN690 | GTA | Plate | Overlay | N | N | Y | N | N | N |
| BWT/5% CS | CRE16-8-2 | GTA | 1/2Tube | Butt | Y | Y | N | Y | Y | N |
| BWT/10% CS | CRE16-8-2 | GTA | 1/2Tube | Butt | Y | Y | N | Y | Y | N |
| BWT/12% CS | CRE16-8-2 | GTA | 1/2Tube | Butt | Y | N | N | N | N | N |
| CE3 | Haynes 556 | GTA | Plate | Butt | Clamp | Y | Y | Y | Y | Y |
| AX5 | Haynes 556 | GTA | Plate | Butt | Clamp | Y | Y | Y | Y | Y |
| AX7 | Haynes 556 | GTA | Plate | Butt | Clamp | Y | Y | Y | Y | Y |
| BWT/crept | CRE16-8-2 | GTA | Tube | Butt | N | Y | Y | Y | N | N |

[a]GTA = gas tungsten arc; SMA = submerged metal arc.

YP9144

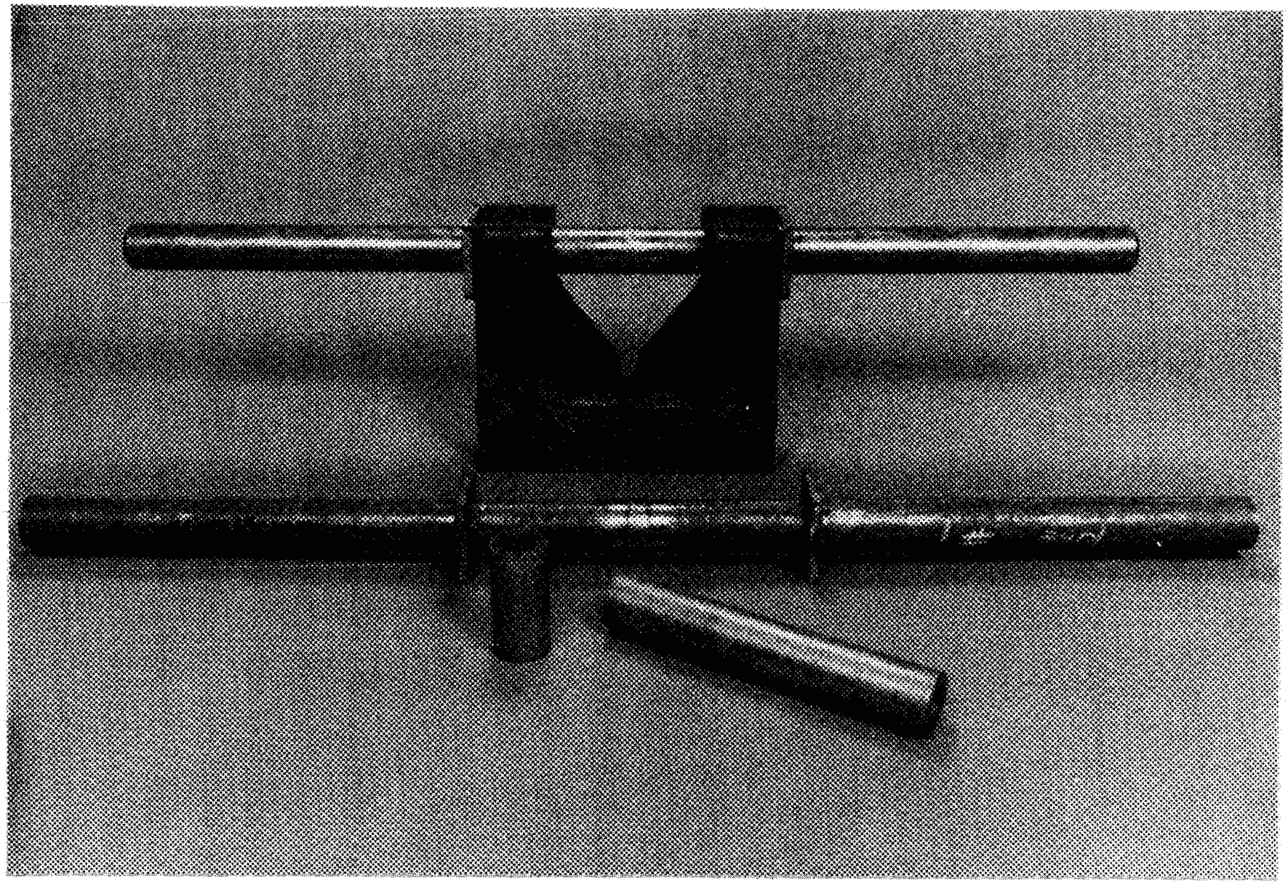

Fig. 19. Photograph of the restraint fixture used in producing gas tungsten arc weld in HT-UPS tubing.

tubing, the base metal was welded with CRE 16-8-2 stainless steel and the cladding with alloy 92. After welding, side bend and metallography evaluations were performed to evaluate the extent of hot cracking. All of the AX series alloys exhibited fusion line or HAZ hot cracking when welded with 17-14CuMo stainless steel. The high phosphorous AX7 heat was the worst and did not pass the visual inspection in the side bend test. Typical microstructures are shown in Fig. 20. No hot cracks were found in the AX6, AX8, CET1, and BWT alloys that were welded with CRE 16-8-2 stainless steel filler metal. No hot cracks were found in welds made with alloy 82. The AX5 and CE3 alloys welded with alloy 556 showed a few, barely detectable hot cracks that were less than 100 μm in length, but the AX7 alloy was cracked to depths of 100 μm in the HAZ. Metallography for some of the successful welds is provided in Fig. 21, and additional information is provided in Appendix D. All alloys exhibited extensive liquation, and in the successful welds it was clear that the hot cracking was avoided by virtue of the liquidity of the weld metal that was able to penetrate the open grain boundary regions.

In summary, there are concerns about the weldability of nearly all of the alloys identified in Table 1. Extreme care will be needed in specifying the welding processes, filler metals, and process variables. Only by testing in actual boiler operating conditions can conformance to Criterion II-F be ensured.

II-G. Standard practices of making tube-to-heater joints will be applicable.

There appear to be no reasons why Criterion II-G cannot be met.

## 5. MECHANICAL PROPERTIES

In specifying the alloy design criteria that address mechanical properties goals, it was intended that the strength of the tubing be sufficient to permit tubing of sizes normally used in superheaters and reheaters to operate at conditions where the fireside metal temperature could reach 700°C and the design steam pressure reach 35 MPa (5000 psi) . To use tubing of convenient diameters and wall thicknesses under these conditions, it was estimated that a design stress of 60 MPa (9 ksi) would be satisfactory. This allowable design stress intensity is approximately twice the allowable stress for any commercially available austenitic stainless steel listed in Sect. I on Power Boilers of the ASME Boiler and Pressure Vessel Code. One might legitimately question the need for such an ambitious target in view of the fact that the near-commercial alloys listed in Table 1 are intended for use in the advanced steam cycle and will probably function quite well at somewhat lower design stress intensities. The answer lies in the desire for an improved design margin. A stronger alloy provides more opportunity to

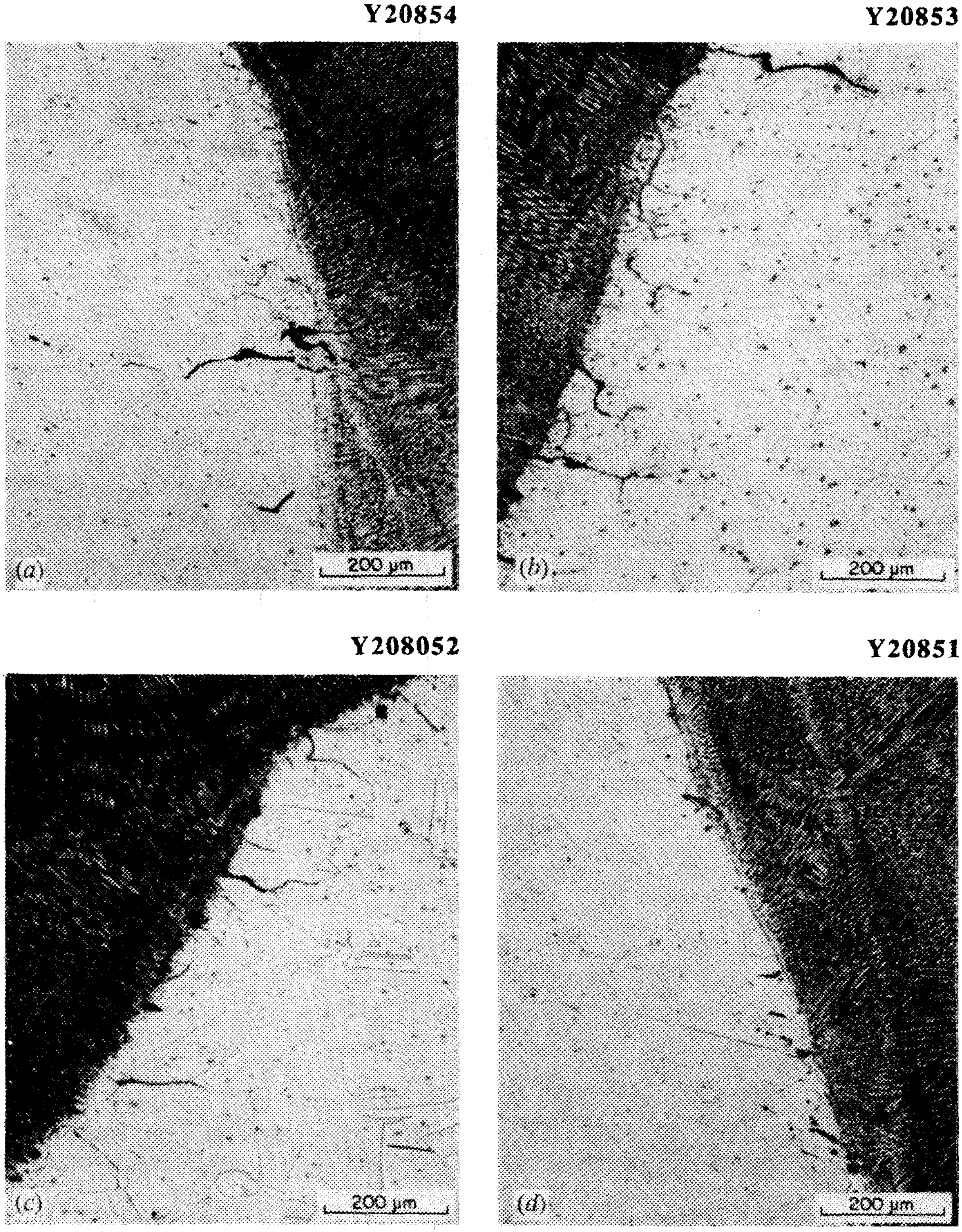


**Fig. 20. Photomicrographs of typical hot cracks produced in the heat-affected zone of butt welds in 13-mm-thick plates of four HT-UPS alloys using the shielded metal arc process with 17-14CuMo stainless steel filler metal: (*a*) alloy AX5 with 0.024% P, (*b*) alloy AX6 with 0.041% P, (*c*) alloy AX7 with 0.076% P, and (*d*) alloy AX8 with 0.043% P.**

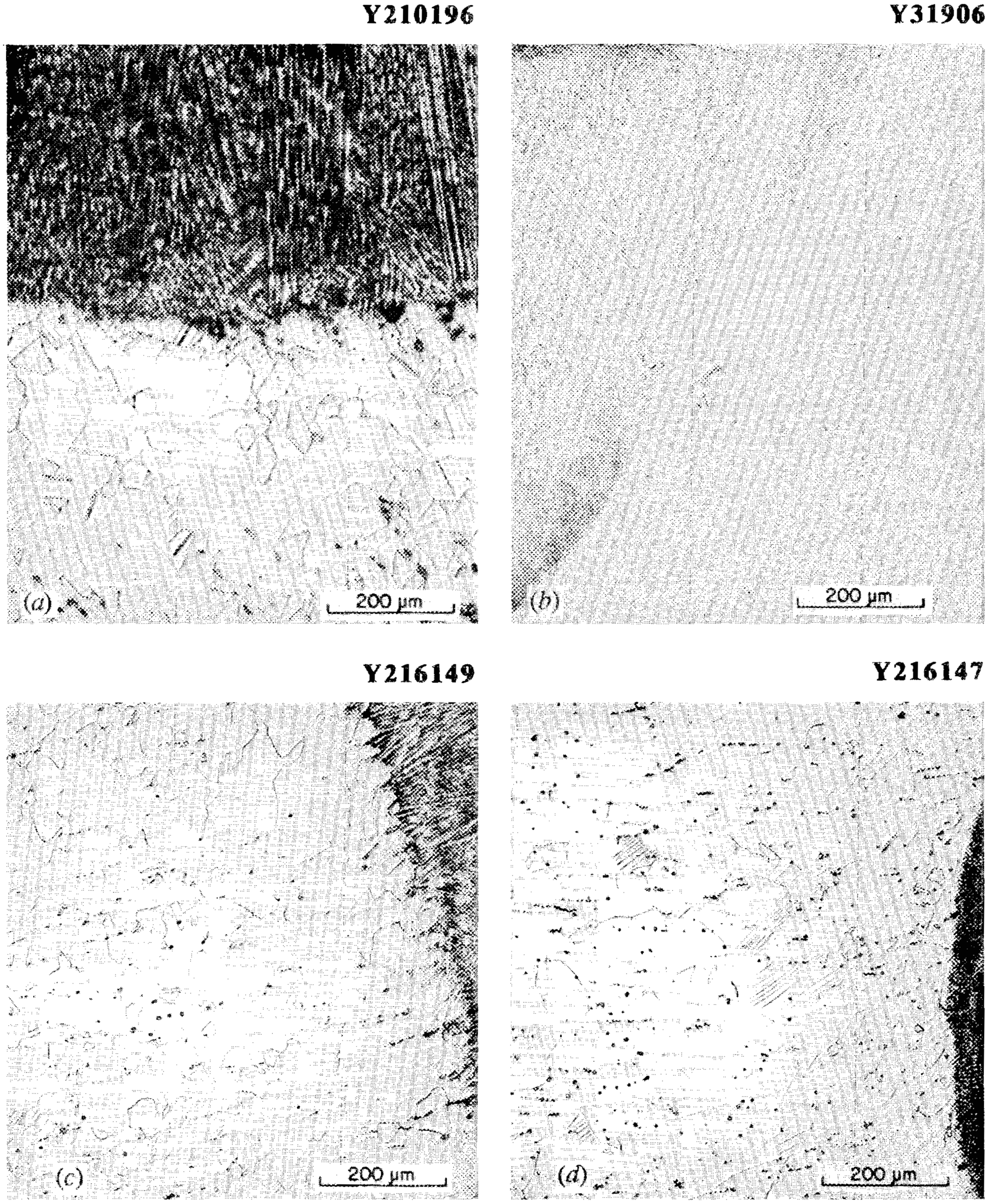


**Fig. 21. Photomicrographs of sound welds in several HT-UPS alloys using different filler metals with the GTA process: (*a*) CRE 16-8-2 filler metal and alloy AX6 with 0.041% P, (*b*) CRE filler metal and alloy BWT with 0.016% P, (*c*) alloy 556 filler metal and alloy CE3 with 0.071% P, and (*d*) alloy 556 filler metal and alloy AX5 with 0.025% P.**

optimize fabrication cost versus performance. It is assumed that a higher strength requirement will exclude the two commercial alloys in Table 1 (types 316 and 347 stainless steels) and require a careful examination of the performance of the near-commercial alloys, as well. In examining relative performance of the alloys listed in Table 1, however, the possibility of improving any of the alloys has not been excluded, with the concomitant problems of qualifying a new grade of steel within the necessary modified specifications for chemistry or thermal-mechanical processing. Nevertheless, most of the emphasis in this section of the report will be placed on the HT-UPS alloys, and comparisons will often be made with type 316 stainless steel.

III-A. The design allowables will be based on the strength criteria set forth in A-150 of the ASME Boiler and Pressure Vessel Code, Sect. I.

Only a Code body can set design stress intensity values, and a well-defined procedure must be followed before any action can be taken by the Code to approve a new material or grade of an existing material. Of utmost importance is the need for a Code stamp on the vessel or piping system in order to meet legal requirements set by the state in which the component is to be used. Currently, there is no specific need in the United States for a high-strength boiler tubing alloy to be used in an advanced steam cycle system. Assuming that the need may exist some day, one can work toward producing materials data that could be used by the Code to establish allowable design stresses. The guidance set forth in paragraph A-150 of Sect. I on Power Boilers is that the allowable design stress intensity for non-age-hardenable austenitic stainless steels will be determined by:

1. 1/4 of the specified minimum tensile strength at room temperature;
2. 1/4 of the tensile strength at temperature;
3. 2/3 of the specified minimum yield strength at room temperature;
4. 2/3 of the yield strength at temperature;
5. 67% of the average stress to produce rupture at the end of 100,000 h;
6. 80% of the minimum stress to produce rupture at the end of 100,000 h; and
7. 100% of the stress to produce a creep rate of 0.01%/1000 h.

For some austenitic alloys, such as types 304 and 316 stainless steels, item (4) above has been waived, and it is permissable to use 90% of the minimum elevated-temperature yield strength. Clearly, more than one heat must be tested and long duration test data are needed.

In addition to these requirements, evidence must be provided that the alloy does not so embrittle in long-time service that catastrophic failure could result.

Substantial data bases exist for type 316 stainless steel; an improved version of type 347 stainless steel, which will be identified here as FG347 stainless steel; and some of the near-commercial alloys listed in Table 1. The National Research Institute for Metals (NRIM) in 1978 published data sheets for nine heats of type 316 stainless steel boiler tubes that have become a standard against which other heats and alloys can be measured. Both tensile and stress rupture data were provided. The temperatures ranged from 600 to 750°C, and stress rupture times extended beyond 50,000 h, thus requiring a minimum of extrapolation to establish design stress allowables with a high degree of confidence.

A plot of the NRIM yield and ultimate strength data versus temperature has been provided in Fig. 22, which also includes a trend line based on a simple polynomial fit through

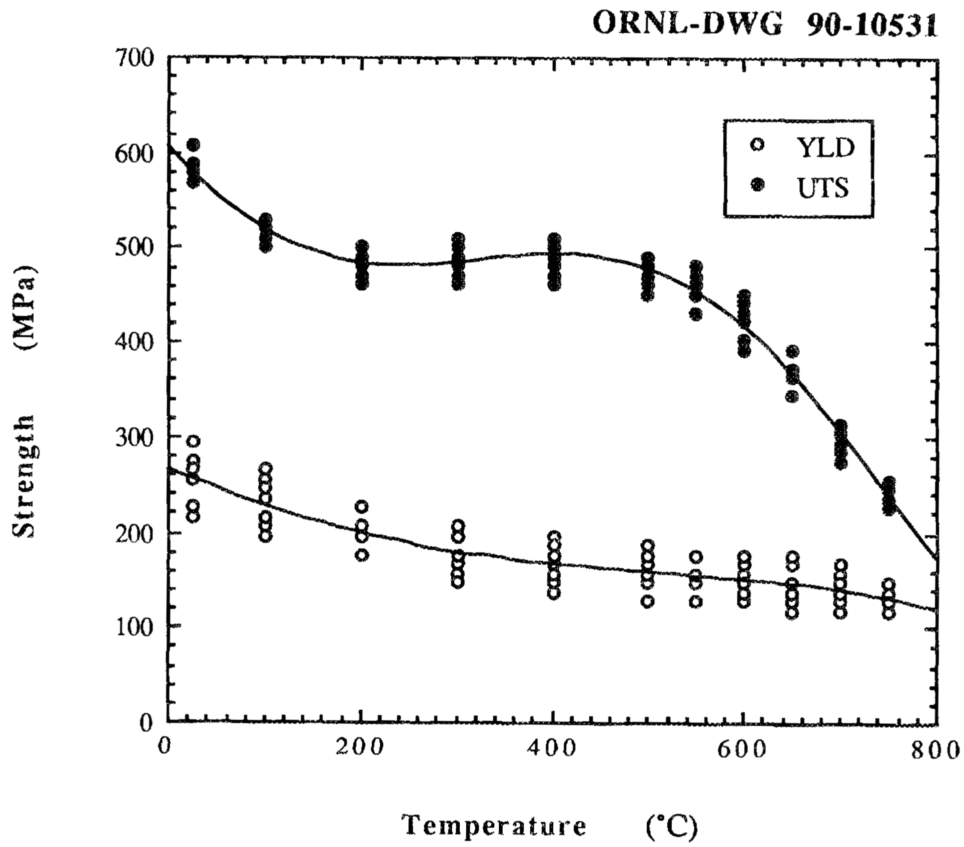


**Fig. 22. Yield and tensile strengths vs temperature for nine heats of type 316 stainless steel tubing tested by the National Research Institute for Metals.**

the data. Since the tubes experienced similar processing histories, a fairly narrow scatter would cover the data, although on a percentage basis it is clear that the yield strength data varied more than the ultimate strengths. The trend of the NRIM data is compared with representative tensile data for FG347 stainless steel, ST3Cu stainless steel, and TEMPALOY 17-14CuMo stainless steel in Fig. 23. The ST3Cu and TEMPALOY 17-14CuMo stainless steels exhibited higher yield strengths, but all four alloys had similar ultimate tensile strengths in the temperature range 200 to 600°C. This is the temperature range where one-fourth of the ultimate strength often limits the allowable stresses, hence there is little to choose from among these four alloys.

Since 17-14CuMo stainless steel was one of the alloys examined experimentally, it is treated in more detail here. Plots of available tensile yield and ultimate strength data versus temperature are provided in Fig. 24. Materials included in the TEMPALOY 17-14CuMo, several heats and heat treatments examined by Armco (1950), and three conditions for the heat are included in the ORNL research. The yield strengths shown in Fig. 24(*a*) varied substantially, with the 1125°C annealed material being the weakest, the 5% cold work material being the strongest, and the materials aged at 732 and 800°C for 5 h and tested by Armco showing good strengths in the range 500 to 700°C. The different heats and heats treatments exhibited about the same scatter in the ultimate strength [Fig. 24(*b*)] as the nine heats of boiler tubing tested by NRIM (Fig. 22). Again, about the same ultimate strengths were observed in the 200 to 600°C temperature range.

Because the quantities of HT-UPS alloys were small and the primary application for the alloys was in the temperature range where creep rupture strength would control the design allowables, the tensile testing of most of the developmental alloys was limited to 25 and 700°C. It was also known from very early in the research work that the HT-UPS alloys in the "laboratory-annealed" condition offered no compelling advantage over the near-commercial alloys identified in Table 1. To conserve material, most of the tensile testing and creep testing was focused on material in the hot- or cold-worked condition, which will be defined here as the "mill-annealed" condition. Even for the mill annealed, however, some distinctions were necessary. Products that received a low-temperature (<1150°C) treatment and small levels of cold work (< 2%) were more typical of laboratory-annealed alloys in regard to creep response. Figure 25 plots the ultimate tensile strength and ductility of the HT-UPS alloys versus the yield strength at 25 and 700°C. Distinctions are made between the mill, mill plus aged, and annealed conditions. In Fig. 25(*a*) it may be seen that at first the room-temperature ultimate strength increased slowly with rising yield but then more rapidly when the yield strength exceeded 500 MPa. The room-temperature ductility data plotted in Fig. 25(*b*)

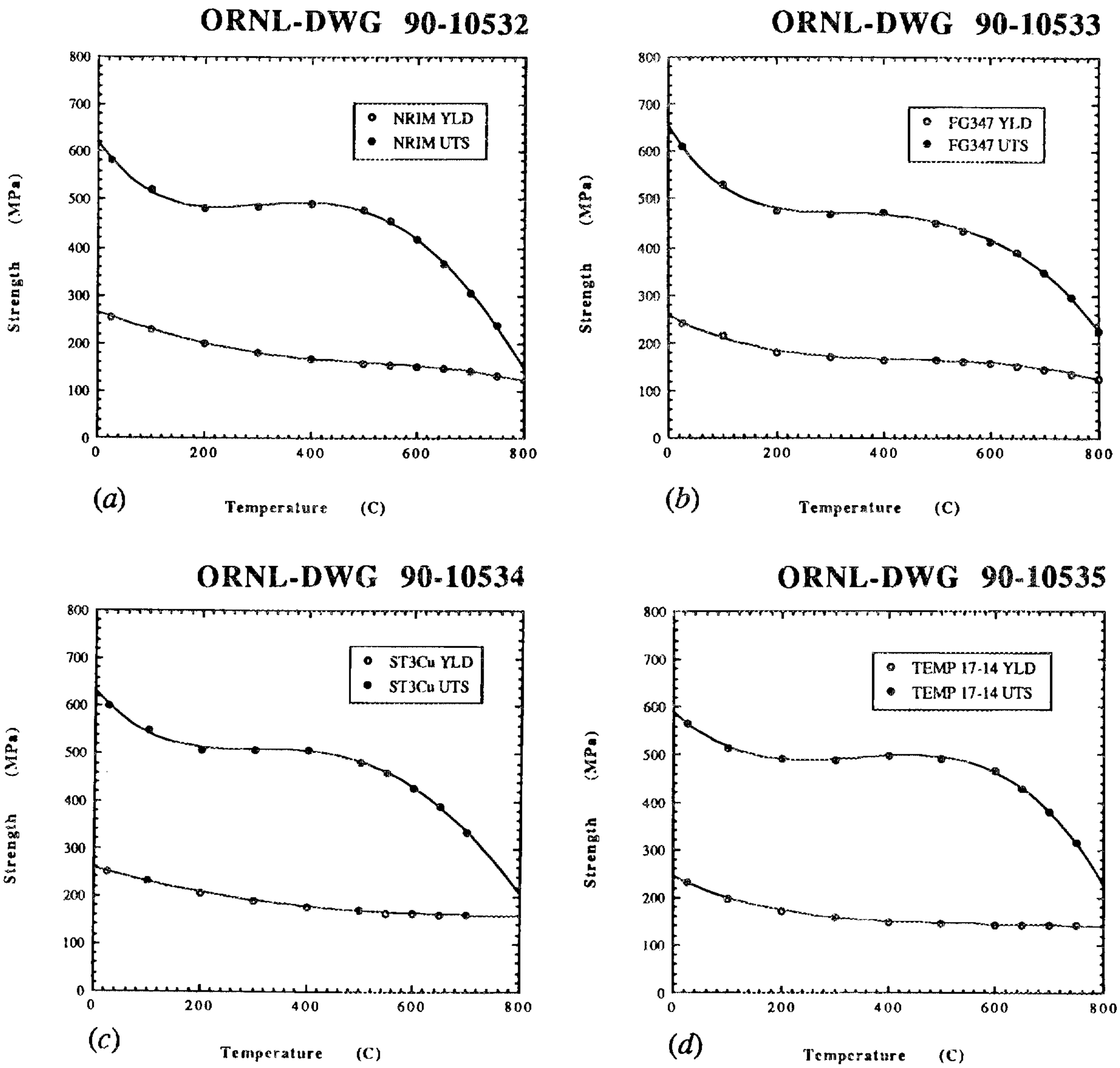


**Fig. 23. Comparision of the yield and tensile strengths vs temperature for four tubing alloys: (*a*) type 316 stainless steel (NRIM 1975), (*b*) fine-grained type 347 stainless steel (Teranishi et al. 1989), (*c*) ST3Cu stainless steel (Sumitomo 1988), and (*d*) TEMPALOY 17-14CuMo stainless steel (Tamura et al. 1987).**

ORNL-DWG 90-10536

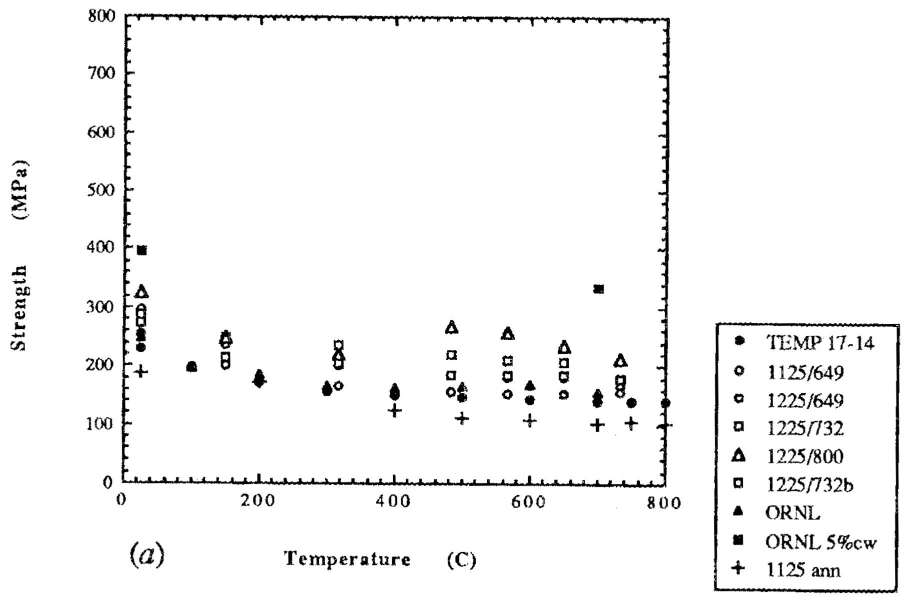


ORNL-DWG 90-10537

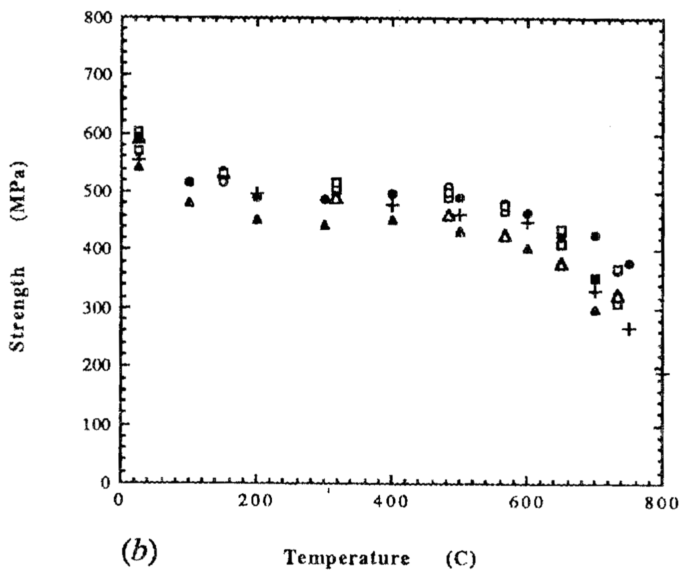


**Fig. 24. Comparison of the strengths for several heats and conditions of 17-14CuMo stainless steel: (*a*) yield strength vs temperature and (*b*) ultimate strength vs temperature.**

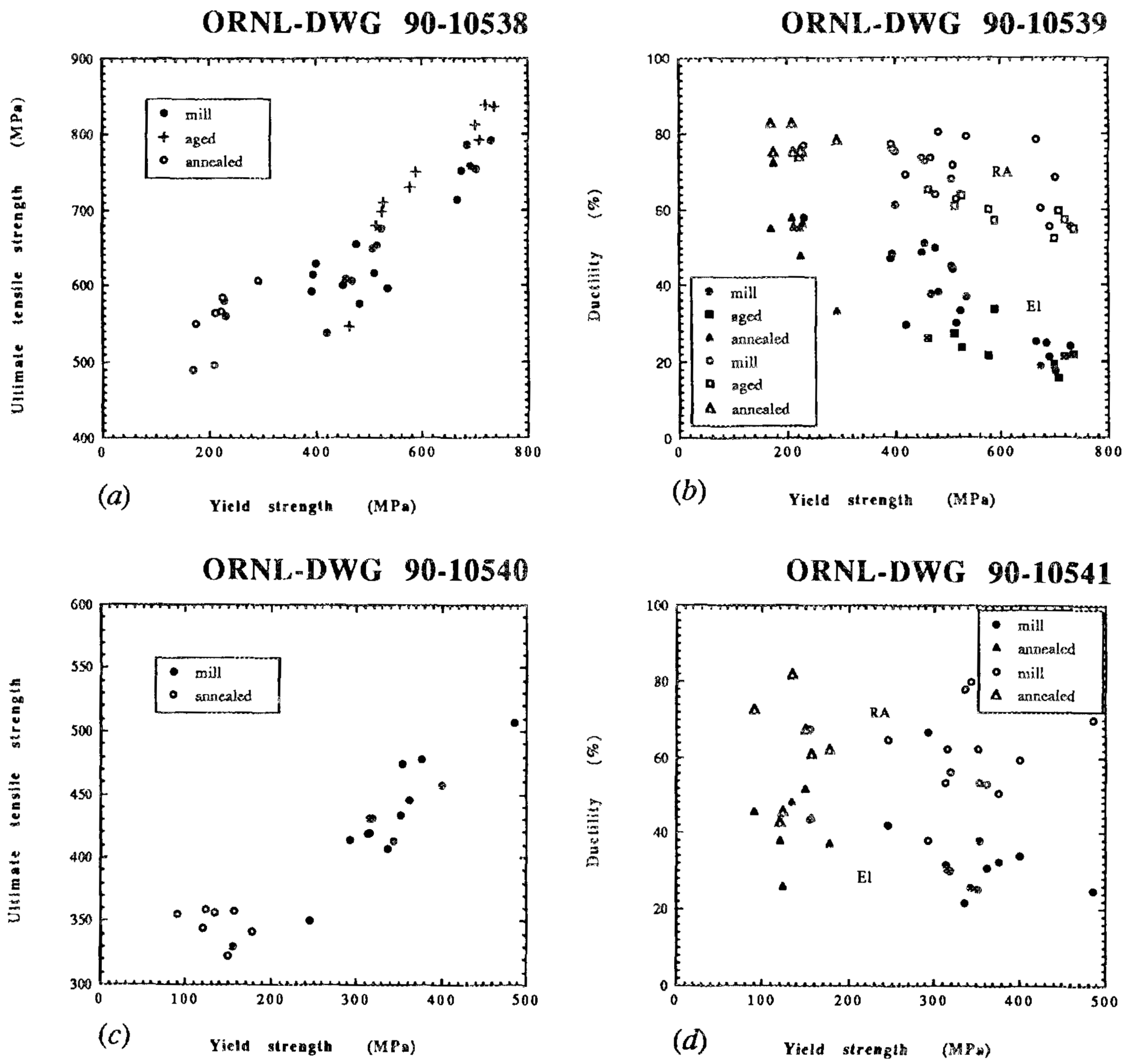


**Fig. 25. Ultimate tensile strength and ductility vs yield strength for HT-UPS alloys: (*a*) UTS at 25°C, (*b*) ductility at 25°C, (*c*) UTS at 700°C, and (*d*) ductility at 700°C.**

revealed excellent reduction of area values at all levels of the yield strength, but elongations decreased below 30% when the yield exceeded 500 MPa. Similar trends were observed in the test data produced at 700°C, with the correspondingly lower yield strength for 700°C, namely 250 MPa. Results from a series of tests over the temperature range 25 to 700°C are shown in Fig. 26 for four alloys. The CE1 alloy was tested in the laboratory-annealed condition (1 h at 1120°C). The yield and ultimate strengths shown in Fig. 26(*a*) were low relative to the commercial and near-commercial alloys discussed earlier. Similarily, data from specimens of

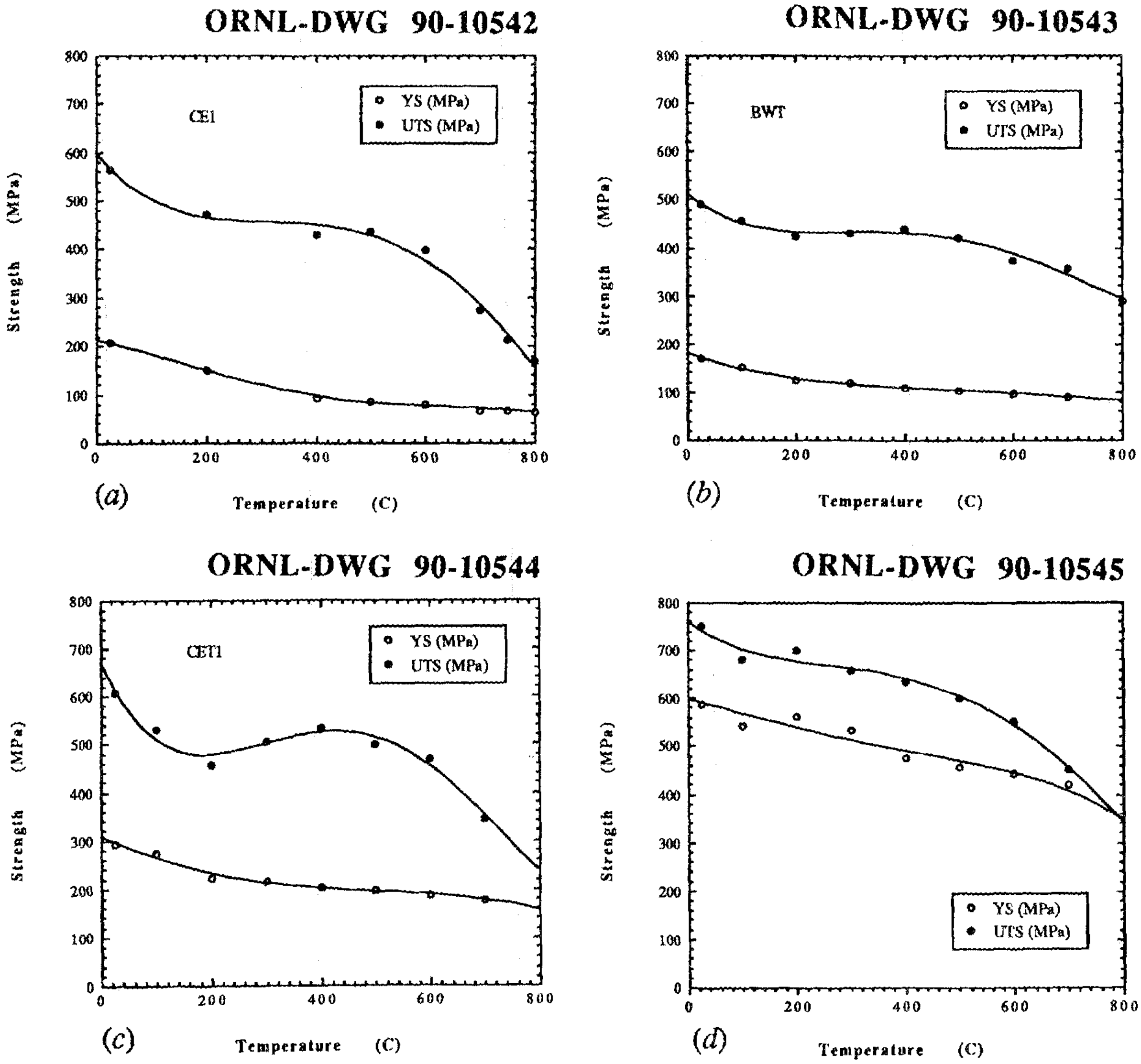


**Fig. 26. Comparision of the yield and tensile strengths vs temperature for HT-UPS alloys: (*a*) hot-rolled CE1, (*b*) as-extruded BWT, (*c*) annealed and rotary straightened CET1, and (*d*) cold-rolled MS5.**

the as-extruded BWT tubing shown in Fig. 26(*b*) revealed strength values in the range 25 to 600°C that were equivalent to or lower than those observed in the CE1 alloy. The CET1 tubing received some work during the rotary straightening process that increased the yield and ultimate strengths to trends similar to those observed in the commercial and near-commercial alloys. This similarity may be seen by comparing Fig. 26(*c*) to the curves in Figs. 23 to 25. The MS5 heat was aged after cold rolling and produced very high yield and ultimate strengths. Data for this alloy are plotted in Fig. 26(*d*) and show that the yield strengths approached the ultimate strengths above 650°C.

The range of yield and ultimate strengths examined in the HT-UPS alloys far exceeded the range for types 316 and 347 stainless steel tubing and piping produced in the United States. Typical yield strengths for 316 stainless steel, for example, are in the range 190 to 340 MPa and type 347 stainless steel varies from 220 to 350 MPa (Smith 1969). Only the HT-UPS products in annealed condition exhibited strengths that consistently fell within these ranges. The mill-annealed alloys were generally stronger. If the higher yield strength is needed to meet the rupture strength Criterion of 60 MPa design stress at 700°C, then the fabrication requirements for the HT-UPS alloys would represent a significant departure from usual boiler tube manufacturing standards.

For purposes of comparison of available data on near-commercial and developmental alloys with the NRIM data base on type 316 stainless steel on a similar time scale, the rupture strengths at 1000 and 10,000 h were interpolated from the NRIM trends and used to construct a curve for log stress versus the Larson-Miller parameter (LMP):

$$\mathrm{LMP} = T\,(20 + \log t_R)\,, \tag{10}$$

where T is temperature in Kelvin and $t_R$ is rupture life in hours. The resulting data are plotted in Fig. 27, where they may be compared with the total NRIM data base, and again in

ORNL-DWG 90-10546

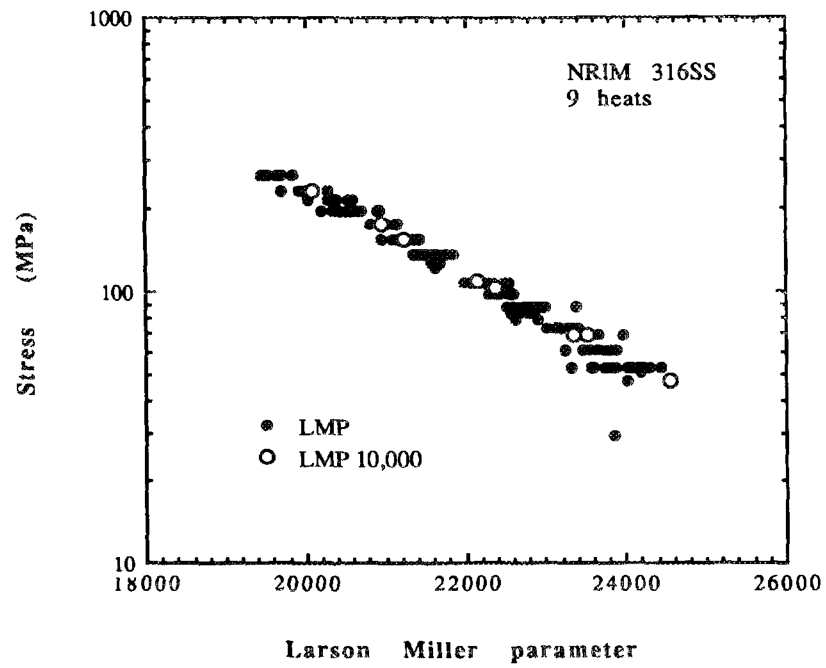


Fig. 27. Log stress vs the Larson-Miller parameter for the rupture life of nine heats of type 316 stainless steel tubing tested by NRIM (1976).

Fig. 28(*a*). The design stress intensity target identified in ORNL-6274 (60 MPa at 700°C) occurs where the LMP is 24330, and a promising alloy should exhibit an average rupture strength that exceeds the target strength by a factor of 1.5. This factor requires that the average strength at 700°C and 100,000 h should meet or exceed 90 MPa.

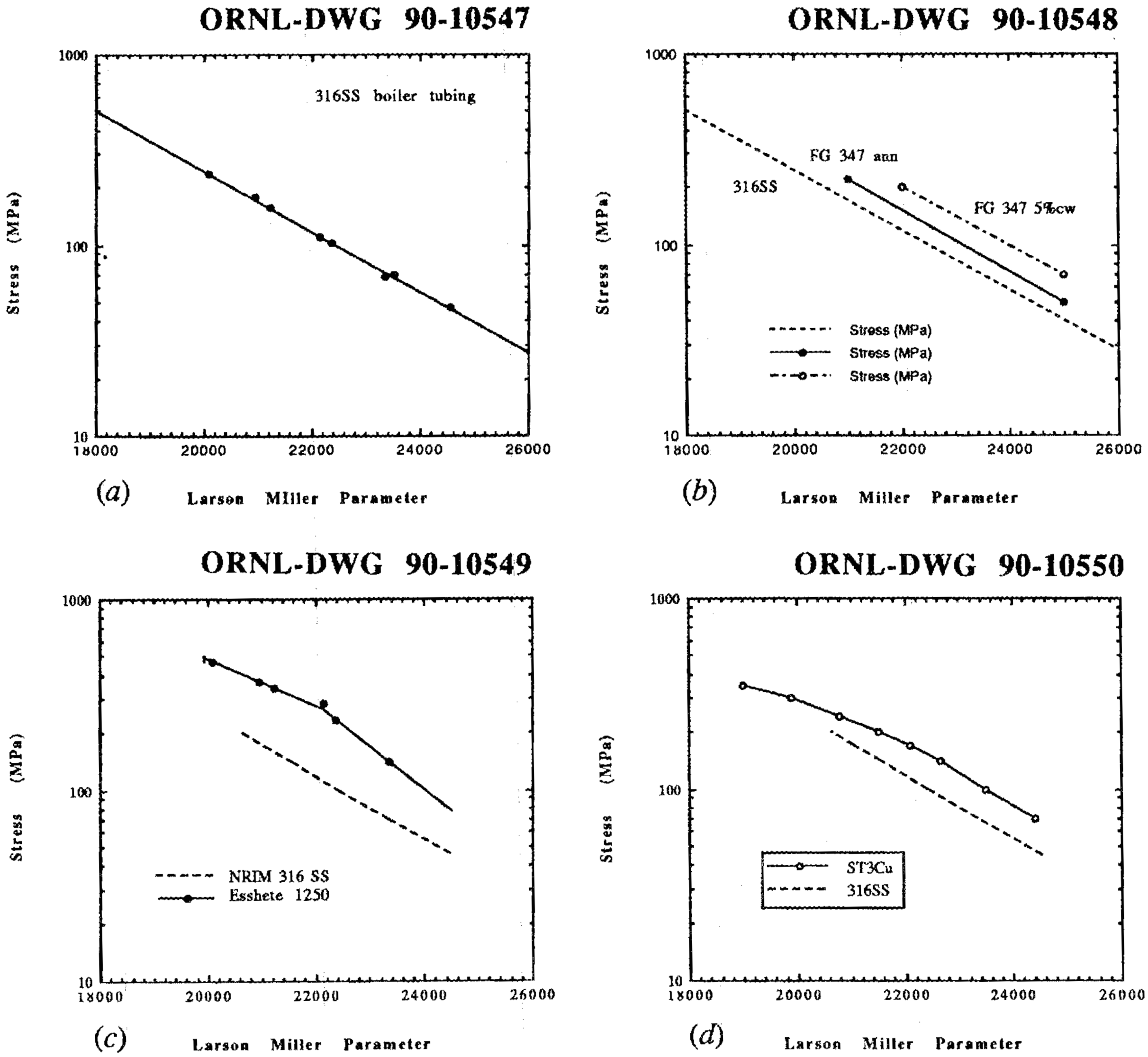


**Fig. 28. Comparison of log stress vs the Larson-Miller parameter for rupture in the time range 1000 to 10,000 h four tubing alloys: (*a*) type 316 stainless steel (NRIM 1976), (*b*) fine-grained type 347 stainless steel (Teranishi et al. 1989), (*c*) Esshete 1250 (Murray et al. 1967), and (*d*) ST3Cu stainless steel (Sumitomo 1988).**

Teranishi et al. (1989) reported creep rate and stress rupture data for nine heats of a fine-grained type 347 stainless steel tested in the temperature range 600 to 800°C for times to 50,000 h. They examined cold working and boiler exposure effects on the tensile and stress rupture life. The performance of the alloy was excellent, and the allowable stress intensity was estimated to be at least 25% higher than standard type 347 stainless steel at 650°C. The intended application for the alloy was in an advanced boiler to produce steam at 566°C and 31 MPa, but the rupture strength at 700°C and 100,000 h was estimated to be in excess of 60 MPa. A log stress versus LMP curve based on the interpolation of their data at 1000 and 10,000 h is provided in Fig. 28(*b*). By cold working the tubing (5 and 10%), the rupture strength was improved; and, by use of the LMP, the strength at 700°C and 100,000 h was estimated to be near 90 MPa. The 90-MPa value meets the average strength needed to produce the 60-MPa design stress.

The creep rupture data base for Esshete 1250 was reviewed by Murray et al. (1967) and included 17 heats and 4 product forms (tubing, bar, piping, and forging). Data extended over the temperature range 600 to 850°C and times to 60,000 h. Various time-temperature correlations were examined, including the LMP, and estimates of the average rupture strength for temperatures to 700°C were made. Again, the average strengths at 1000 and 10,000 h were interpolated from curves provided by Murray et al. (1967) and used to construct the low-stress versus LMP plot shown in Fig. 28(*c*). This plot reveals the excellent strength possessed by Esshete 1250 at lower temperatures. With suitable thermal-mechanical treatment, it may be possible to achieve the target design stress level.

The data base for ST3Cu stainless steel reported by Sumitomo (1988) included seven heats tested over the temperature range 600 to 750°C and times to 10,000 h. Sumitomo analyzed their data using a LMP with an optimized constant of 20.83, rather than 20 as used to construct Fig. 27. The strengths at 1000 and 10,000 h were interpolated from the reported stress rupture curves and used to construct the log stress versus LMP curve shown in Fig. 28(*d*). Here, the parameter constant was 20. The average strength when the LMP was 24330 was estimated to be near 70 MPa. Sumitomo estimated a value near 65 MPa, hence further optimization of ST3Cu stainless steel would be needed to meet the strength Criterion set forth in ORNL-6274.

At times in this report, TEMPALOY 17-14CuMo stainless steel has been treated separately from the standard version of 17-14CuMo stainless steel. In regard to creep rupture strength, it is convenient to include the alloy with the historical data base and the experimental work performed at ORNL. A Larson-Miller plot of all creep rupture data is provided in Fig. 29 in which the test data produced at ORNL are distinguished from the literature data.

ORNL-DWG 90-10551

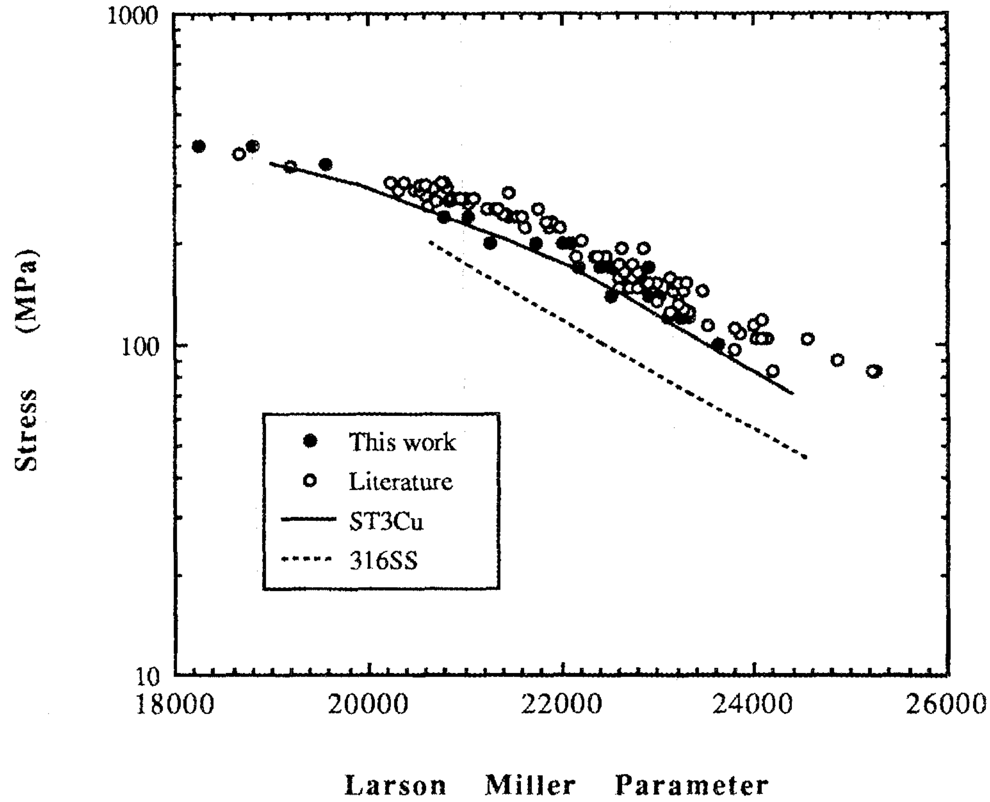


**Fig. 29. Comparison of stress vs the Larson-Miller parameter for rupture of 17-14CuMo stainless steel with the trend lines for type 316 stainless steel and ST3Cu stainless steel.**

The data produced by ORNL indicated lower strength for this material. A single test on a specimen annealed at 1200°C exhibited slightly longer life, and two specimens of the same heat cold rolled to 5% reduction in thickness fell on the upper side of the trend. These test data are included in Appendix C. For comparison, the curves for type 316 stainless steel and ST3Cu stainless steel are included in Fig. 29. Both alloys were weaker than 17-14CuMo stainless steel, although the ST3Cu alloy came very close to matching the strength of the material tested at ORNL. Inspection of the data trend revealed that the strength range for 17-14CuMo stainless steel when the LMP was 24330 was from 70 to 105 MPa. The average was near 90 MPa, which meets the strength Criterion in ORNL-6274. Thus it appears that 17-14CuMo stainless steel deserves consideration when selecting an alloy for the advanced steam cycle.

The creep rupture response of the HT-UPS alloys was devided into two categories — annealed and mill annealed. Annealed was meant to imply that the material was heated to at least 1110°C, held for at least 0.5 h, and air cooled. Mill annealed for purposes of evaluating the creep rupture response implied that the material was annealed at 1150°C or higher and received some degree of warm or cold work after the anneal. Creep rupture tests were performed on several of the HT-UPS alloys in both of the conditions. Testing covered all 14 alloys, a variety of heat treatments, temperatures in the range 600 to 850°C, and times to beyond 35,000 h. Data are reported in Appendix C, but results are too extensive to be fully described in this report. Briefly reviewing the findings in regard to stress rupture, data for the HT-UPS alloys have been plotted as log stress versus LMP in Fig. 30. A significant

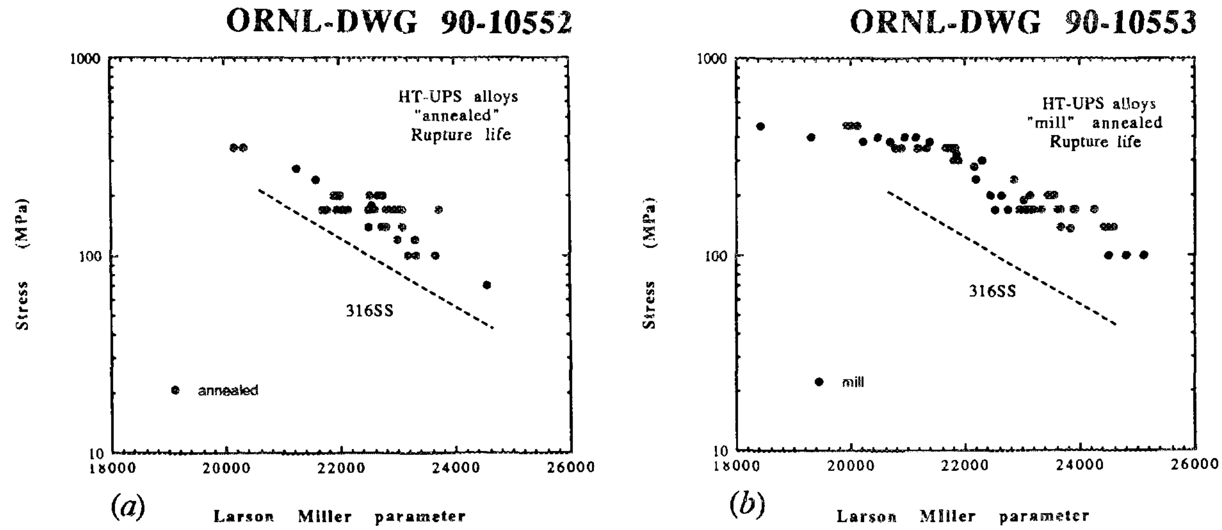


**Fig. 30. Comparison of log stress vs the Larson-Miller parameter for HT-UPS alloys with the trend for type 316 stainless steel: (*a*) annealed material and (*b*) mill-annealed material.**

difference in the strength is apparent in comparing Fig. 30(*a*) for fully annealed materials with Fig. 30(*b*) for the mill annealed-materials. The downward trend for the annealed materials extrapolated to stress around 60 MPa when the LMP was 24330. Hence, the strength of the annealed HT-UPS alloys was similar to some of the near-commercial alloys discussed earlier. The mill-annealed condition produced some extraordinary strengths. Extrapolation of data indicated that strengths in the range 100 to 160 MPa could be achieved. Such values would easily meet the rupture strength Criterion in ORNL-6274.

Much of the scatter in the log stress versus LMP curves for the annealed alloys may be attributed to the limitations of the LMP in correlating the time-temperature behavior of alloys that undergo strengthening due to the precipitation of carbides during service. In particular, at temperatures below 700°C, rupture data were often produced at stresses that exceeded the yield strength, as mentioned earlier in this report, and the strain associated with this deformation promotes the precipitation of carbides, especially MC, which cause strengthening that would not be present at stresses closer to the design levels. Fortunately, below 700°C, the allowable design stress may be controlled by the tensile strength, which provides an extra margin of safety when such alloys are used.

The considerations in determining the design stress allowables for high temperatures require knowledge of the creep rate and preferably the whole creep curve. Except for type 316 stainless steel, very few data were available for the alloys listed in Table 1. Teranishi et al. (1989) reported creep rate data for one heat of the fine-grained 347 stainless steel that indicated that the stress for the 0.01%/1000 h was greater than 67% of the average stress to produce creep in 100,000 h. A similar approach was used by Sumitomo in working with data for ST3Cu stainless steel (1988). Murray et al. (1967) reported an analysis for Esshete 1250 that included the times to specific creep strains in the range 0.1 to 1%. Again, it appeared that 67% of the rupture strength at 100,000 h, rather than the stress for the 0.01%/1000 h creep rate, was the controllingCriterion in setting allowable stresses in the creep range.

Chapman and Lorentz (1960) included creep rate data in their analysis of 17-14CuMo stainless steel, and additional information was produced by Armco (1950). Some information on actual creep curves and relaxation rates was also available. The experiments at ORNL on 17-14CuMo stainless steel included the measurement of the entire creep curve, hence the times to various creep strains and the minimum creep rates (mcr) were determined for nearly every test. Some of this information has been included in Appendix C. The shape of the creep curve for 17-14CuMo stainless steel was discussed by Swindeman and Bolling (1990). They observed very little primary creep. Further, the time to 1% creep was a high fraction of the rupture life. This trend implied that the rupture life, rather than the mcr or the time to 1% creep, would control the allowable design stresses at high temperatures. Some data for the heat of 17-14CuMo stainless steel are provided in Fig. 31. These are plots of the stress against the value of the LMP for the minimum creep rate [Fig. 31(*a*)] and the time to 1% creep [Fig. 31(*b*)]. To calculate the LMP for these indices, the time to 1% creep or the reciprocal mcr data were inserted into Eq. (10). The wide scatter in the data plotted in Fig. 31 was an indication that the LMP was not a very good correlating parameter for either damage measurement. The time to 1% creep strain was better behaved than the mcr, however, and the

ORNL-DWG 90-10554

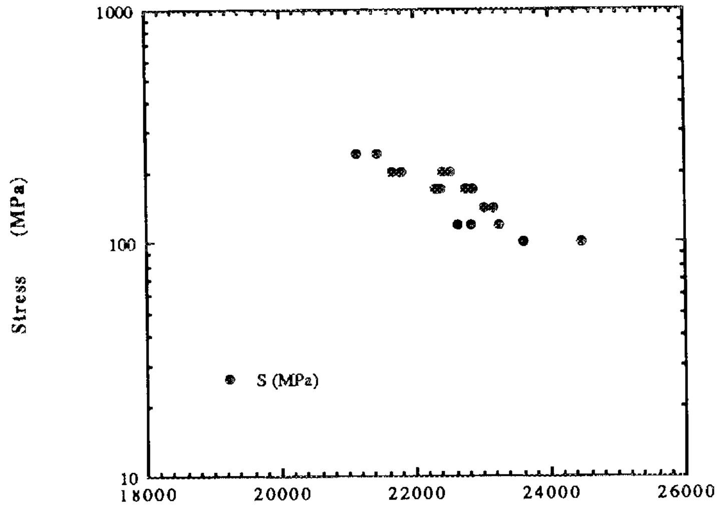


(*a*) Larson Miller Parameter

ORNL-DWG 90-10555

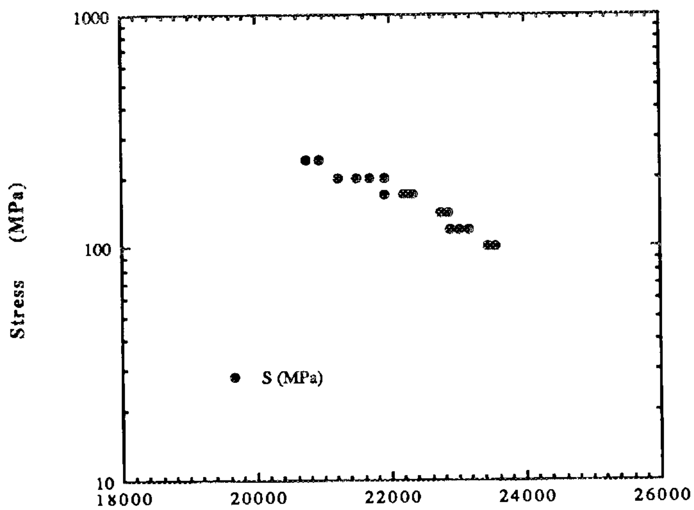


(*b*) Larson Miller Parameter

**Fig. 31. Log stress vs the Larson-Miller parameter for (*a*) minimum creep rate and (*b*) time to 1% creep strain for 17-14CuMo stainless steel.**

trend indicated that the stress to produce 1% creep was only slightly less than that to produce rupture. Since the Code uses 100% of the average stress for 1% creep in 100,000 h and only 67% of the stress to produce rupture in a similar time, it appeared that the stress associated with the rupture life would be controlling.

A very large body of information has been amassed on the creep behavior of the HT-UPS alloys, but the subject will be only briefly discussed here. Some typical curves for the CE3 alloy are shown in Fig. 32 for low stress tests at 700°C extending to beyond 30,000 h.

ORNL-DWG 90-10556

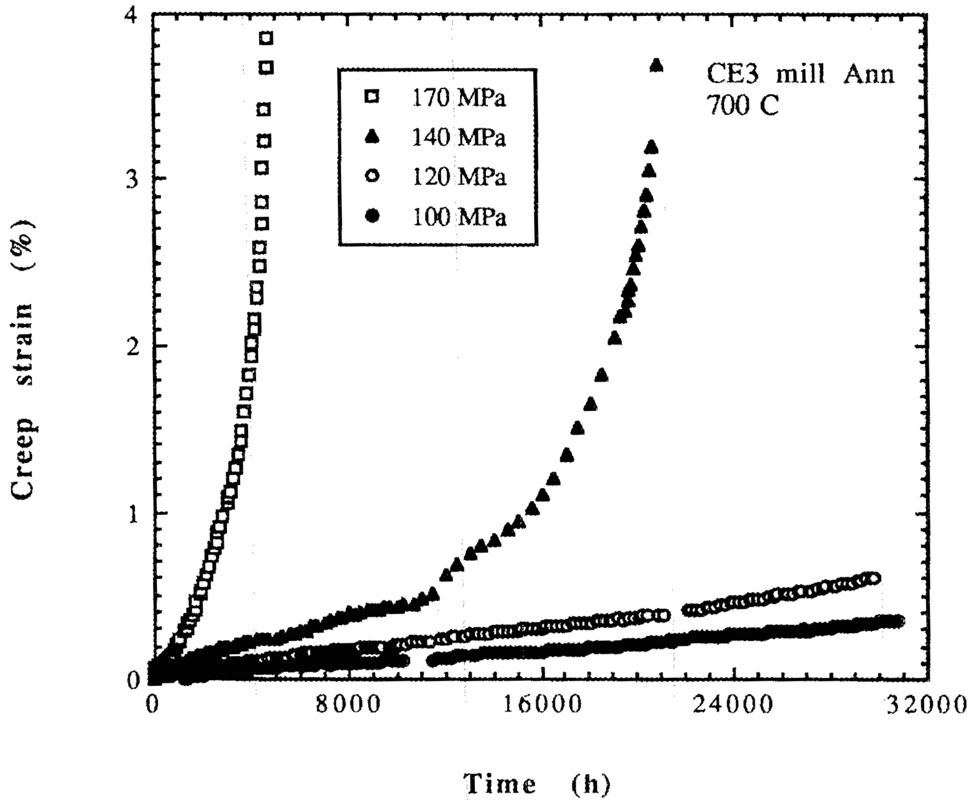


**Fig. 32. Low stress creep curves for HT-UPS alloy CE3 at 700°C.**

The lack of significant primary creep and the general linearity of the curves suggested that very few microstructural modifications occur in the alloy over long periods of time at low stresses and high temperatures. This observation was consistent with the analytical work performed by Todd and Ren (1989), Maziasz (1989), and Carolan et al. (1989) on the HT-UPS alloys. However, it was also clear that the strains prior to the initiation of tertiary creep are very small, typically 1% for the mill-annealed condition. As for the case of 17-14CuMo stainless steel, such trends indicated the stress to rupture, rather than stress for a mcr of 0.01%/1000 h or stress for 1% creep in 100,000 h, would be the governing property. Curves for the log stress versus the LMP minimum creep rate and time to 1% creep data are shown in Fig. 33 for both the annealed and mill-annealed HT-UPS alloys. Here it may be seen that the trends for the mill-annealed material [Figs. 33(*b*) and 33(*d*)] were somewhat better defined than the trends for the annealed material [Figs. 33(*a*) and 33(*c*)]. This was partially due to a larger number of tests that were performed on the mill-annealed materials at low stresses. The trends for the annealed materials were so poorly defined that it was difficult to draw any meaningful conclusions. The trends for the mill-annealed materials clearly indicated that the strengths derived from the deformation data would be comparable to those derived from the rupture data plotted in Fig. 30. Again, with theCriterion that the design stress be based on 100% of the average strength derived from deformation and only 67% of the average strength derived from rupture testing, it was clear that rupture strength would be the controlling strength. It is also clear from Figs. 30 and 33 that the HT-UPS alloys have more than adequate strength potential to meet the target design stress.

The data produced on the HT-UPS were not intended to be an engineering data base on which to determine design stress allowables. Rather, the data were intended to guide in the selection of suitable fabrication and heat-treating schedules that would ensure that the target design stress could be reached. To a great extent, the estimation of the design stress depends on the selection of the methods by which the data are extrapolated, and many elegant procedures have been developed to accomplish this task. It is well beyond the scope of this report to delve into this sophisticated technology area. Some work on modeling of the mcr data was reported by Black et al. (1989), but the major effort has yet to be undertaken. Before this is done, testing must be completed on tubing products fabricated to achieve tensile strength properties that fall near the upper limit of the 300 series stainless steel tubing. Most likely, the optimum tubing condition would correspond to a room-temperature yield strength in the range 350 to 450 MPa.

In summary, further optimization and analysis of the near-commercial and developmental alloys identified in Table 1 are required before it can be certain that the target design stress of 60 MPa at 700°C can be achieved in fabricated boiler tubing alloys. The 17-14CuMo, ST3Cu, and HT-UPS alloys show excellent potential.

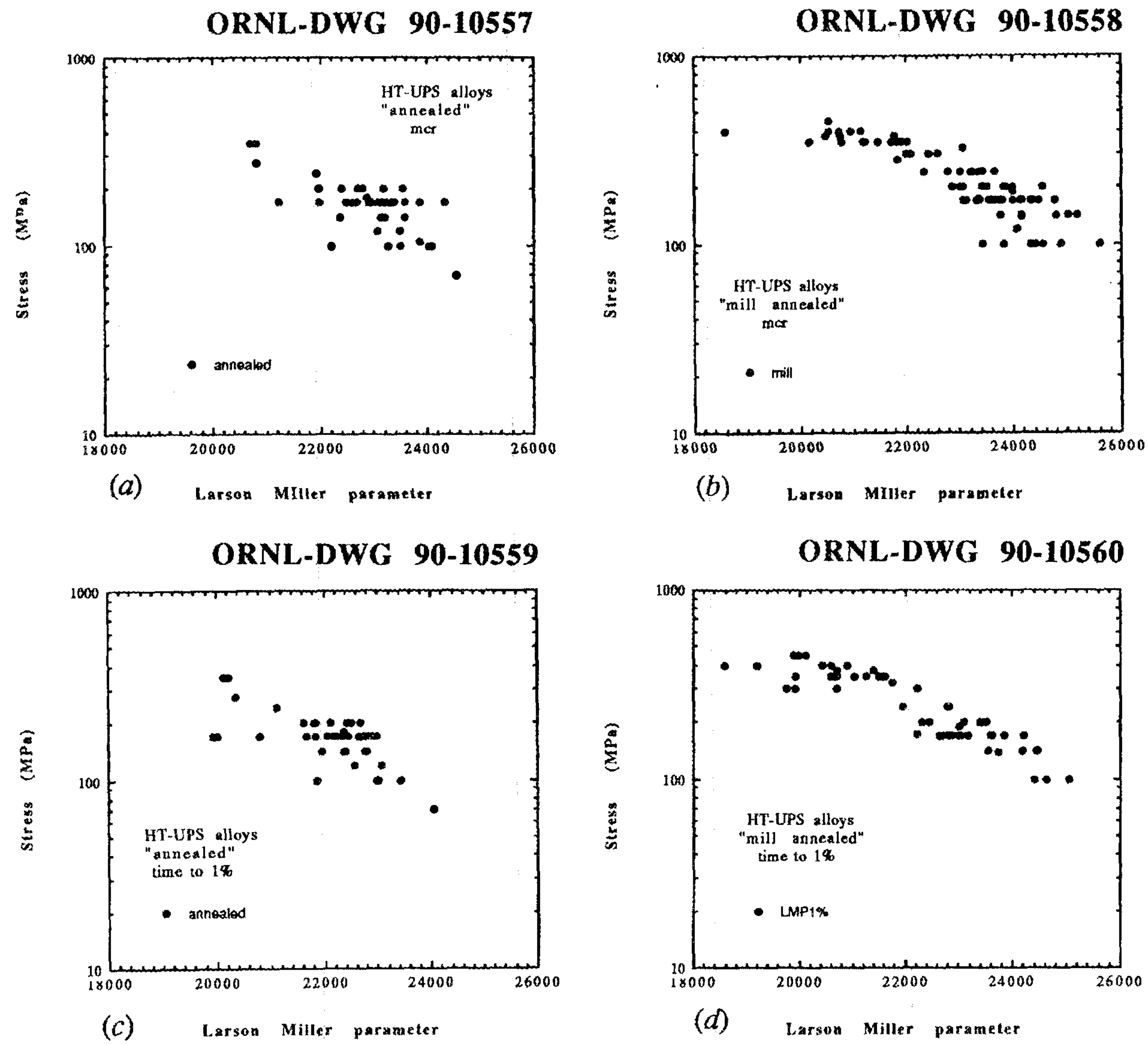


**Fig. 33. Log stress vs the Larson-Miller parameter for minimum creep rate (mcr) and time to 1% creep strain for HT-UPS alloys: (*a*) and (*b*) for annealed material, (*c*) and (*d*) for mill-annealed material.**

<u>II.B. Creep rupture ductilities will be such as to produce at least 2% circumferential strain after 100,000 h under pressurized tube rupture conditions.</u>

Many indices have been proposed which correlate creep rupture ductilities measured under contant-load, isothermal, uniaxial stress conditions with performance under more realistic loading conditions. Twenty-one of these indices were reviewed by Manjoine (1975), and the triaxiality factor (TF) proposed by Davis and Connelly (1959) emerged as a useful index for evaluating ductility requirements for pressurized tubing. Here the TF is defined as the ratio of the normal stress to the shear stress on the octahedral plane, normalized to unity for simple tension:

$$TF = \sqrt{2}\,(\sigma_1 + \sigma_2 + \sigma_3) \,/\, [(\sigma_1 - \sigma_2)^2 + (\sigma_2 - \sigma_3)^2 + (\sigma_3 - \sigma_1)^2]^{1/2} \ , \qquad (11)$$

where the principal stresses are $\sigma_1$, $\sigma_2$, and $\sigma_3$. The strain measured in the stress rupture experiment is then plotted against the TF to estimate ductility. Manjoine provided data for type 304 stainless steel, but very little information is available for the alloys listed in Table 1, with the exception of type 316 stainless steel.

The performance of type 316 stainless steel was reviewed by Marshall (1984), who showed data revealing a very wide variation in creep rupture ductilities from heat to heat. The elongation and reduction of area data report by NRIM (1978) also revealed a wide range of ductilities (1 to 40%) after long times at 700°C. This trend is shown in Figs. 34(*a*) and 34(*b*). Experience with low ductility failures of type 316 stainless steel piping in the Eddystone Unit #1 plant was discussed by Masuyama et al. (1987) and Ellis et al. (1988). They found that the steels that were balanced toward the higher $Cr_{eq}$(B) were more prone to low ductility failures than those with higher $Ni_{eq}$(B). Compositions that minimized hot cracking tendencies in welding tended to promote low ductility cracking in service. The issue is yet to be resolved, but it seems as if the intermetallic embrittling phases are more likely in the higher chromium alloys.

Of the steels listed in Table 1, Teranishi et al. (1989) provided data that revealed excellent uniaxial ductilities (10 to 40% elongations) in fine-grained type 347 stainless steel specimens which ruptured in times to 10,000 h and temperatures in the range 600 to 750°C. They also performed pressurized tube stress-rupture tests, but did not report ductilities. Murray et al. (1967) provided elongation data for Esshete 1250 that showed values exceeding 10% strain for times in the range 100 to 30,000 h and temperatures from 600 to 700°C. Pressurized tube stress rupture testing of Esshete 1250 was reported by Mantle and Gemmill (1967), but no data on ductilities were provided. Similarly, testing of tubes of 17-14CuMo stainless steel was undertaken by Chapman and Lorentz (1960). They reported good ductility in the ruptured tubes, but provided no numerical data. The uniaxial creep rupture elongations were in the range 3 to 21% and reductions of area were from 6 to 40%. Higher elongations were observed in TEMPALOY 17-14CuMo stainless steel by Tamura et al. (1987). Information of the creep rupture ductility of type 17-14CuMo stainless steel, including the

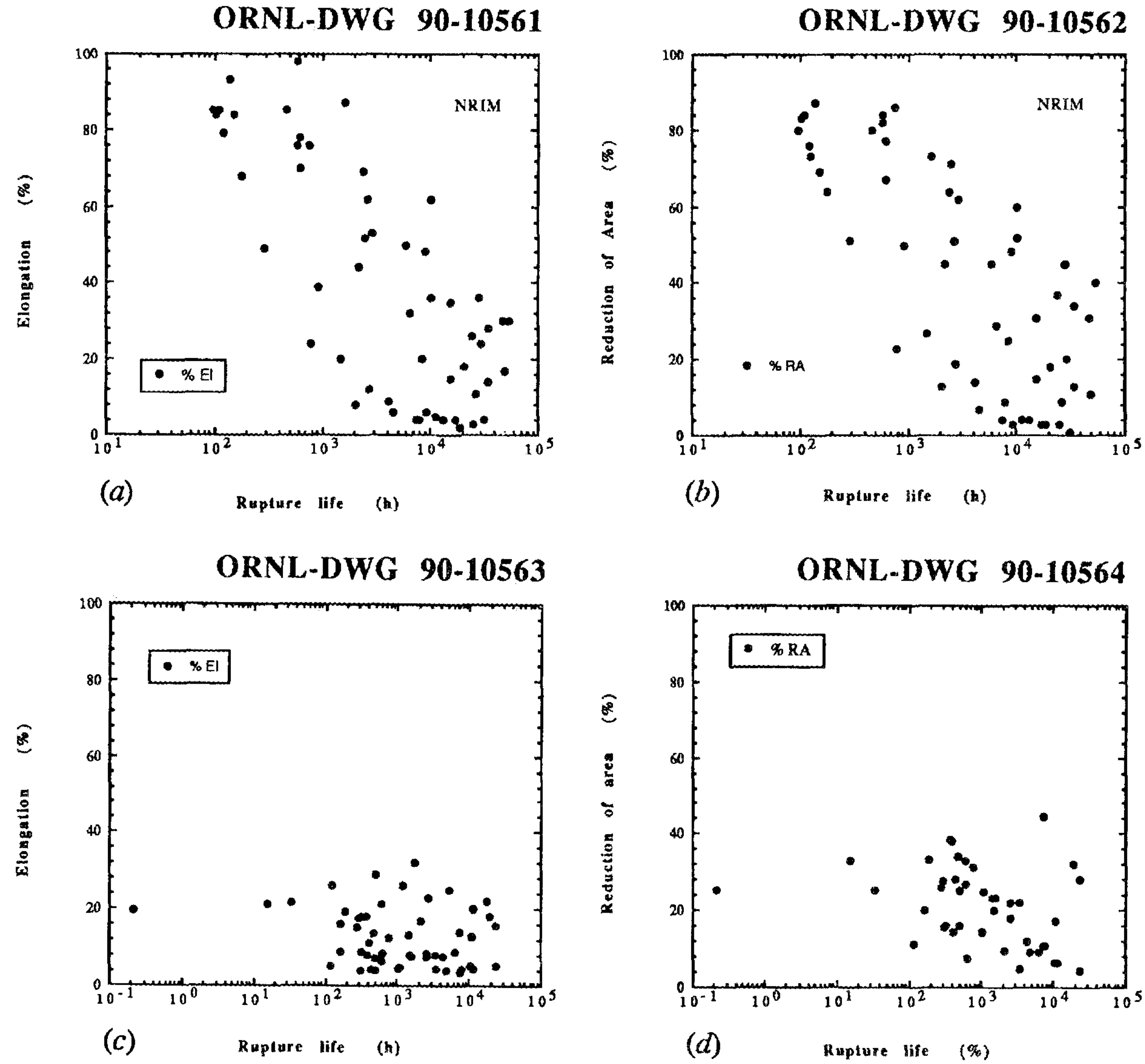


**Fig. 34. Elongation and reduction of area vs log rupture life for two tubing alloys: (*a*) and (*b*) for type 316 stainless steel at 700°C, (*c*) and (*d*) for 17-14CuMo stainless steel at temperatures in the range 600 to 815°C.**

ORNL work, is summarized in Figs. 34(*c*) and 34(*d*). Ductility in this alloy was marginal, with both elongation and reduction of area data often falling below 10%. This may be due to the tendency for this alloy to form Laves phase.

Elongation and reduction of area data for the HT-UPS alloys are plotted in Figs. 35(*a*) and 35(*b*). For the most part, excellent ductilities were observed for times to beyond 10,000 h at all temperatures. A few test data corresponding to the more heavily cold-rolled

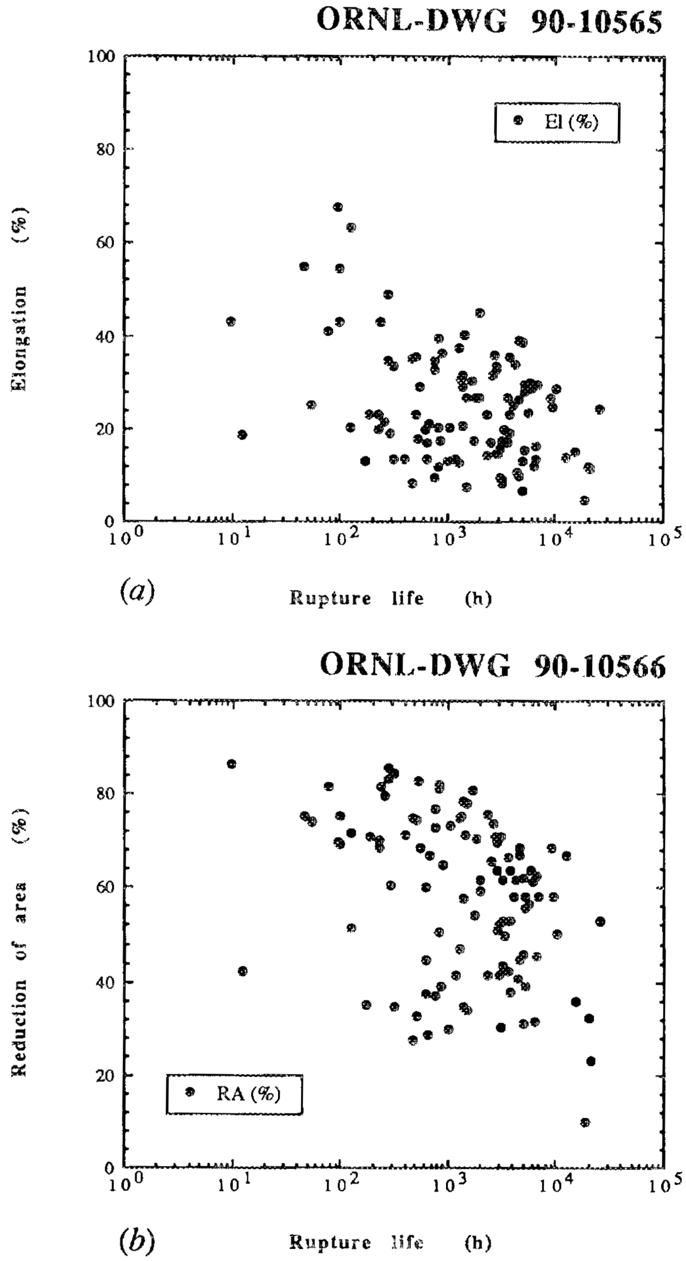


**Fig. 35. Ductility vs log rupture life for HT-UPS alloys: (*a*) elongation data and (*b*) reduction of area data.**

MS alloy series fell below 10%, and one specimen of the AX8 alloy exhibited an elongation of only 6% and a reduction of area approaching 10% in 18,745 h. Knowing the long-time ductility for the HT-UPS alloys, an estimate may be made of the strain at rupture in a pressurized tube from the curves developed by Manjoine (1975) from type 304 stainless steel data, using the TF defined in Eq. (11) above. The ratio of ductility in a pressurized tube to the uniaxial ductility for a creep rate near 0.01%/1000 h would be near 0.7. Assuming that the trend for elongation versus log time in Fig. 34(*a*) extrapolates to 4% in 100,000 h, the expected ductility in a pressurized tube would be around 3%. This exceeds the specified 2% strain.

Some concerns remain in regard to rupture ductilities under pressurized stress conditions because of the unusual failure mode exhibited by the HT-UPS alloys. As may be seen in the creep curves shown earlier, the alloys often experienced little or no creep for long times. Over a short time span tertiary creep occurred and the specimens necked down and failed by a plastic instability mechanism. This necking and instability appeared to be brought about by a combination of factors. First, oxide cracks developed on grain boundaries, as shown in Fig. 36(*a*), and worked inward both on the grain boundaries and through the grains. Possibly, the increase in stress associated with the local reduction in load-bearing area promoted recrystallization on grain boundaries and within the matrix. The MC was then dissolved into the dislocation-free recrystalized regions, as shown in Fig. 37 for a specimen that failed in 18,000 h. Both transgranular and intergranular cracks grew and produced the relatively high reduction of area creep rupture failure as shown in Fig. 36(*b*).

To better examine the stability of the HT-UPS alloys under high-temperature creep, four creep crack growth tests were performed on 17-14CuMo stainless steel and the AX5 alloy at 700°C, and some results are provided in Table 6. The specimens were of a compact tension (CT) design with thickness of 12.7 mm and width of 25.4 mm. They were chevron notched, precracked by fatigue, side grooved 20% of the thickness, and tested in a dead-load lever-arm creep machine. Crack growth was monitored by a dc potential drop (PD) technique. Current leads and voltage pickup leads for the tests were located at positions described by McGowan and Nanstad (1984). The first 17-14CuMo stainless steel specimen failed on loading to 4.26 kN. The stress intensity factor, K, calculated from the equation in ASTM E 399-83 Appendix A4, was estimated to be less than 44 MPa-$m^{1/2}$. The second 17-14CuMo stainless steel specimen was loaded to 2.66 kN (K = 25 MPa-$m^{1/2}$) and lasted 122 h. Posttest examination revealed that the crack grew from an a/w of 0.6 to 0.7, whereupon a gross overload failure occurred. The value of K, calculated from the load and dimensions obtained from the rupture surface, was near 42 MPa-$m^{1/2}$. Examination of the rupture surface of the specimen revealed intergranular creep propagation to the point of overload, then transgranular tearing. The potential drop and load line displacement data were examined on the basis of equations for C* and $C_t$ proposed by Saxena and Han (1987) and $C_j$ proposed by Jaske and Begley (1978), but the results were inconclusive because of uncertainties in the interpretation of the data. For example, the rupture surface revealed creep

Y211526

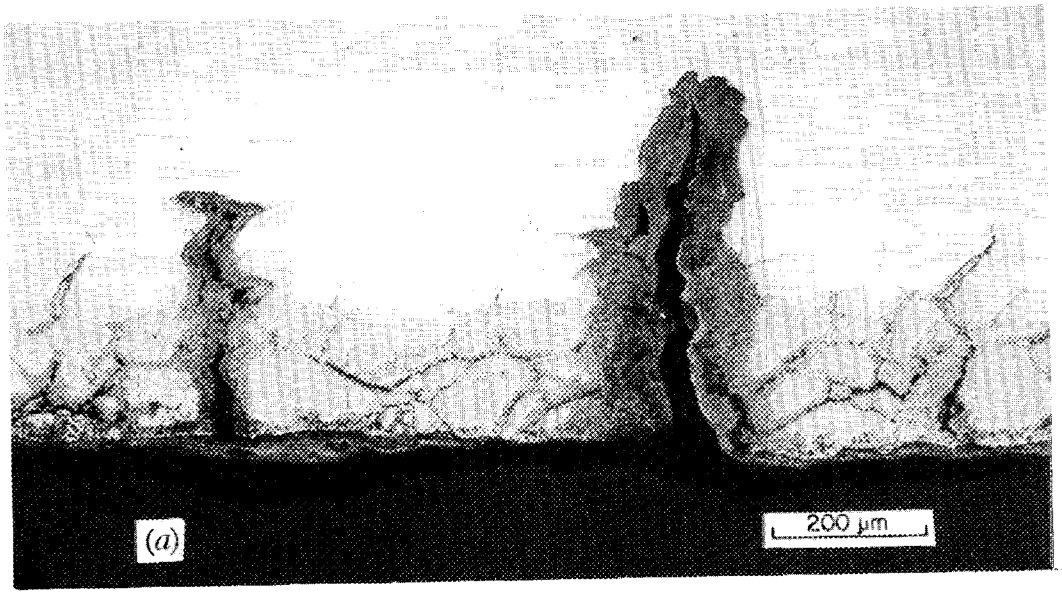


Y211520

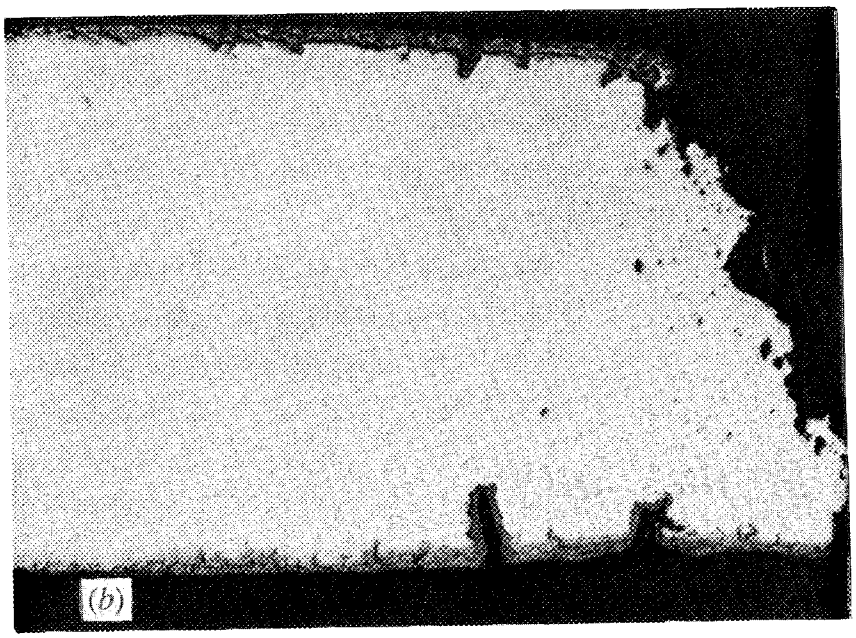


**Fig. 36. Photomicrographs of HT-UPS alloy CE3 that ruptured after 21,204 h at 700°C and 140 MPa: (*a*) oxide penetration along grain boundaries and (*b*) necking in the rupture area.**

YE-14156

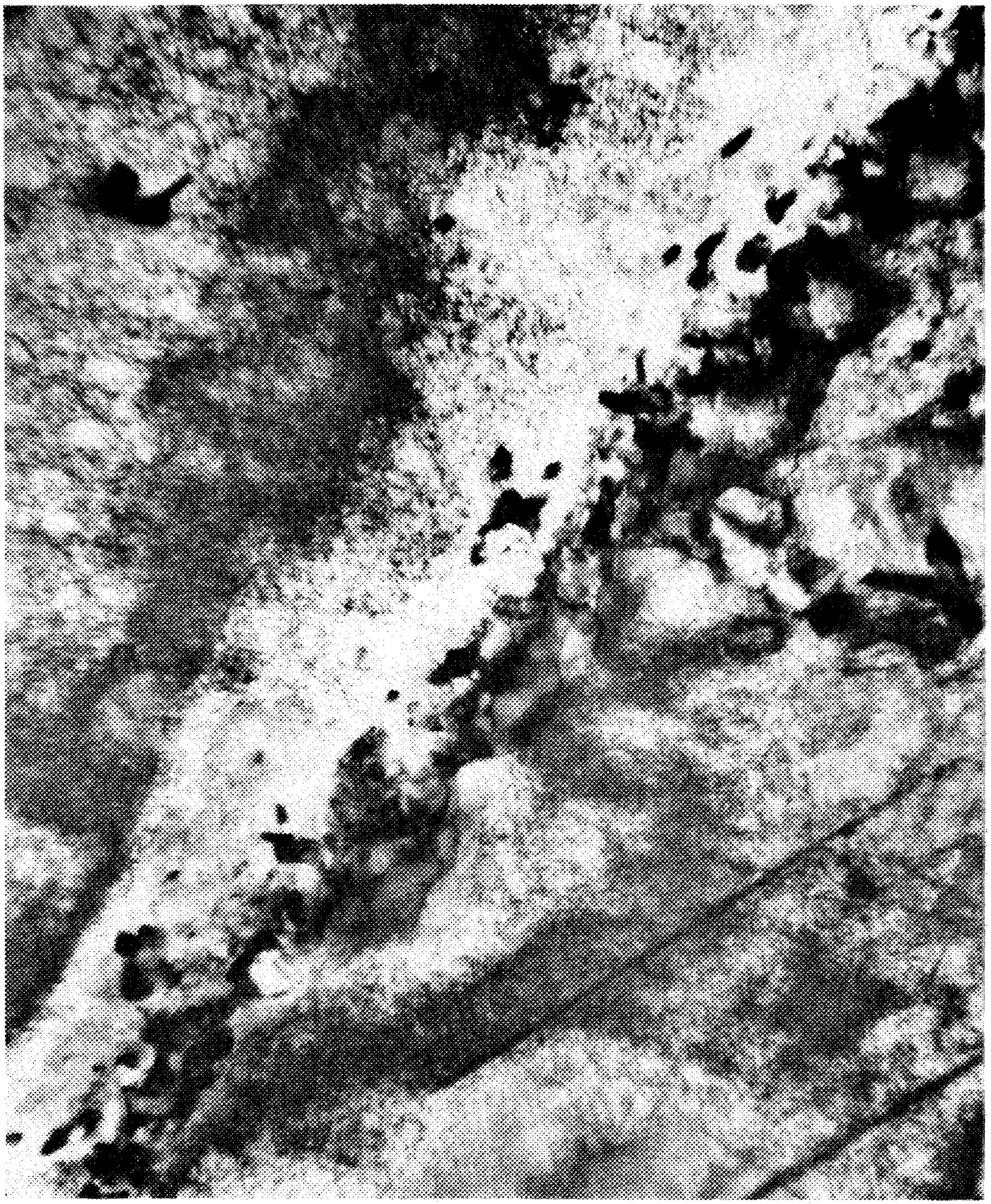

Fig. 37. Transmission electron micrograph of HT-UPS alloy AX8 that ruptured after 18,745 h at 700°C and 170 MPa. Recrystallization along the grain boundary was evident.

Table 6. Summary of creep crack growth tests

| Test | Specimen | Material | Time (h) | Load (kN) | K (MPa$\sqrt{m}$) | Comment |
|---|---|---|---|---|---|---|
| 25490 | CCG1 | CuMo SS | 0 | 4.26 | 44 | K estimated from fracture surface |
| 25600 | CCG2 | CuMo SS | 0 | 2.66 | 25 | |
| | | | 122 | 2.66 | 42 | K estimated from fracture surface |
| 25494 | CCG7 | AX5 mill | 0 | 2.66 | 25 | K estimated from fracture surface |
| | | | 423 | 3.19 | | |
| | | | 590 | 3.72 | | |
| | | | 758 | 4.26 | | |
| | | | 930 | 4.79 | | |
| | | | 1099 | 5.32 | | |
| | | | 1373 | 5.32 | 74 | K estimated from fracture surface |
| 25606 | CCG6 | AX5 ann | 0 | 2.12 | 17 | K estimated from sectioning |
| | | | 1844 | 2.66 | | |
| | | | 2490 | 2.66 | 22 | K estimated from sectioning |

crack growth near 2.5 mm, while the potential drop measurements indicated only 0.8 mm. In the same time period the load line displacement was near 0.18 mm. Use of the PD and load line data without any corrections to resolve the inconsistencies produced C* data that deviated by an order of magnitude from the trend observed by Marriott and Stubbins (1988) on center-cracked-tension (CCT) specimens machined from the same heat of 17-14CuMo stainless steel.

A creep crack growth specimen of the AX5 alloy was loaded at 700°C to 2.66 kN, which produced a starting stress intensity factor near 25 MPa-m$^{1/2}$. After 423 h, with no apparent load line displacement, the load was increased to 3.19 kN. Again, nothing happened in a week, so the load was increased to 3.72 kN. Eventually, after increments to 4.26 and 4.79 kN and 1099 h in test, significant load line displacement was observed when the load was increased to 5.32 kN. The specimen failed after an additional 274 h. Examination of the rupture surface revealed a ductile tearing failure mode starting near the fatigue crack tip and progressing to the front where overload failure occurred, an a/w distance of approximately 0.1. The stress intensity was estimated to be near 74 MPa-m$^{1/2}$ when the overload condition was reached. Assuming little or no crack growth at the lower loads, the crack grew from a value for a/w near 0.6 at 1099 h to 0.7 at 1373 h as the stress intensity increased from 50 to 74 MPa-m$^{1/2}$. The evidence suggested that the AX5 alloy had approximately 80% higher resistance to creep crack growth than 17-14CuMo stainless steel at 700°C. A longer time test was performed on an annealed AX5 specimen at 700°C. Here, the starting stress intensity was equal to, or greater than, 17 MPa-m$^{1/2}$. After 1844 h the load was increased to produce an estimated K near 22 MPa-m$^{1/2}$. Very little load line displacement was observed for an additional 646 h. The specimen was removed from testing and cross sectioned. A photomicrograph of the crack tip region is provided in Fig. 38. This revealed a blunt crack with some oxide penetration along grain boundaries at angles to the crack growth direction but no evidence of creep crack growth or cavitation at the crack tip.

Y209857

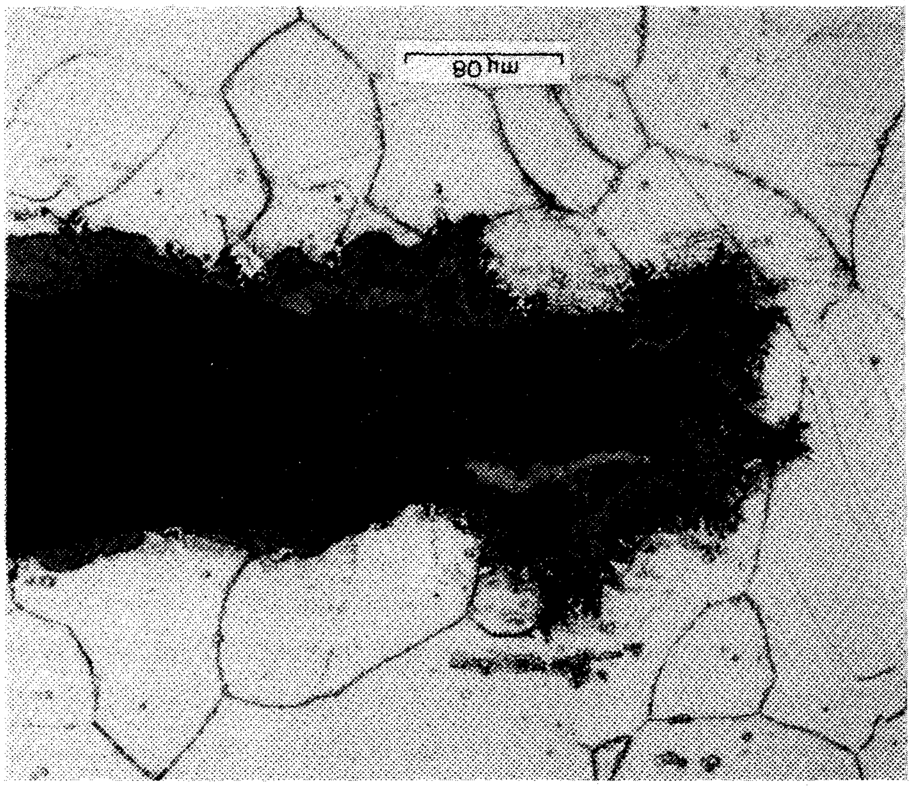


**Fig. 38. Photmicrograph of the crack tip of HT-UPS alloy AX5 that sustained 1844 h at K = 17 MPa-m$^{1/2}$ and 646 h at K = 22 MPa-m$^{1/2}$ with no apparent crack growth. Plasticity-induced crack blunting and oxide penetration along grain boundaries are evident.**

In summary, the alloys identified in Table 1 appear to have adequate ductility to meet Criterion III-B. However, the low creep ductilities reported in some heats of type 316 stainless steel and 17-14CuMo stainless steel suggest that these alloys may be marginal. There is some evidence that the creep crack growth resistance of the HT-UPS alloys is unusually high, and further work to explore this attribute would be of value.

III-C. Overtemperature excursions of 50°C for up to 1% of life will not degrade long-time strength by more than 10%.

High temperature heat recovery systems generally experience overtemperature transients with various degrees of severity. Very little testing has been performed to assess the ability of alloys to resist such transients without undergoing damage. One significant symposium was held by ASTM (1954) that collected work on cyclic heating and stressing of materials, and the trends revealed in the papers on austenitic stainless steels indicated that the linear damage summation proposed by Robinson (1952) was satisfactory in correlating data. Here, the creep damage fraction, $d_{ci}$, during any transient to temperature $T_i$ is calculated by

$$d_{ci} = \delta t_i / t_{ri} \ , \tag{12}$$

where $\delta t_i$ is the time at $T_i$, and $t_{ri}$ is the time to rupture at that temperature and stress. When the sum of all damage fractions reaches unity, failure occurs:

$$\Sigma\, d_{ci} = 1.0 \ . \tag{13}$$

Of the alloys listed in Table 1, only type 316 stainless steel has been extensively examined, and a summary of work performed in connection with the failures in the Eddystone Unit #1 main steam line piping has been provided by Masuyama et al. (1987). They found Robinson's rule to be a reasonable estimate of remaining life. Toft and Broom (1963) performed temperature cycling creep tests on both type 316 stainless steel and Esshete 1250 at 600°C, but found no significant acceleration of damage. Criterion III-C assumes the validity of linear damage, but allows a significant extent of damage caused by transients to be accumulated. Examining the general trend of the LMP curves plotted earlier and taking 90% of the stress for any LMP value, the reduced LMP value and the original LMP value for that stress may be used to estimate the percentage of life corresponding to a 10% loss of strength. For the HT-UPS alloys, this procedure estimated an allowable 50% loss in life at stresses in the range of the LMP curve. In other words, if the damage fraction summation for tests involving temperature changes exceeds 0.5, Criterion III-C can be satisfied for a given alloy.

A few tests were undertaken on some of the HT-UPS alloys to examine damage under temperature change conditions, but the lack of a complete data base to estimate $t_{ri}$ presented a handicap. Data are summarized in Table 7. Included are results from one experiment on the AX7 and four experiments on the BWT alloy. Several different temperatures were examined and stresses were in the range 170 to 240 MPa. The life for any condition was estimated from

**Table 7. Damage summations for variable temperature tests**

| Test | Specimen | Temp (C) | Stress (MPa) | Time (h) | Summation damage (min) | Summation damage (max) |
|---|---|---|---|---|---|---|
| 25611 | AX7-12 | 650 | 200 | 20,000 | 0.17 | 0.17 |
| | | 760 | 200 | 174 | 0.85 | 0.85 |
| 26028 | BWT-27 | 700 | 170 | 10,000 | 0.50 | 0.28 |
| | | 730 | 170 | 3,685 | 0.98 | 0.55 |
| 26053 | BWT-27 | 650 | 200 | 10,084 | 0.08 | 0.04 |
| | | 760 | 200 | 537 | 2.18 | 1.06 |
| 26087 | BWT-31 | 650 | 170 | 10,050 | 0.02 | 0.01 |
| | | 700 | 170 | 480 | 0.04 | 0.02 |
| | | 730 | 170 | 513 | 0.18 | 0.10 |
| | | 760 | 170 | 1,002 | 1.46 | 0.84 |
| | | 730 | 170 | 193 | 1.51 | 0.86 |
| | | 700 | 170 | 984 | 1.56 | 0.89 |
| 26607 | CS5-03 | 700 | 240 | 835 | 0.28 | 0.16 |
| | | 730 | 240 | 145 | 0.52 | 0.31 |
| | | 700 | 240 | 611 | 0.72 | 0.62 |

the LMP in which the parametric constant was selected to be 20. Since the log stress versus the LMP data for the BWT alloy exhibited scatter, maximum and minimum values were selected for estimating maximum and minimum $t_{ri}$ values in Eq. (11). The damage summations in the five experiments ranged from 0.55 for the worst case to 2.18 for the best case. Thus, in no case was there an indication that the HT-UPS alloys would not meet Criterion III-C. However, it may be that thermal cycling could punch out dislocations around the large precipitates. These dislocations could produce enhanced creep rates or promote local recrystallization; to ensure that such a creep enhancement mechanism would not occur, more testing under thermal cycling is needed.

III-D. Stress-temperature cycling will not degrade the long-time strength by more than 10%.

Reflecting the concerns in the boiler industry about material degradation under cyclic loads, Criterion III-D addresses the need for an understanding of damage accumulation under both temperature and load cycling. Toft and Broom (1963) examined the behavior of type 316 stainless steel and Esshete 1250 under combined load and temperature changes and found only small effects. However, fatigue and creep-fatigue interaction phenomena are known to produce significant damage in austenitic stainless steels at high temperatures, and much is being done to reduce the likelihood of cycle-induced failures. Currently, the most often used rules for evaluating damage under combined stress- (or strain-) temperature cycling are those in the high-temperature extension of the ASME BVP Code, Sect. VIII, namely, Code Case N-47. Here, continuous cycling design fatigue curves were constructed from uniaxial, strain-range controlled, low-cycle fatigue (LCF) tests. It was then recommended that the fatigue damage for any arbitrary cycling histogram be calculated from Minor's rule. Various types of creep damage are then introduced in the cycle and the creep damage fraction calculated from Robinson's rule. The fatigue damage fraction, $d_{fi}$, for any cycle at strain range, $\Delta\varepsilon_i$, is given by

$$d_{fi} = 1/N_{fi} , \tag{14}$$

where $N_{fi}$ is the number of cycles to failure at $\Delta\varepsilon_i$. Again, damage is summed over all cycles, but, for creep fatigue interactions, the creep damage and fatigue damage fractions are again summed and the total damage, D, restricted to a number equal to or less than 1. Thus:

$$D = \Sigma\, d_{ci} + \Sigma\, d_{fi} . \tag{15}$$

For austenitic stainless steels, D is sometimes chosen to be 0.3.

Of the alloys identified in Table 1, only type 316 stainless steel has a sufficient data base to estimate the D value by the analysis method developed for Code Case N-47. A review of the data base for type 316 stainless steel was provided by Marshall (1984). However, Teranishi et al. (1989) examined the fatigue behavior of fine-grained type 347 stainless steel at 750°C and 1% strain range. They did not interpret their data on the basis of Eq. (15), but reported the cyclic lives with and without creep damage being introduced. These lives were found to be 80 and 450 cycles, respectively, for 40-μm grain size material. Dawson et al. (1967) and Skelton and Beckett (1987) discussed the creep-fatigue behavior of Esshete 1250. At 600°C and 1% strain range, they found the fatigue life was near 2000 cycles under continuous cycling conditions and, depending on the heat treatment, 400 to 1000 cycles when a 0.5-h creep relaxation period was introduced between cycles.

A few exploratory fatigue and creep-fatigue tests have been performed on 17-14CuMo stainless steel and on one of the HT-UPS alloys (AX8). Marriott and Stubbins (1988) tested 17-14CuMo stainless steel at 700°C and two strain rates. At 1% strain range, the life of 17-14CuMo stainless steel was about 800 cycles for the $4 \times 10^{-3}$/s strain rate and near 100 cycles for the $1.4 \times 10^{-5}$/s strain rate. These lives were longer than those reported by Teranishi et al. (1987) for fine-grained type 347 stainless steel at 750°C, but they indicated poorer creep-fatigue resistance than Esshete 1250 at 650°C. One test was performed at ORNL on the same heat of 17-14CuMo stainless steel at 650°C and 1% strain range. A 0.5-h relaxation hold was introduced at the tensile strain limit of each cycle. The specimen lasted 176 cycles. The relaxation curve at half-life and the creep rupture data for 650°C were used to calculate the creep damage in the cycle as specified in Eq. (12), and a value of $2.2 \times 10^{-4}$/cycle was produced. Assuming that the continuous cycling life would be around 1000 cycles and that the half-life damage fraction was applicable throughout the life, the damage D was determined from Eq. (15) to be around 0.21 and not far from the 0.3 value used in Code Case N-47 for austenitic stainless steels. By calculation, most of the damage was found to be fatigue damage, yet the failure mode was predominantly intergranular. Similar relaxation hold experiments were performed on the AX8 alloy and type 316 stainless steel (1% strain range with a 0.5-h hold at the tensile strain limit). The cyclic lives were 677 and 530 cycles, respectively. Calculation of the damage during the relaxation cycle was handicapped by the lack of creep rupture data for the AX8 alloy at 650°C. Damage calculations based on the trend for other cold-rolled HT-UPS alloys, however, produced a damage per cycle near $2.6 \times 10^{-5}$/cycle which was almost an order of magnitude lower than for 17-14CuMo stainless steel. The value of D, assuming a continuous cycling life of 1000 cycles, was found to be near 0.7. The damage mode for the AX8 alloy was primarily transgranular cracking that was promoted by oxide wedges similar to those shown in Fig. 36(*a*). The damage calculated for type 316 stainless steel was near $1.35 \times 10^{-3}$/cycle and the value for D near 1.25. The failure mode was primarily intergranular cracking. Thus, only the type 316 stainless steel accumulated significant creep damage, based on the use of Eq. (12); yet, on a relative strength basis, the relaxation response was not much different for the three alloys. Plots of the relaxation data for the alloys near their half-lives are provided in Fig. 39(*a*). Here it may be seen that the AX8 alloy was very strong, but the stress relaxation increment in 0.5 h was about the same as that for 17-14CuMo stainless steel and type 316 stainless steel (about 80 MPa). The creep rupture strength of the HT-UPS alloys was very high relative to the rapid relaxation, however, and this fact led to the small creep damage accumulation, as may be seen in Fig. 39(*b*).

Data for all alloys, including type 316 stainless steel, are too meager to determine if Criterion III-D can be met. Further studies on cyclic operation and the way in which damage is summed are needed. The current creep-fatigue interaction diagram recommended for use in high-temperature nuclear service implies, by virtue of the fact that D is limited to 0.3, that a small amount of fatigue damage can greatly reduce long-time creep strength (and vice versa).

ORNL-DWG 90-10567

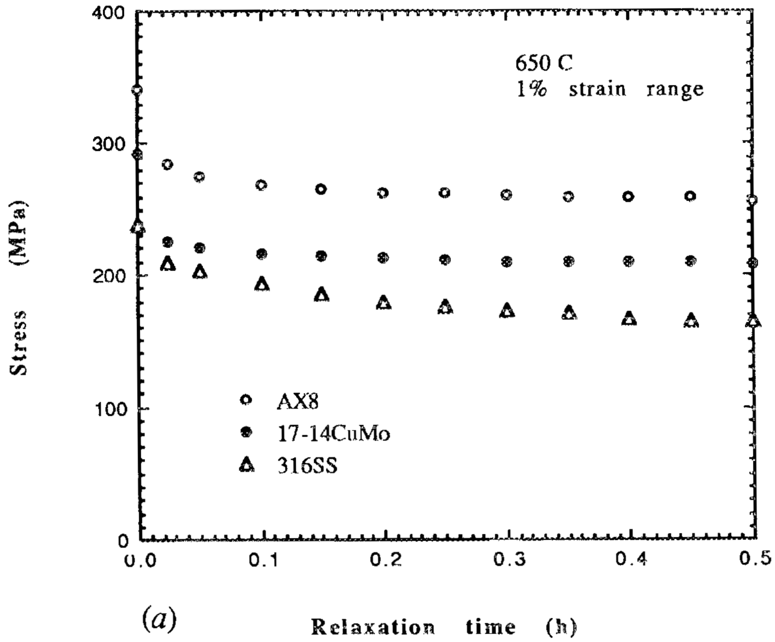


(*a*)

ORNL-DWG 90-10568

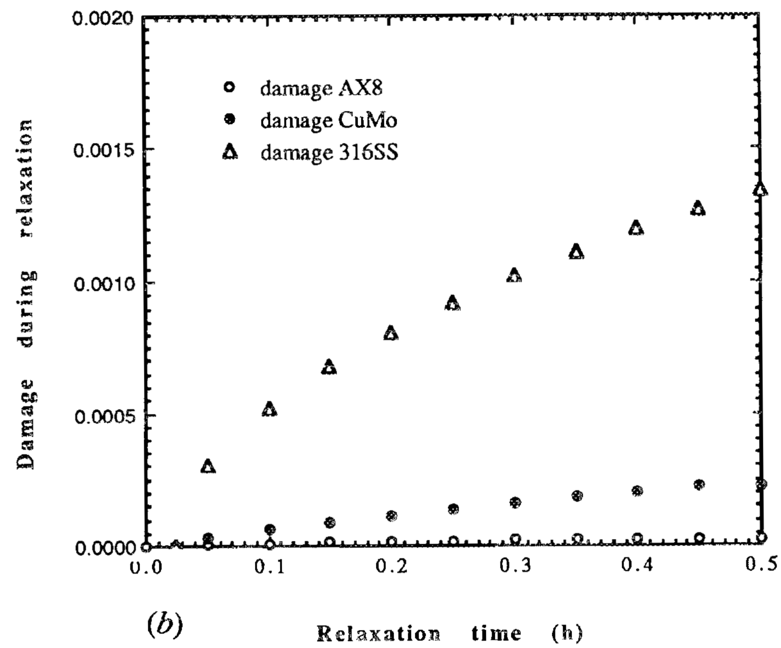


(*b*)

**Fig. 39. Creep damage introduced during relaxation periods of fatigue tests at 650°C and 1% strain range for type 316 stainless steel, 17-14CuMo stainless steel, and HT-UPS alloy AX8: (*a*) relaxed stress vs relaxation time and (*b*) creep damage vs time.**

III-E. Notched-to-smooth bar creep rupture strength ratios will exceed unity at temperatures in the range 600 to 760°C.

Williams and Willoughby (1963) found that type 316 stainless steel and Esshete 1250 were notch strengthened at temperatures in the range 600 to 700°C. It was found that the presence of the stress concentration associated with the notch produced local warm work that promoted the precipitation of MC in Esshete 1250, thereby improving the strength. No data for the other alloys, except type 316 stainless steel, are available; however, it seems likely that those alloys that produce copius amounts of intermetallic phase could be susceptible to notch embrittlement. Possibly, 17-14CuMo stainless steel could be in this category, as well as some heats of type 316 stainless steel. The HT-UTS alloys, with their exceptional ductility and resistance to creep crack growth, are likely to be notch strengthened.

III-F. Charpy V impact energy at room temperature will exceed 20 J at the end of life.

Marshall (1984) has reviewed the work of Sikka (1982) and others who addressed the influence of aging on the impact energy and fracture toughness of 300 series stainless steels. The impact energy (Charpy V, Charpy keyhole, or Izod) has been observed to diminish to 20% of the starting value as a result of long-time aging. Values for the Charpy V-notch may approach 60 J at long times for initially tough alloys and less than 40 J for low-toughness alloys. Teranishi et al. (1989) aged the fine-grained 347 stainless steel for times to 10,000 h at temperatures in the range 650 to 800°C and found the Charpy energies to be around 55% of the starting value at 0°C. Minami et al. (1986), on the other hand, aged type 347 stainless steel for times to 50,000 h and found that the impact toughness was reduced to 20% of the starting value. They did not specify the type of test, but reported values as low as 50 J. Murray reported that Esshete 1250 suffered less embrittlement due to aging than type 316 stainless steels. The Izod impact energy at room temperature diminished to 50% of the unexposed energy after 10,000 h at 700°C and 40% after 10,000 h at 800°C. Clark et al. (1960) found that the room-temperature Charpy V-notch toughness for 17-14CuMo stainless steel was in the range 40 to 60 J after aging approximately 4300 h (6 months) at temperatures in the range 650 to 800°C. In the worst case, the toughness diminished to 33% of the starting value. Sumitomo (1988) exposed ST3Cu for 3000 h at temperatures in the range 600 to 750°C and found the remaining Charpy V-notch toughness to be approximately 55% of the starting value at 0°C. These data reported in the literature are summarized in Table 8. Tensile and Charpy V-notch impact tests were performed on several of the HT-UPS alloys aged approximately 10,000 h at 700°C. The tensile data are provided in the appendices and Charpy V-notch data are summarized in Table 8. Several of the alloys did not meet the 20-J impact

**Table 8. Typical impact data for several aged alloys**

| Alloy | Condition | Type test | Temperature (°C) | Time (h) | Toughness (J) | Reference |
|---|---|---|---|---|---|---|
| Esshete 1250 | Mill | Izod | 600—800 | 10,000 | 40—115 | Murray et al. 1967 |
| 17-14CuMo | Mill | Charpy V | 650—815 | 4,300 | 40—60 | Clark et al. 1960 |
| 316 SS | Mill | Charpy V | 700 | 10,000 | 28.9, 28.8 | ORNL |
| 17-14CuMo | Mill | Charpy V | 700 | 10,000 | 56.70 | ORNL |
| 17-14CuMo | Mill | Charpy V | 700 | 10,000 | 19.4, 27.3 | ORNL |
| AX7 | Mill | Charpy V | 700 | 10,000 | 9.6, 10.4 | ORNL |
| AX8 | Mill | Charpy V | 700 | 10,000 | 18.4, 18.4 | ORNL |
| BWT | Extruded | Charpy V | 700 | 5,000 | 95.6, 96.5 | ORNL |
| 17-14CuMo | SMA weld | Charpy V | 700 | 10,000 | 35.9, 28.4 | ORNL |
| 17-14CuMo | SMA weld | Charpy V | 700 | 10,000 | 32.9, 35.9 | ORNL |
| 17-14CuMo | GTA weld | Charpy V | 700 | 10,000 | 18.9 | ORNL |

energy end-of-life criterion. These included AX7 (10 J) and AX8 (18 J). 17-14CuMo stainless steel produced values near 19, 27, and 57 J, while the toughness for type 316 stainless steel was close to 29 J. The best HT-UPS alloy was the BWT material with an impact energy near 96 J. Charpy V notch impact data for the starting HT-UPS materials were not obtained, so a comparison with the other alloys discussed above cannot be made on the basis of the percentage of retention of toughness.

In summary, all of the alloys listed in Table 1 will lose toughness as a result of exposure to high-temperature service. Indications are that some of the alloys (AX7 and AX8) may be so embrittled at room temperature that they will not meet the 20-J impact energy identified as a desirable Criterion. Discrepancies exist in regard to the aging embrittlement of 17-14CuMo stainless steel and 347 stainless steel that may reflect heat to heat variations. Further studies of loss of toughness in a service environment will be needed.

III-G. Impact properties of weld metal will meet the requirements of the ASME BPV Code.

Austenitic alloy weldments that contain significant amounts of ferrite could suffer embrittlement if the ferrite were to transform to sigma or α' during service. The alloys listed in Table 1 are not expected to contain much ferrite in welds, hence it should be possible to meet this Criterion III-G. Nevertheless, sigma and Laves could develop in the weldment, just as it could in the base metals. Impact and fracture toughness data for the alloys are of interest. Again, Marshall (1984) provided a review of the toughness of weldments in 300 series stainless steels, while Williams and Willoughby (1963) examined Esshete 1250. Little information has been reported about the impact toughness of welds in the fine-grained 347 stainless steel, 17-14CuMo stainless steel, or ST3Cu. A few Charpy V-notch tests were performed at ORNL on weldments of 17-14CuMo stainless steel aged 10,000 h at 700°C, and results are reported in Table 8. The SMA weld exhibited room temperature impact energies in the range 28 to 72 J. The GTA weld produced an impact value near 19 J. No information has been produced on the aging embrittlement of CRE 16-8-2 stainless steel and alloy 556 filler metals. However, it is known from the work of McCoy and King (1985) that base metals such as alloy 617 and alloy 556 will exhibit Charpy V impact values less than 20 J after long-time aging at 700°C and higher. There is reason to expect that similar embrittlement would occur in filler metals of similar composition.

In summary, more information is needed on the toughness of aged filler metal for all alloys listed in Table 1. In particular, the CRE 16-8-2 stainless steel and alloy 556 filler metals should be investigated to determine their tendency toward embrittlement.

III-H. The creep rupture strength of weldments will exceed 90% of the base metal strength.

Data for the strength of weldments has been reported for nearly all of the alloys in Table 1. Generally, the Criterion of 90% of the base metal strength has been met. The data base for weldments in type 316 stainless steel is vast, and the Code has developed weld strength reduction factors that may be used for this alloy when weldment integrity is of concern. Over most of the useful range for type 316 stainless steel these stress reduction factors indicate weldment strengths in excess of 90% of base metal. Teranishi et al. (1989) tested weldments of the fine-grained type 347 stainless steel over the temperature range 650 to 750°C and to times beyond 10,000 h. They found that the rupture lives for weldments fell within the scatter band for base metal. Lister et al. (1967) examined the creep rupture response of Esshete 1250 at 600 and 650°C for times beyond 10,000 h. They found that weldments had comparable strength to base metal at 650°C, but rupture lives consistently fell near the lower limit of the base metal strength at 600°C. The weldments appeared to have only 85% of the average base metal strength at this temperature. Sumitomo (1988) used 17-14CuMo stainless steel to produce GTA welds in ST3Cu stainless steel tubing. They performed creep rupture tests in the range 600 to 750°C and found that the weldments had strengths that fell within the scatter band for base metal for times to 10,000 h. Masuyama et al. (1988) reported creep rupture data for transverse weld in 17-14CuMo stainless steel at 700 and 750°C and for times to 10,000 h. Specimens were postweld heat treated for 5 h at 730°C prior to testing, and the rupture lives scattered about the curves drawn for base metal. They extrapolated the trend at 700°C and found the rupture strength to be near 100 MPa.

As discussed in the section of this report addressing fabrication, the results of the tests for weldability of the HT-UPS alloys indicated that their high nickel balance would preclude autogenous welding, and in Table 5 the alternate filler metals and processes are identified. These included alloy 82 (a nickel base alloy), 17-14CuMo stainless steel, CRE 16-8-2 strainless steel, alloy 690 (a nickel base alloy cladding), and alloy 556 (a Fe-Ni-Cr-Co alloy). Screening tests of weldment strength and ductility consisted of tensile tests on transverse weldments at 25 and 700°C, creep tests on transverse weldments at 700°C and 170 MPa, a few tensile tests and impact tests on aged weldments, a few creep tests at temperatures in the range 600 to 800°C to examine time-temperature-stress effects, two axial-load creep tests on full-size piping at 700°C, and two longitudinal weldment creep tests.

The tensile data are reported in Appendix B, and trends are summarized in Fig. 40. The ultimate tensile strengths (UTS) at 25 and 700°C are shown in the form of bar charts in Figs. 40(*a*) and 40(*c*), respectively, while the reduction of area (RA) data for the two temperatures are displayed as bar charts in Fig. 40(*b*) and 40(*d*). The data are difficult to interpret because of the large number of material variables, but Fig. 40(*a*) revealed that all weldments produced similar ultimate tensile strengths at 25°C, except for BWT2, which was a relatively weak base metal. All weldments exceeded the minimum UTS specified for 300H series stainless steels (515 MPa). At 700°C, alloys welded with CRE 16-8-2 stainless steel filler metal were weak relative to alloys welded with 17-14CuMo stainless steel and alloy 556. All weldments exhibited acceptable UTS values. In spite of fusion line cracking in the high-phosphorous-containing alloys (CE1, CE3, and AX7), the RA values at 25°C exceeded 40%, and most failures occurred in the base metal. At 700°C, however, the RA values were strongly influenced by the base metal composition, filler metal composition, and metallurgical condition of the base metal. The cold-rolled AX5, AX6, AX7, and AX8 exhibited low ductilities when welded with 17-14CuMo stainless steel. Better ductilities were observed when CRE 16-8-2 stainless steel and alloy 556 were used, and RA values exceeding 50% were achieved. The alloy 82 weld was found to be weak, and the GTA 17-14CuMo stainless steel weld was found to be brittle. Data for specimens welded with these filler metals are provided in Appendix D.

Creep rupture data produced on transverse weldment specimens are provided in Appendix D and summarized in Fig. 41 on the basis of log stress versus the LMP [Fig. 41(*a*)] and RA versus log time to rupture [Fig. 41(*b*)]. Here it may be seen that the CRE 16-8-2 exhibited the lowest strength but the best ductility. Alloy 556 exhibited both good strength and good ductility. The 17-14CuMo stainless steel weldments exhibited the poorest ductility. Examining the trend of the data, it appeared that the weldment strength was

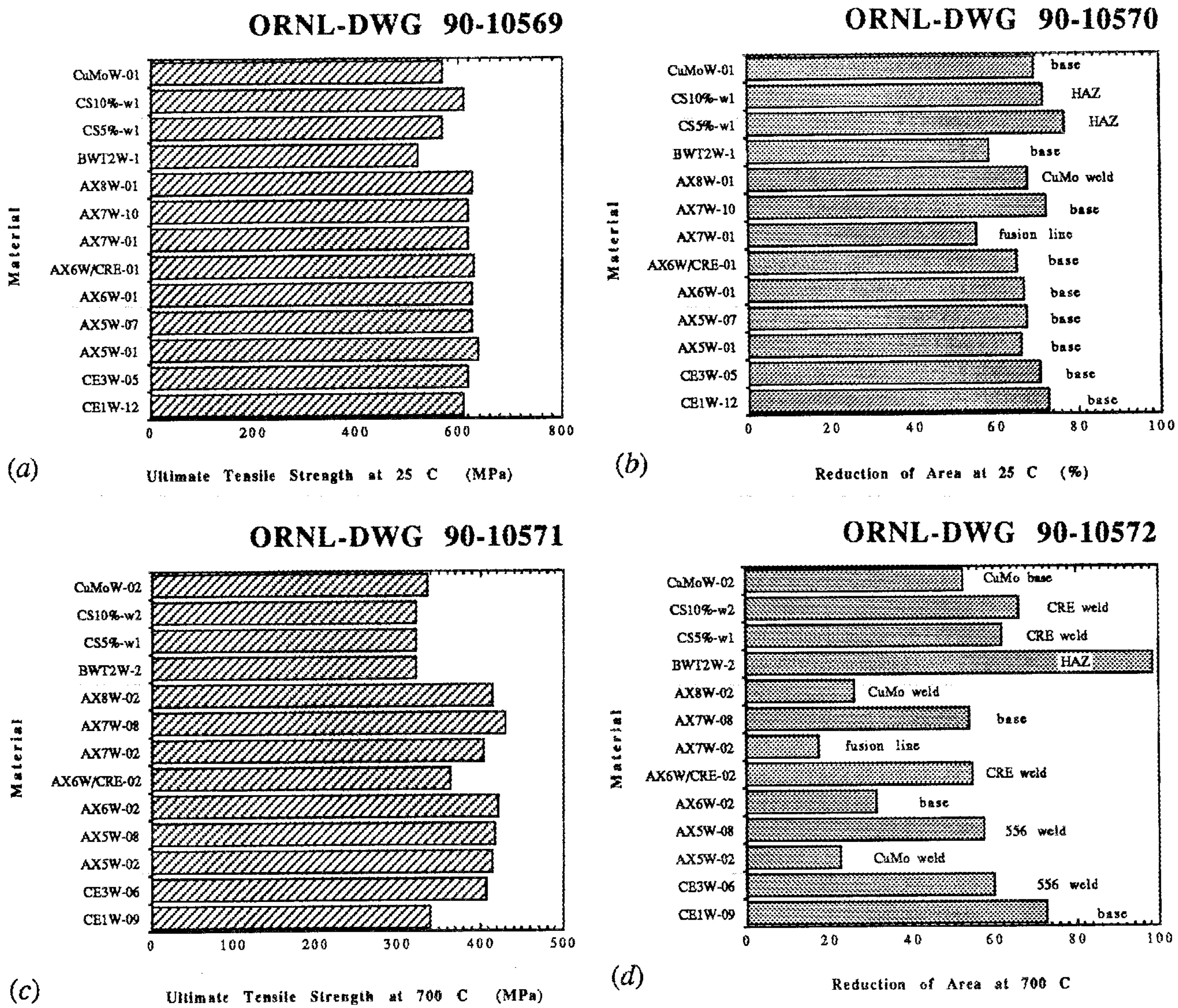


Fig. 40. Bar charts comparing the ultimate tensile strength (UTS) and reduction of area (RA) for weldments of HT-UPS weldments: (*a*) UTS at 25°C, (*b*) RA at 25°C, (*c*) UTS at 700°C, and (*d*) RA at 700°C. For specimen codes see appendix tables.

ORNL-DWG 90-10573

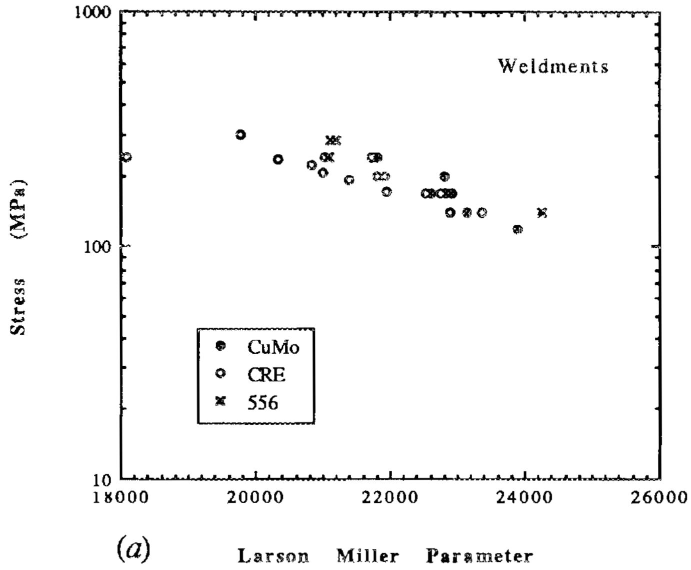


(*a*)

ORNL-DWG 90-10574

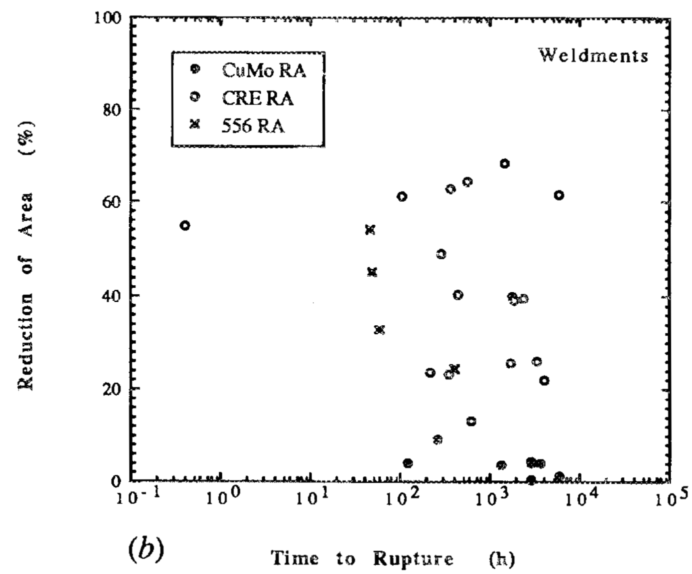


(*b*)

**Fig. 41. Creep-rupture data for weldments in HT-UPS alloys welded with 17-14CuMo stainless steel, CRE 16-8-2 stainless steel, and alloy 556 filler metals: (*a*) log stress vs LMP and (*b*) RA vs time to rupture.**

sufficient to meet Criterion III-H. To further examine the weldment behavior, however, a few larger weldments were tested.

The photographs of the creep ruptures in full-section welded tubes are shown in Fig. 42. The as-extruded BWT alloy tube was welded with CRE 16-8-2 stainless steel, as shown in Fig. 19, and loaded in a 444-kN creep testing machine. A butt weld was at the center, fillet welds were at the ends of the gage length, and butt welds to type 316 stainless steel were made at the ends. The specimen was stressed to 140 MPa at 700°C and failed in 2600 h. The failure appearance may be seen in Fig. 42(*a*). The CRE 16-8-2 stainless steel weld provided extra strength to the tube, causing the tube to fail in a region remote from the weld. The second test was performed on clad tubing. In addition to the butt weld at the center, simulated "repair" welds were placed in longitudinal and transverse locations. The specimen was stressed to 217 MPa (assuming no strength contribution from the cladding) and failed in 478 h. See Fig. 42(*b*). Again, the welds produced strengthening, and failures occurred remote to the welds. Both tubes failed in half the lives expected from small specimen test data; hence, additional studies are needed to determine the cause for the differences.

Two longitudinal weldment tests were performed at 650°C. Type 316 stainless steel and the AX8 alloy were selected, since the former is considered to have reasonable weldability and the latter was known to contain hot cracks of the type shown in Fig. 20. It was of interest to examine the possible growth of hot cracks under creep conditions. Butt welds were made in 13-mm-thick plates of AX8 and type 316 stainless steel. Specimens were machined approximately 44 mm wide, 2.5 mm thick, and 95 mm in length. These were tested in a 222-kN creep testing machine, and the crack initiation and growth were visually monitored during testing at 650°C, where it was expected that crack growth would be of more concern than at 700°C. The type 316 stainless steel was stressed to 170 MPa and failed in 525 h. Cracks developed in the HAZ and propagated through the weld metal and base metal to produce the type of failure shown in Fig. 43(*a*). This is a common mode of failure in type 316 stainless steel at temperatures in the range 550 to 650°C. The AX8 alloy was stressed to 240 MPa, but after little or no creep in 1000 h, the stress was increased to 290 MPa. After an additional 1000 h and with less than 1% creep strain accumulated, the stress was increased to 340 MPa. Cracks were soon seen in the CRE 16-8-2 stainless steel weld metal. (They may have existed at the time the stress was increased.) These cracks propagated across the weld region, which constituted approximately 25% of the cross-sectional area, and the subsequent increase in the stress in the AX8 alloy ligament exceeded its ultimate strength. A ductile overload failure occurred, as shown in Fig. 43(*b*).

YP-8538 YP-9918

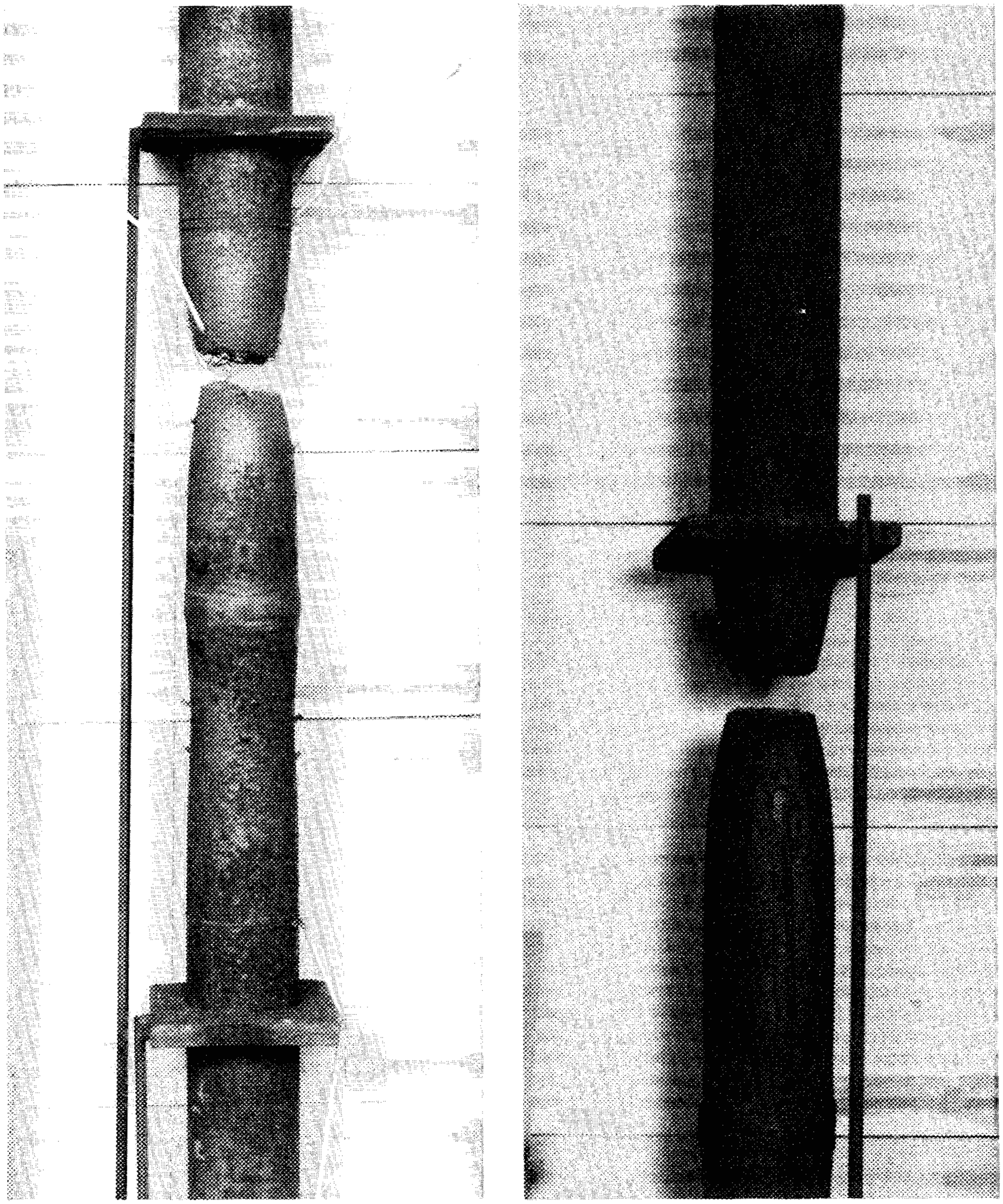

Fig. 42. Rupture appearance of full-sized butt-welded tubing tested at 700°C: (*a*) BWT tubing welded with CRE 16-8-2 that failed in the base metal after 2600 h at 140 MPa and (*b*) BWT tubing clad with alloy 71 and welded with CRE 16-8-2 stainless steel with alloy 92 corrosion overlay that failed in the base metal after 478 h at 217 MPa.

Y216637

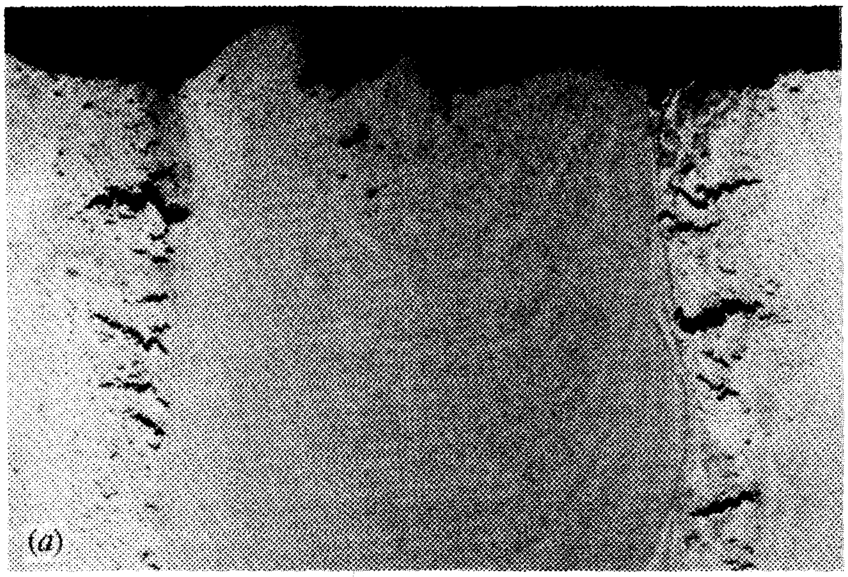


Y216636

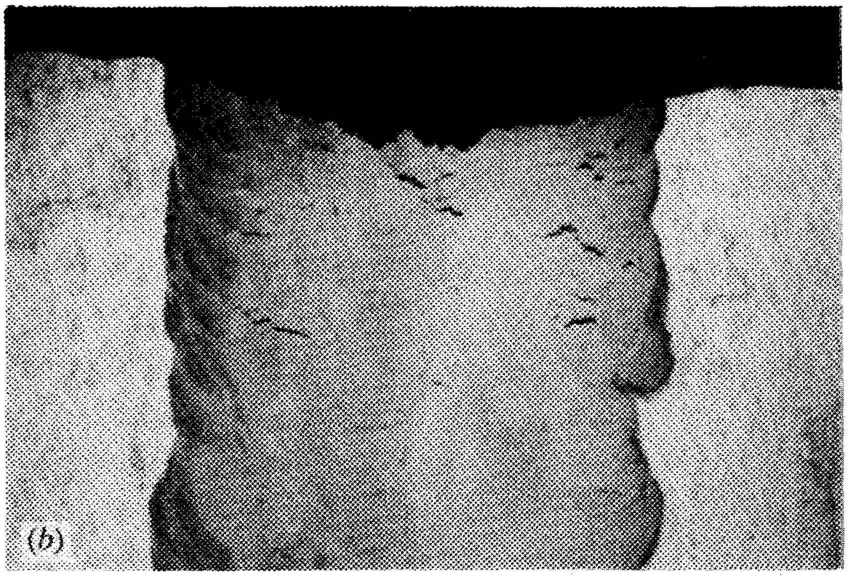


Fig. 43. Comparison of cracking patterns in longitudinal weldments tested at 650°C: (*a*) type 316 stainless steel welded with CRE 16-8-2 that failed after 525 h at 170 MPa from cracks that initiated in the HAZ; and (*b*) AX8 alloy welded with 16-8-2 stainless steel that survived 1000 h at 240 MPa and 1000 h at 290 MPa, and failed after 22 h at 340 MPa from cracks that initiated near the center passes of filler metal.

To examine the possibility that hot cracks could initiate crack growth under fatigue loading, two tests were performed on CRE 16-8-2 weldments in the BWT alloy at 650°C and 1% strain range. The testing section contained base metal, HAZ, and weld metal, so the possibilities of strain concentration in any one region was a possibility. A continuous cycling test failed after 556 cycles with the crack propagating through the weld metal. A test with a 0.5-h hold at the test strain limit failed after 254 cycles, again with the crack propagating through the weld metal. The hold time fatigue life of the BWT weldment proved to be superior to the 17-14CuMo stainless steel base metal and nearly as good as the type 316 stainless steel and AX8 alloy base metal. These exploratory tests were positive indications that welds in the BWT alloy could withstand significant strain fatigue loadings.

In summary, it appears that some of the HT-UPS alloys may be welded successfully with CRE 16-8-2 stainless steel weld metal, or perhaps alloy 556. Test data to 10,000 h indicate that brittle failures as a result of the growth of hot cracks would be unlikely. On the other hand, the alloys tend to have low Charpy V impact toughness and would have to be treated in a manner similar to nickel base alloys with similar properties. More testing of full-scale weldments and pressurized tubes with weldments and thermal cycling is needed to assure that dissimilar weld failures of the type reviewed by Roberts et al. (1985) would not occur. Further, additional work on weldments in 17-14CuMo stainless steel, ST3Cu stainless steel, and Esshete 1250 would be of value.

## 6. FIRESIDE CORROSION

Fireside corrosion is probably the most severe problem to be addressed in the selection of materials for heat recovery in an advanced steam cycle pulverized-coal-fired boiler. Corrosion is largely due to the formation of liquid trisulfate deposits on the tubing that suppress the formation of protective oxides. In applications where the coal may have lower ash content, it is possible that corrosion would not be so limiting. In specifying criteria for fireside corrosion, it was assumed that a coal such as Illinois No. 6 would be used. The corrodents produced by the combustion of this material are severe. The subject has been considered in the early work of Clark et al. (1960), and much has been examined in the ensuing 30 years. Current studies are under way by Nakabayashi et al. (1986), Wolowodiuk et al. (1989), and Plumley and Roczniak (1989), to name a few. Alloys include several of those listed in Table 1, and these are being tested both in the laboratory and as probes in boilers. Among the lean stainless steels are type 347 stainless steel, Esshete 1250, and 17-14CuMo stainless steel. Higher chromium alloys, aluminum-bearing alloys, and nickel base alloys are also being evaluated, but they are not the subject of this report. A full interpretive report is being written by Blough (1990) that will address the problems and solution of problems in regard to the use of lean stainless steel. Alloys listed in Table 1 that will be investigated by Blough as part of this work include 17-14CuMo stainless steel, type 347 stainless steel, and the BWT alloy. Claddings for these alloys include alloy 671, alloy 690, and alloy 692. No new data are available at this time, so the criteria specified in ORNL-6274 will be covered briefly.

IV-A. Alloys will be amenable to claddings and coatings.

It has been shown in earlier sections of this report that alloys listed in Table 1 can be clad with a variety of corrosion-resistant alloys. The long-time performance of some claddings has been demonstrated in boilers that operate at steam temperatures as high as 570°C by Flately et al. (1987). Chromized coatings may be too thin to be of value. This subject will be addressed by Blough (1990).

IV-B. Alloys will be amenable to protection by metallic or ceramic shields.

Shields have been used in the Eddystone Unit #1, so their use with 17-14CuMo stainless steel has been demonstrated. Shields have been used on type 347 stainless steel tubes installed in conventional power plant boilers for many years, so there appears to be no problem with type 347 stainless steel in boilers that operate at lower temperatures. The ability to fillet weld on bare and clad BWT tubing has been demonstrated in this report, so it may be possible to shield a candidate HT-UPS alloy. More study of shield attachments under cyclic conditions is needed.

IV-C. Corrosion in beneficiated coal will not exceed 10% of the wall thickness during the design lifetime.

Typically, tube thinning in the Eddystone Unit #1 plant reaches 30% of the wall thickness (see Fig. 44). This is one reason that a high-strength alloy is desired for tubing. When cladding is used, it must be thick enough to protect the lean stainless steel base metal throughout the design lifetime. Most laboratory testing is of short duration, and in-boiler probe testing is expensive. Models are now under development by Blough (1990) that will use laboratory data, probe data, and power plant experience to predict performance of alloys as a function of time, temperature, and coal chemistry.

YP10019

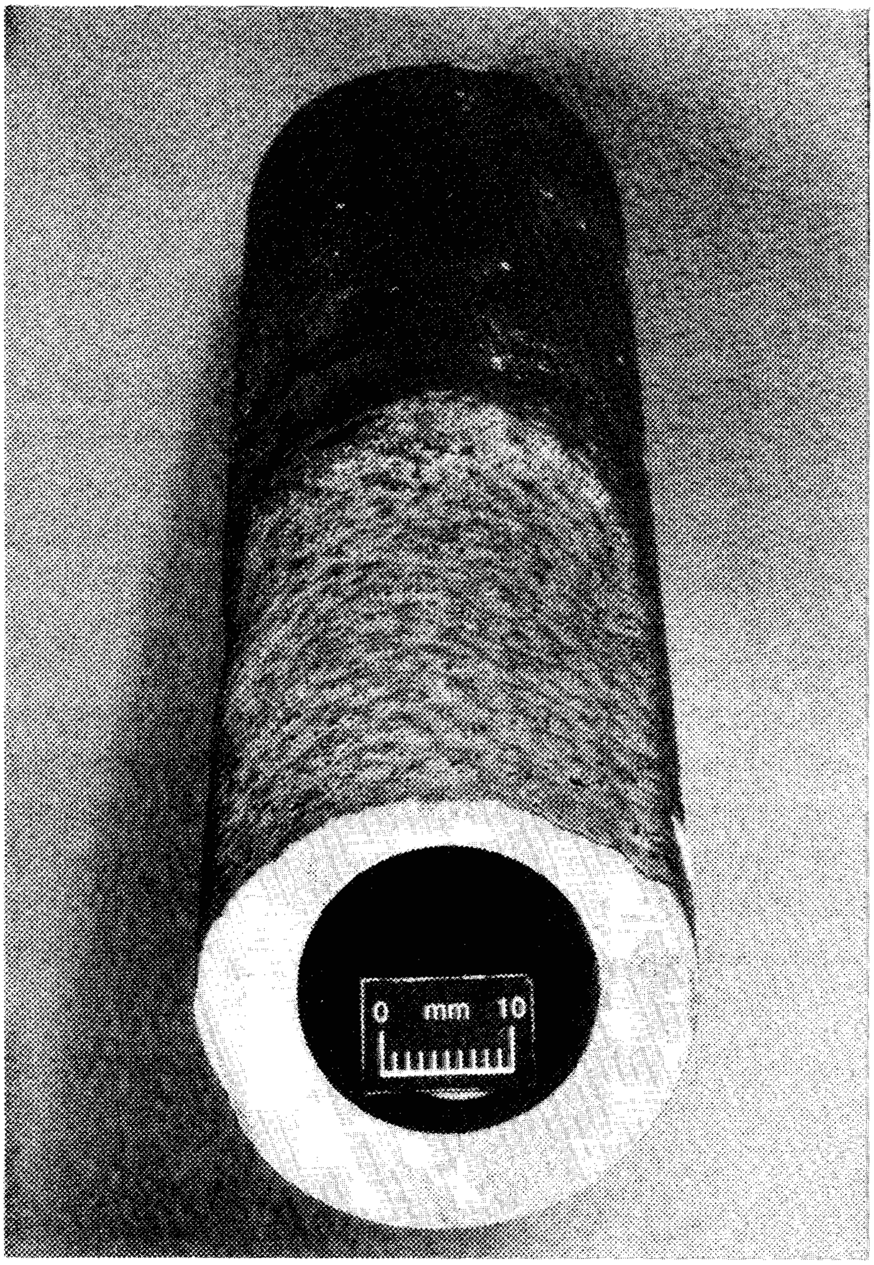


Fig. 44. Typical loss of tubing thickness produced in 17-14CuMo stainless steel superheater tubing due to long-time exposure in an advanced steam cycle boiler.

IV-D. Alloys will be corrosion resistant in a limestone-scavanged environment.

Testing of the lean stainless steels in fluidized bed combustors has not been undertaken as part of this research effort.

In summary, much has yet to be accomplished in the area of addressing the fireside corrosion problems, especially with respect to the HT-UPS alloys. Probe testing in boilers would be of considerable value.

## 7. STEAMSIDE CORROSION

Because of concern about exfoliation of oxides that form on the steam side of the tubing and the possible damage that particulates could inflict on the turbine at the pressures and temperatures of the advanced steam cycle (Rehn 1981), a relatively stringent requirement was placed on the steamside corrosion resistance. The Criterion was that the corrosion resistance be equivalent to alloy 800. To meet such a target, cladding, chromizing, aluminizing, chromating, or some similar treatment may be necessary. Cold working is known to improve oxidation resistance, as well. Clearly, if steamside oxidation equivalent to alloy 800 is required, then alloy 800H could be used for tubing. Research on this material is under way, and much progress has been made in developing strong, fabricable modifications to alloy 800. However, the topic is beyond the scope of this report. There remains concern that the low chromium in 17-14CuMo stainless steel and the HT-UPS alloys will be insufficient to prevent severe oxidation on the steamside. Earlier, Swindeman et al. (1987) reported severe oxidation in some of the HT-UPS alloys. However, no occurences of such oxidation has been observed in long-time, low-stress testing. A HT-UPS CE3 alloy specimen was removed after 21,000 h of testing under variable stresses (50 to 150 MPa) at 700°C and had the appearance shown in Fig. 45. Oxides had exfoliated from the surface, and penetration of oxides to a depth of 200 μm was observed. Work is currently under way by DeVan at ORNL to examine the oxidation of the HT-UPS alloys as a function of cold work. Early data suggest that significant improvements can be made to the oxidation resistance by modest amounts of cold work near the surface.

## 8. SUMMARY

When this research was begun in 1985 there was considerable interest in an advanced steam cycle pulverized-coal power plant. A large, high-efficiency plant reduces overall coal

YP6604

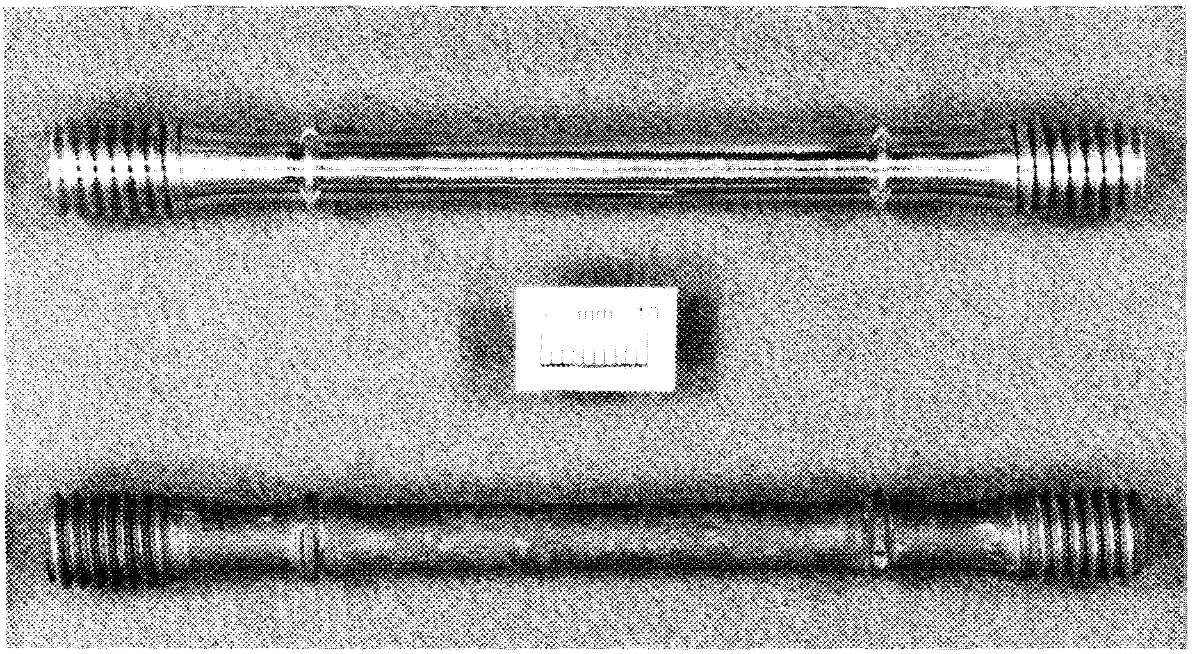


**Fig. 45. Appearance of a specimen of HT-UPS alloy CE3 after 21,000 h at 700°C and cyclic stresses in the range 50 to 150 MPa.**

consumption and is attractive from a viewpoint of reducing $CO_2$ emission. The alloy design criteria set forth in ORNL-6274 (Rittenhouse et al. 1985) were developed around this concept. This was especially true in regard to those criteria addressing corrosion resistance. It was the original intent that this activity evaluate several classes of alloys and develop an information base by 1990 that could assist in the selection of a material that could be further developed on a commercial scale. While this work was under way, research in Japan produced the FG347 stainless steel, ST3Cu stainless steel, and several higher chromium alloys not considered in this report. It is fairly clear that there are a number of excellent alloys that are available for commercialization.

The lean stainless steels have good fabricability. The research on the HT-UPS alloys suggests that clean steel-making practices should be followed; and vacuum melting, electroslag remelting, and ladle refining would be helpful in reducing undesirable residual elements. The alloys show their best strength properties after a high-temperature solution treatment and subsequent warm or cold working to raise the yield strength to values above 250 MPa. This could be accomplished in a rotary tube straightener. If any problems exist in the fabricability area, they relate to welding. To minimize the tendency toward the formation of brittle intermetallic phases, it has been necessary to increase the nickel equivalent in the lean stainless steels. The consequence of this chemistry adjustment is the tendency toward hot cracking during welding. The HT-UPS alloys seem to be the most susceptible, although the other alloys have not been examined in the same detail. The solution, if there is a solution, requires the use of a filler metal that can lessen the cracking at the fusion line. When this is done, side bend, tensile tests, and creep tests of weldments on most of the lean stainless steels considered in this report suggest that acceptable weldability is obtained. The exceptions are the HT-UPS alloys containing more than 0.04% phosphorous. Indeed, phosphorous should be kept to a minimum. In both longitudinal and transverse creep rupture tests, the HT-UPS alloys welded with CRE 16-8-2 stainess steel exhibited less heat-affected zone cracking than standard type 316 stainless steel. This trend is encouraging.

All of the lean stainless steels evaluated here owe their strength to the formation of the MC phase. The work performed to identify carbide precipitates and construct time-temperature-precipitation diagrams is too extensive to be treated in this report, but it can be said that the thermal-mechanical treatment can be optimized to produce a very stable and fine MC precipitate. For the case of the HT-UPS alloys, this involves a solution treatment above 1150°C followed by enough cold or warm work to introduce an equivalent of 5% strain. The HT-UPS alloys, however, are found to be remarkably stable for long times and high temperatures. In spite of the high nickel equivalencies, all of the lean stainless steels produced intermetallic phases. The sigma phase occurs in FG347 stainless steel and Esshete 1250, while Laves phase forms in 17-14CuMo stainless steel and the HT-UPS alloys. The 17-14CuMo stainless steel appears to be the most embrittled under creep conditions, while the HT-UPS alloys show the best creep rupture ductilities. The room-temperature impact energy of all the MC-forming alloys is reduced. The reduction of impact energy is most likely due to the increase in matrix strengthening by the MC precipitate along with the formation of brittle carbides and intermetallic compounds on the grain boundaries. The impact energies are no lower than seen in some nickel-base alloys and other 300 series stainless steels, although some of the HT-UPS alloys were judged to be unacceptable.

The allowable design stress for the MC-forming lean stainless steels is controlled by the short-time (tensile) properties up to fairly high temperatures. Techniques to increase the yield strength include controlling thermal-mechanical processing to (1) precipitate copper in ST3Cu stainless steel, (2) refine grain size in FG347 stainless steel, (3) age harden 17-14CuMo stainless steel, or (3) simply cold work the HT-UPS alloys. For service to 600°C, any of the alloys will serve quite well, while at 650°C Esshete 1250 is attractive. At 700°C, all indicators favor the cold-worked HT-UPS alloys if creep strength is the governing Criterion.

Exploratory studies reveal that the HT-UPS alloys have excellent creep crack growth resistance and good creep-fatigue resistance.

The research on oxidation and corrosion resistance has been extensive for FG347 stainless steel, 17-14CuMo stainless steel, and Esshete 1250. For service to 600°C, these alloys are satisfactory. The FG347 may be suitable for service to 650°C. However, the lean stainless steels need protection on the fireside when high-ash and chlorine-containing coals are burned. Although chromizing works well on ferritic alloys, it may not be suitable for the lean stainless steels due to the formation of a relatively thin but brittle surface layer on a coarse-grained soft substrate. Considerable more research is needed on the optimization of coatings for the lean stainless steels. Cladding is not a problem, but more operational experience is needed.

Since 1985, interest has shifted away from large pulverized-coal plants toward small gas-fired turbines, fluidized-bed combustors (both atmospheric and pressurized), and a gasification combined-cycle concept. New alloy design criteria could be developed for these applications. However, the need for high-performance alloys in heat recovery systems remains. It is expected that the research efforts on the lean stainless steels will be phased out within the next year, while the efforts on higher chromium alloys and aluminum-bearing alloys will continue.

## 9. CONCLUSIONS

1. Lean stainless steels containing MC-forming elements can be processed to produce strengthening microstructures that are stable for times exceeding 35,000 h at 700°C. The embrittling influence of intermetallic phases can be minimized by reducing the content of elements that promote sigma and Laves phase fields.

2. High-strength, high-quality superheater tubing can be readily fabricated from lean austenitic stainless steels. For optimum properties, the HT-UPS alloy tubing should be solution treated at a temperature above 1150°C and subjected to small amounts of cold or warm work to promote the precipitation of fine MC carbides.

3. To minimize weldability problems, the HT-UPS alloys should have low phosphorous, sulfur, and other residual elements. Alloys with high nickel equivalencies, such as the HT-UPS alloys, are subject to hot cracking and require special filler metals for joining.

4. With optimized heat treatment, it should be possible to produce superheater tubing that will achieve a design stress close to 60 MPa at 700°C. Commercial and near-commercial

lean stainless steels that are close to meeting the strength requirements include 17-14CuMo stainless steel, fine-grained type 347 stainless steel, ST3Cu stainless steel, Esshete 1250, and some of the HT-UPS steels.

5. The practicality of protecting lean stainless steels from corrosion in high ash content coal by high-chromium-bearing cladding seems likely.

6. The HT-UPS alloys possess the best strength and ductility, but techniques to produce clad tubing with controlled cold or warm work must be demonstrated.

## REFERENCES

American Society for Testing Materials. 1954. *Symposium on Effect of Cyclic Heating and Stressing on Metals at Elevated Temperatures,* STP 165, Philadelphia, Pa.

Armco Steel, 1950, unpublished information.

Asbury, F. E., and Willoughby, G. 1972. "Aging and Creep Behavior of a Cr-Ni-Mn Austenitic Steel," pp. 144-51 in *Creep Strength in Steel and High-Temperature Alloys*, The Metals Society, London.

Asbury, F. E., and Brooks, S. 1987. "Superheater Tubes for Advanced Coal-Fired Power Plant in the U. K.," pp. 213-18 in *Advances in Material Technology for Fossil Power Plants*, ASM International, Materials Park, Ohio.

Black, R. D., et al. 1989. "A Comparison of Creep and Load Relaxation Data of a Modified 316 Stainless Steel," pp. 1-8 in *Collection and Uses for Relaxation Data in Design*, PVP Vol. 172, ASME, New York.

Blough, J. F. 1990. "Fireside Corrosion Testing of Candidate Superheater Tube Alloys, Coating, and Cladding," pp. 251-52 in *Fossil Energy Advanced Research and Technology Development Materials Program Semiannual Progress Report for Period Ending September 30, 1989*, ORNL/FMP-89/2, Martin Marietta Energy Systems, Inc., Oak Ridge Natl. Lab.

Carolan, R. A., Li, Che-Yu, and Swindeman, R. W. 1987. in "The Effect of Minor Alloying Additions on the Mechanical Properties of Type AISI 316 Stainless Steel," pp. 275-81 *Advances in Material Technology for Fossil Power Plants*, ASM International, Materials Park, Ohio.

Carolan, R. A., et al. 1989. "Effect of Copper on the Strength of AISI 316 Stainless Steel," *Metall. Trans.* **20A**, 421-29.

Chapman, E. C., and Lorentz, Jr., R. E. 1960. "The Selection of Materials and Fabricating Techniques for the Eddystone Boiler and Sulzer Control Valves," *J. Eng. Power, Trans. Am. Soc. Mech. Eng*. pp. 275-85.

Clark, C. L., et al. 1960. Metallurgical Evaluation of Superheater-Tube Alloys After Six-Months' Exposure at Temperatures of 1100 to 1500 F," *J. Eng. Power, Trans. Am. Soc. Mech. Eng*. pp. 35-67.

Davis, E. A., and Connelly, F. M. 1959. "Stress Distributions and Plastic Deformation in Rotating Cylinders of Strain Hardening Materials," *J. Appl. Mech.* **81**, 25-30.

Dawson, R. A. T., et al. 1967. *Thermal and High Strain Fatigue*, Metals and Metallurgy Trust, London, pp. 239-69.

DeLong, W. T. 1974. "Ferrite in Austenitic Stainless Steel Weld Metal," *Weld. J.* 273-s-286-s.

Doi, H., et al. 1986. "Effects of Nb and Mo on Creep Rupture Strength of 23Cr-34Ni Iron Based Alloy," pp. 227-32 in *Proceedings, International Conference on Creep*, Japan Society of Mechanical Engineers, Tokyo, Japan.

Domian, H. A., and LeBeau, S. E. 1989. *Literature Review of Workability and Phase Stability Relative to Advanced Austenitic Alloys in Steam Service*, ORNL/Sub/88-SB775/01, Martin Marietta Energy Systems, Inc., Oak Ridge Natl. Lab.

Dulis, E. J., and Kasak, A. 1967. "Use of Cold-Formable Austenitic Stainless Steel for Valves for Internal-Combustion Engines," U.S. patent 3,303,023.

Ellis, F. V., et al. 1988. *Composition and Sigma Phase Determination in Eddystone No. 1 Main Steam Piping*, final report to Electric Power Research Institute on Research Project 1403-13, Combustion Engineering, Chattanooga, Tenn.

Flately, T., Latham, E. P., and Morris, C. W. 1987. "CEGB Experience with Co-Extruded Tubes for Superheated and Evaporative Sections of PF Fired Boilers," pp. 219-29 in *Advances in Material Technology for Fossil Power Plants*, ASM International, Materials Park, Ohio.

Gold, M., Leyda, W. E., and Zeisloft, R. H. 1975. "The Effect of Varying Degrees of Cold Work on the Stress-Rupture Properties of Type 304 Stainless Steel," *J. Eng. Mater. Technol.* **97**, 305-12.

Gold, M., and Jaffee, R. I. 1984. "Materials for Advanced Steam Cycles," *J. Mater. Energy Syst.* **3**, 138-45.

Goodwin, G. M. 1987. "Development of a New Hot-Cracking Test - The Sigmajig," *Weld. J. (Miami)* **66**, 33s-38s.

Grover, H. K., and Wickens, A. 1982. "Effects of Minor Elements on the Long-Term Creep-Rupture Properties of 316 Austenitic Stainless Steel," pp. 81-87 in *Mechanical Behavior and Nuclear Applications of Stainless Steel at Elevated Temperatures*, The Metals Society, London.

Hanada, T., Takahashi, M., and Sotooka, M. 1989. "EPDC's Atmospheric Fluidized Bed Combustion and Super Critical R&D," *Second International Conference on Improved Coal Fired Power Plants*, EPRI publication GS-6422, paper 3-1, Electric Power Research Institute, Palo Alto, Calif.

Harries, D. R. 1982. "Physical Metallurgy of Fe-Cr-Ni Austenitic Steels," pp. 1-14 in *Mechanical Behavior and Nuclear Applications of Stainless Steel at Elevated Temperatures*, The Metals Society, London.

Irvine, K. J., Gladman, T., and Pickering, F. B. 1969. "The Strength of Austenitic Stainless Steels," *J. Iron Steel Inst.* **207**, 1017-28.

Jaske, C. E., and Begley, J. A. 1978. "An Approach to Assessing Creep/Fatigue Crack Growth," pp. 381-409 in *Ductility and Toughness Considerations in Elevated Temperature Service*, MPC-8, American Society of Mechanical Engineers, New York.

Kaufman, L., and Nesor, H. 1974. "Calculation of Superalloy Phase Diagrams: Part I," *Metall. Trans.* **5**, 1617-21.

Keown, S. R., and Pickering, F. B. 1972. "Effect of Niobium Carbide on the Creep Rupture Properties of Austenitic Stainless Steels," pp. 134-43 in *Creep Strength in Steel and High-Temperature Alloys*, The Metals Society, London.

Kimura, H, and Minami, Y. 1986. "The Effect of Cu Additions on the Creep Rupture Strength of 17Cr-14Ni-Cu-Mo Stainless Steel," pp. 221—28 in *Proceedings, International Conference on Creep*, Japan Society of Mechanical Engineers, Tokyo, Japan.

King, R. T., Cole, N. C., and Goodwin, G. M. 1976. "Creep Behavior of SMA Type 316 Weld Metal With Controlled Residual Elements," *Trans. ASME J. Pressure Vessel Technol.* **98**, 194-98.

Kinoshita, K., et al. 1973. "Improved Superheater Tubing Material - Ti and Nb Bearing Austenitic Steel," pp. 162.1-162.6 in *International Conference on Creep and Fatigue in Elevated Temperature Applications*, Inst. Mech. Engineers, London.

Kujanpää, V. P., David, S. A., and White, C. L. 1987. "Characterization of Heat-Affected Zone Cracking in Austenitic Stainless Steel Welds," *Weld. Res. Suppl.* 221s-228s.

LeBeau, S. E. 1988. *Production of Small Heats of Austenitic Tubing - Final Report CRD No. 1191*, Babcock & Wilcox report RDD; 89:4423-01-01:01, Alliance, Ohio.

LeBeau, S. E. 1990. "Evaluation of the Fabricability of Advanced Austenitic Tubing," pp. 219-27 in *Fossil Energy Advanced Research and Technology Development Materials Program Semiannual Progress Report for Period Ending September 30, 1989*, ORNL/FMP-89/2, Martin Marietta Energy Systems, Inc., Oak Ridge Natl. Lab.

Lee, D., and Hart, E. W. 1971. *Metall. Trans.* **2**, 1245-55.

Lister, E., Mickleraith, J., and Higgenbottom, A. 1967. "High Temperature Properties of Steampipe Welds," pp. 474-81 in *High Temperature Properties of Steels*, Publication 97, Iron and Steel Institute, London.

Lundin, C. D., et al. 1985. "New Concepts in Varestraint Testing for Hot Cracking," *Welding Research, The State of the Art, Proceedings of the JDC University Symposium*, 1985 International Welding Congress, ASM, Toronto, Canada.

Lundin, C. D., Qiao, C. Y. P., Gill, T. P. S., and Ren, W. 1989. *The Hot Ductility and Hot Cracking Behavior of Modified 316 Stainless Steels Designed for High Temperature Service*, ORNL/Sub/88-07685/01, Martin Marietta Energy Systems, Inc., Oak Ridge Natl. Lab.

Machlin, E. S., and Shao, J. 1978. "SIGMA-SAFE: A Phase Diagram Approach to the Sigma Phase Problem in Base Superalloys," *Metall. Trans.* **9A**, 561-68.

Manjoine, M. J. 1975. "Ductility Indices at Elevated Temperatures," *J. Eng. Mater. Technol.* **97**, 156-60.

Mantle, K. G., and Gemmill, M. G. 1967. "Integrity of Attachment Welds to Superheater Tubing," pp. 496-504 in *High Temperature Properties of Steels*, Publication 97, Iron and Steel Institute, London.

Marriott, D. L., and Stubbins, J. F. 1988. *Development of a Design Methodology for High Temperature Cyclic Application of Materials Which Experience Cyclic Softening*, ORNL/Sub/85-55904/02, Martin Marietta Energy Systems, Inc., Oak Ridge Natl. Lab.

Marshall, P. 1984. *Austenitic Stainless Steels Microstructure and Properties*, Elsevier Science Publishing Co., Inc., New York.

Masuyama, F., et al. 1985. "Findings on Creep-Fatigue Damage in Pressure Parts of Long-Term Service-Exposed Thermal Power Plants," pp. 79-90 in *Residual-Life Assessment, Nondestructive Examination, and Nuclear Heat Exchanger Materials*, PVP-Vol. 98-1, American Society of Mechanical Engineers, New York.

Masuyama, F., et al. 1987. "Investigation of the Deformation Plus Restoration Behavior of Fourteen Heats of TP316 Stainless Steels Removed from Eddystone Unit No. 1 Main Steam Lines After 130,520 Hours of Service," pp.173-88 in *Properties of Stainless Steels in Elevated Temperature Service*, ed. by M. Prager, MPC-Vol. 26/PVP-Vol. 132, American Society of Mechanical Engineers, New York.

Masuyama, F., et al. 1988. "Update Survey and Evaluation of Materials for Steam Generators for Improved Coal-Fired Power Plants," pp. 5-85-5-109 in *First International Conference on Improved Coal Fired Power Plants*, EPRI publication CS-5581-SR, Electric Power Research Institute, Palo Alto, Calif.

Maziasz, P. J. 1988. "Microstructural Stability for Improved Irradiation Resistance and for High Temperature Strength of Austenitic Stainless Steels," pp. 116-65 in *MiCon 86: Optimization of Processing, Properties, and Service Performance Through Microstructural Control*, ASTM STP 979, Philadelphia, Pa.

Maziasz, P. J. 1989. "Developing an Austenitic Stainless Steel for Improved Performance in Fossil Power Facilities," *J. Met.* **41**, 14-20.

Maziasz, P. J., Braski, D. N., and Rowcliffe, A. F. 1989. "Radiation Resistant Austenitic Stainless Steel Alloys," U.S. patent 4,818,485.

Maziasz, P. J., and McHargue, C. J. 1987. "Microstructural Evolution in Annealed Austenitic Steels During Neutron Irradiation," *Int. Metall. Rev.* **32**, 190-218.

McCoy, H. E., and King, J. F. 1985. *Evaluation of HD 556 and Incoloy 802 for High-Temparature Gas-Cooled Reactor Applications*, ORNL/TM-9382, Martin Marietta Energy Systems, Inc., Oak Ridge Natl. Lab.

McGough, T. C., et al. 1985. "Selection and Fabrication of Replacement Main Steam Piping for the Eddystone No. 1 Supercritical Pressure Unit," *Weld. J.* 29-36.

McGowan, J. J., and Nanstad, R. K. 1984. "A Direct Comparison of Unloading Compliance and Potential Drop Techniques in J-Integral Testing," pp. 136-40 in *Computer-Aided Testing and Model Analysis*, Proceedings of the 1984 SEM Fall Conference, Milwaukee, Wis.

Minami, Y., Kimura, H., and Tanimura, M. 1986. "Creep Rupture Properties of 18%Cr-8%Ni-Ti-Nb and Type 347H Austenitic Stainless Steels," pp. 231-40 in *New Developments in Stainless Steel Technology*, American Society for Metals, Metals Park, Ohio.

Moen, R. A., and Farwick, D. G. 1978. "Limiting Recrystallization in Austenitic Stainless Steels for Structural Applications," pp. 235-46 in *Characterization of Materials for Service at Elevated Temperatures*, MPC-7, ASME, New York.

Murray, J. D., Hacon, J., and Wannell, P.H. 1967. "The High Temperature Properties on an Advanced Austenitic Steel: Esshete 1250," pp. 403-25 in *High Temperature Properties of Steels*, Publication 97, Iron and Steel Institute, London.

Myllykosi, L. 1983. "Hot Ductility of Austenitic Stainless Steels." pp. 61-6 in *Third Scandanavian Symposium in Materials Science.*

Nakabayashi, Y., et al. 1986. *Field Test and Evaluation of High Temperature Materials for Ultra Super Critical (USC) Power Boiler*, Technical Review, Mitsubishi Heavy Industries, Ltd., Tokyo, Japan.

National Research Institute for Metals. 1978. "Data Sheets on the Elevated Temperature Properties of 18Cr-12Ni-Mo Stainless Steel for Boiler and Heat Exchanger Tubes (SUS 316 HTB)," *Creep Data Sheet No. 6A*, Tokyo, Japan.

Naylor, E. R., et al. 1989. "Fundamental Study of Aluminizing and Chromizing Processes," pp. 273-87 in *Fossil Energy Materials Program Semiannual Progress Report for the Period Ending March 31, 1989*, ORNL/FMP-89/1, Martin Marietta Energy Systems, Inc., Oak Ridge Natl. Lab.

Pickering, F. B. 1979. "Introduction," pp. 1-43 in *The Metallurgical Evolution of Stainless Steels*, Am. Soc. Metals, Metals Park, Ohio.

Plumley, A. L., and Roczniak, W. R. 1989. "Coal Ash Corrosion Field Testing of Advanced Boiler Tube Materials - II," *Second International Conference on Improved Coal Fired Power Plants*, EPRI publication GS-6422, paper 34-1, Electric Power Research Institute, Palo Alto, Calif.

Rehn, I. M. 1981. *Corrosion Problems in Coal Fired Boiler Superheater and Reheater Tubes: Steam Side Oxidation and Exfoliation*, EPRI CS-1812, Electric Power Research Institute, Palo Alto, Calif.

Rittenhouse, P. L., et al. 1985. *Assessment of Materials Needs for Advanced Steam Cycle Coal Fired Plants*, ORNL-6274, Martin Marietta Energy Systems, Inc., Oak Ridge Natl. Lab.

Roberts, B. W., and Canonico, D. A. 1988. "Candidate Uses for Modified 9Cr-1Mo Steel in an Improved Coal-Fired Power Plant," *First International Conference on Improved Coal Fired Power Plants*, EPRI publication CS-5581-SR, paper 5-4, Electric Power Research Institute, Palo Alto, Calif.

Roberts, D. I., Ryder, R. H., and Viswanathan, R. 1985. "Performance of Dissimilar Welds in Service, 1985," pp. 55-63 in *Residual-Life Assessment, Nondestructive Examination, and Nuclear Heat Exchanger Materials*, PVP-Vol. 98-1, American Society of Mechanical Engineers, New York.

Robinson, E. L. 1952. "Effect of Temperature Variation on Long Time Rupture Strength of Steels," *Trans. Am. Soc. Mech. Eng.* **74**, 777-81.

Rundell, G. R. 1987. "Evaluation of a High Silicon-Aluminum Alloy for Waste Incineration and Fluidized Bed Combustion Systems," paper 8715-004, *Proceedings of the Conference on Performance of High Temperature Materials in Fluidized Bed Combustion Systems and Process Industries*, ASM, Materials Park, Ohio.

Saxena, A., and Han, J. 1987. *Evaluation of Crack Tip Parameters for Characterizing Crack Growth Behavior in Creeping Materials*, Fracture and Fatigue Research Laboratory, Georgia Institute of Technology, Atlanta, Ga.

Shinoda, T., Matsuo, T., and Tanaka, R. 1973. "Method for Improving the Creep Strength in Austenitic Heat Resisting Steel," pp. 175.1-175.9 in *International Conference on Creep and Fatigue in Elevated Temperature Applications*, Institute of Mechanical Engineers, London.
Sikka, V. K. 1982. *Effects of Aging on the Mechanical Properties of Type 316 Stainless Steel- Elevated-Temperature Properties*, ORNL/TM-8371, Martin Marietta Energy Systems, Inc., Oak Ridge Natl. Lab.

Skelton, R. P., and Beckett, B. J. E. 1987. "Thermal Fatigue Properties of Candidate Materials for Advanced Steam Plant," pp. 359-66 in *Advances in Material Technology for Fossil Power Plants*, ASM International, Materials Park, Ohio.

Smith, G. V. 1969. *An Evaluation of the Yield, Tensile, Creep, and Rupture Strengths of Wrought 304, 316, 321, and 347 Stainless Steels at Elevated Temperature*, ASTM Data Series DS 5S2, American Society for Testing and Materials, Philadelphia, Pa.

Spaeder, C. E., and Defilippi, J. D. 1974. "A Statistical Study of the Effect of Composition on the Creep-Rupture Properties of AISI Type 304 Stainless Steel," pp. 65-77 in *Symposium on Elevated Temperature Properties of Austenitic Stainless Steels*, ASME, New York.

Sumitomo Metal Industries, Ltd. 1988. *Properties of High Strength ST3Cu Austenitic Stainless Steel Tubing for Boiler Application*, document 808 F-No 1858, Japan.

Swindeman, R. W., et al. 1986. *Alloy Design Criteria and Evaluation Methods for Advanced Austenitic Alloys in Steam Service*, ORNL-6274, Martin Marietta Energy Systems, Inc., Oak Ridge Natl. Lab.

Swindeman, R. W., et al. 1987. *Procurement and Screening Test Data for Advanced Austenitic Alloys for 650 °C Steam Service (Part 1, 14Cr-16Ni Steels and 20Cr-30Ni Fe Alloys)*, ORNL/TM-10206/P1, Martin Marietta Energy Systems, Inc., Oak Ridge Natl. Lab.

Swindeman, R. W., et al. 1988. *Procurement and Screening Test Data for Advanced Austenitic Alloys for 650 °C Steam Service (Part 2, Final Report)*, ORNL/TM-10206/P2, Martin Marietta Energy Systems, Inc., Oak Ridge Natl. Lab.

Swindeman, R. W., Bolling, E., and Li, C-Y. 1990. "Copper Bearing Stainless Steels for High Temperature Applications," *New Alloys for Pressure Vessels and Piping*, ASME Pressure Vessels and Piping Conference, to be published.

Takahashi, T., et al. 1989. "Development of a High Strength 25Ni-20Cr Steel for Tubes in Ultra Supercritical Power Boilers," *Second International Conference on Improved Coal Fired Power Plants*, EPRI publication GS-6422, paper 41-1, Electric Power Research Institute, Palo Alto, Calif.

Tamura, K., et al. 1988. "Study on Applicability of Tubing and Piping Materials for Improved Coal-Fired Power Boiler," pp. 5-131-5-146 in *First International Conference on Improved Coal Fired Power Plants*, EPRI publication CS-5581-SR, Electric Power Research Institute, Palo Alto, Calif.

Tamura, M., et al. 1987. *TEMPALOY 17-14CuMo/NAC CR35A Composite Tubing for the Superheaters of Advanced Coal Fired Boilers*, Nippon Kokan Technical Report No. 49, Japan.

Teranishi, H., et al. 1989. "Fine Grained TP347H Steel Tubing with High Elevated Temperature Strength and Corrosion Resistance for Boiler Applications," *Second International Conference on Improved Coal Fired Power Plants*, EPRI publication GS-6422, paper 33-1, Electric Power Research Institute, Palo Alto, Calif.

Todd, J. A., and Ren, J-C. 1989. *Microstructural Studies of Advanced Austenitic Steels*, ORNL/Sub/19X-SA663C, Martin Marietta Energy Systems, Inc., Oak Ridge Natl. Lab.

Toft, L. H., and Broom, T. 1963. "Exploratory Tests on the Effect of Temperature and Load Cycling on the Creep Resistance and Microsructure of Two Austenitic Steels," pp. 3-77-3-83 in *Joint International Conference on Creep*, Institute of Mechanical Engineers, London.

Townsend, R. D. 1987. "CEGB Experience and UK Developments in Materials for Advanced Plant," pp. 11-20 in *Advances in Material Technology for Fossil Power Plants*, ASM International, Materials Park, Ohio.

Turner, D. L. 1987. Babcock & Wilcox Research & Development Division, Alliance, Ohio, letter report CRD 1185 to R. W. Swindeman, ORNL.

Williams, N. T., and Willoughby, G. 1963. "The Notch Rupture Behavior of Some Austenitic Steels," pp. 4-11-4-17 in *Joint International Conference on Creep*, Institute of Mechanical Engineers, London.

Wolowodiuk, W., Blough, J. L., and Kihara, S. 1989. "Coal-Ash Corrosion - An Update," *Second International Conference on Improved Coal Fired Power Plants*, EPRI publication GS-6422, paper 32-1, Electric Power Research Institute, Palo Alto, Calif.

Woodyatt, L. R., Sims, C. T., and Beattie, Jr., H. J. 1966. "Prediction of Sigma-Type Phase Occurrence from Compositions in Austenitic Superalloys," *Met. Trans.* **236**, 519-27.

# APPENDIX A

# MICROSTRUCTURES OF HT-UPS ALLOYS

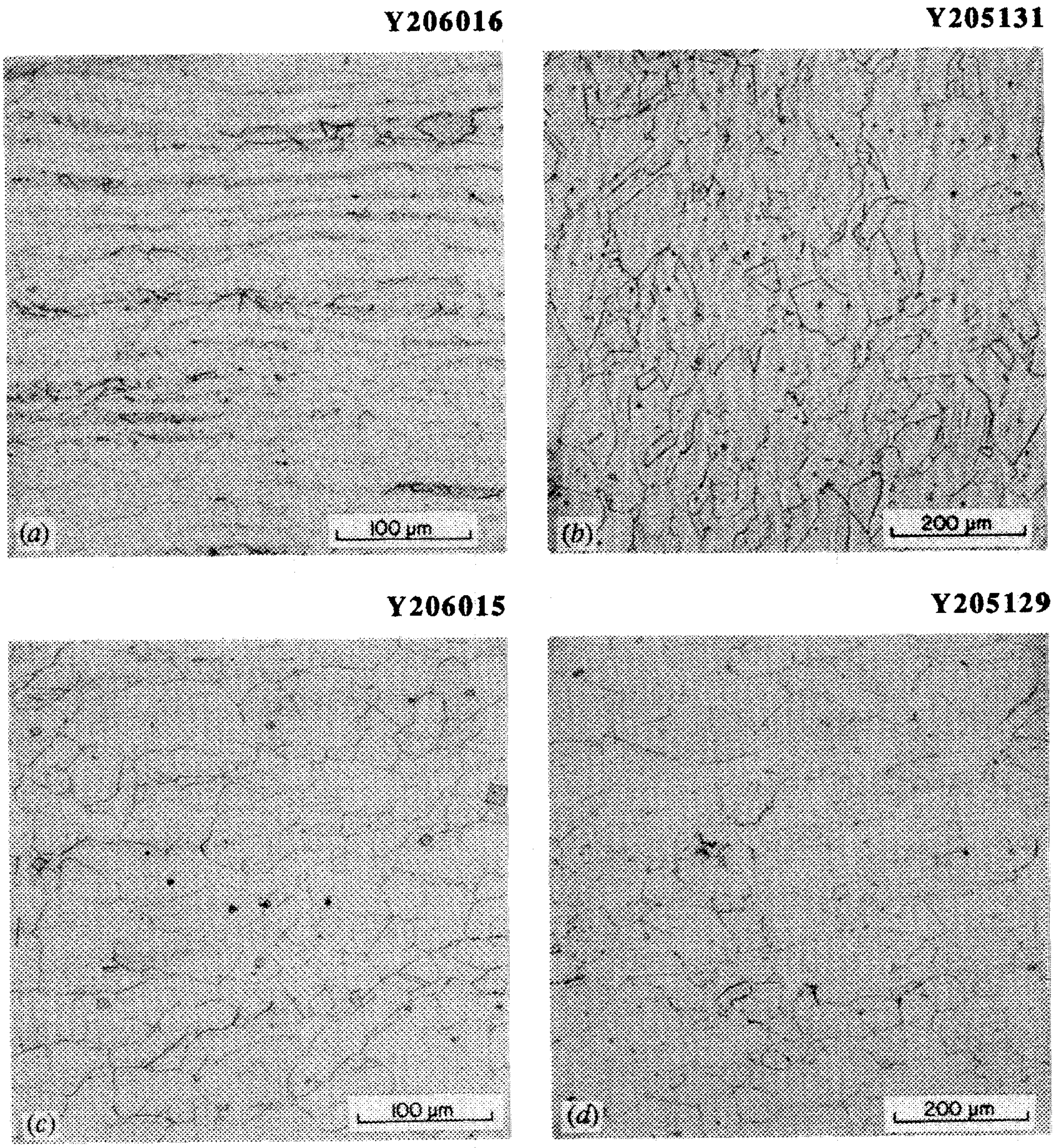


**Fig. A.1. Photomicrographs of the microstructures of the hot-rolled CE series of HT-UPS alloys: (*a*) CE0, (*b*) CE1, (*c*) CE2, and (*d*) CE3.**

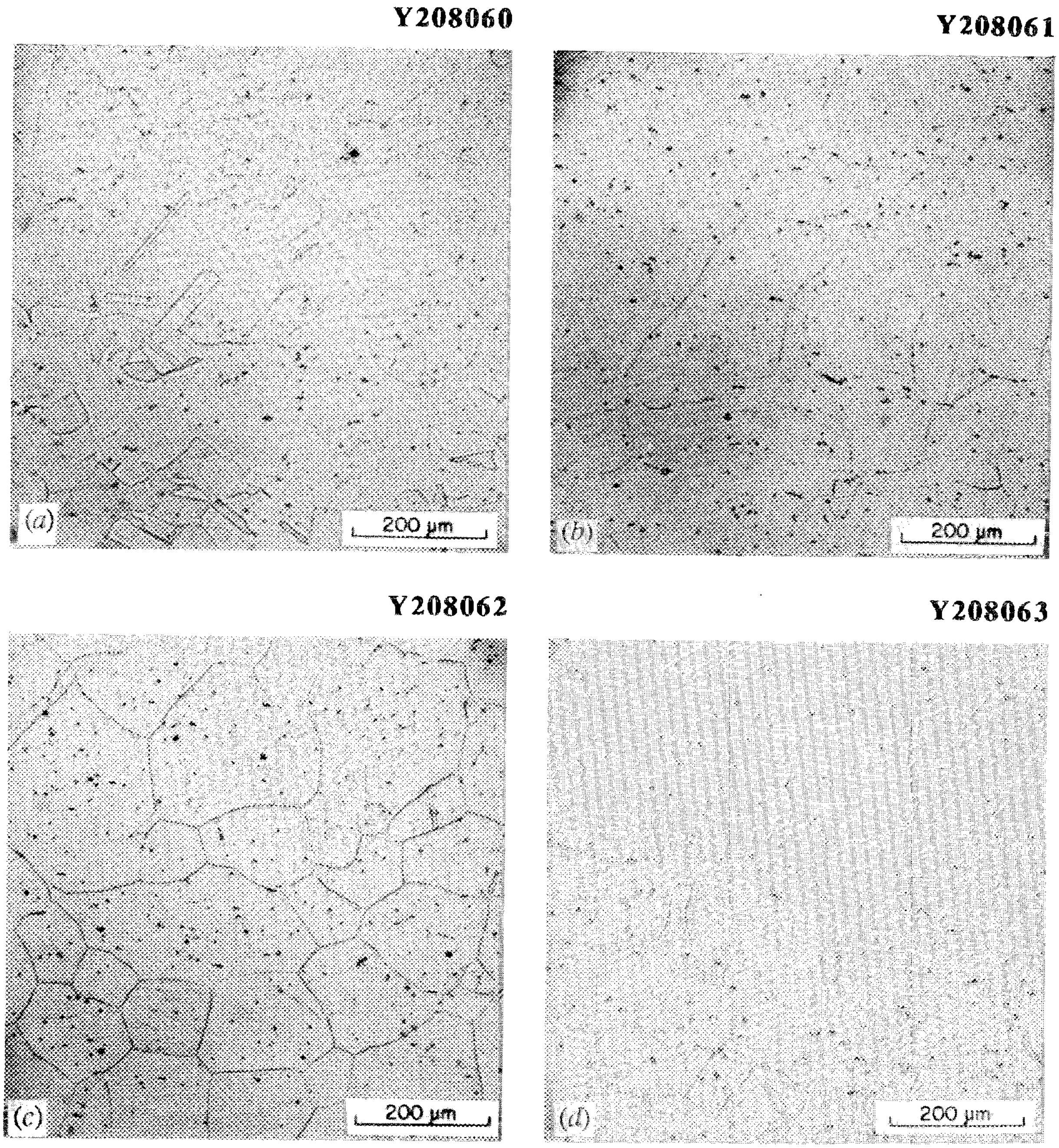


**Fig. A.2. Photomicrographs of microstructures of the cold-rolled AX series of HT-UPS alloys: (*a*) AX5, (*b*) AX6, (*c*) AX7, and (*d*) AX8.**

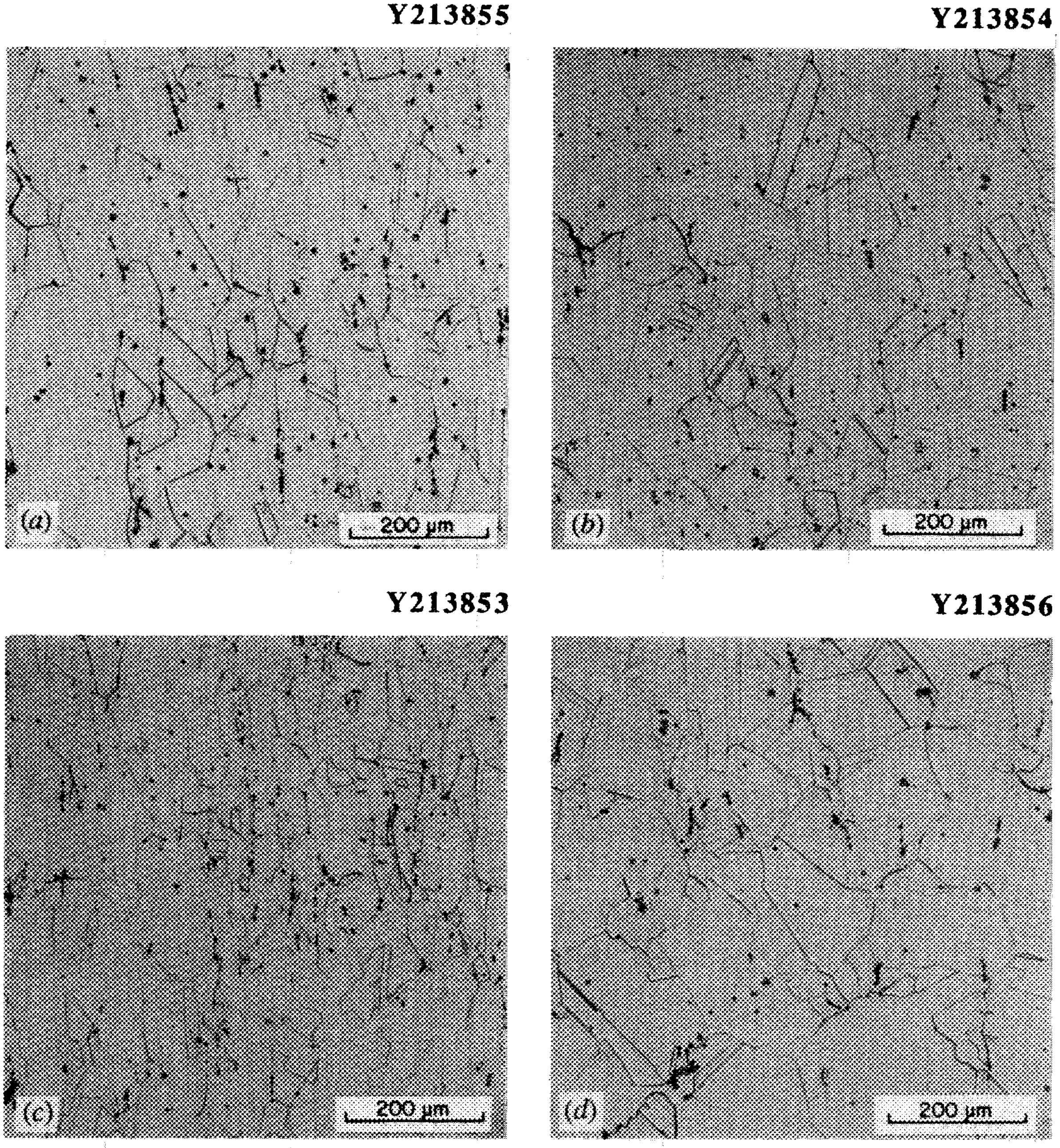


**Fig. A.3. Photomicrographs of the microstructures of the cold-rolled 13-mm plates of the MS series of HT-UPS alloys: (*a*) MS1, (*b*) MS4, (*c*) MS4, and (*d*) MS6.**

Y213849

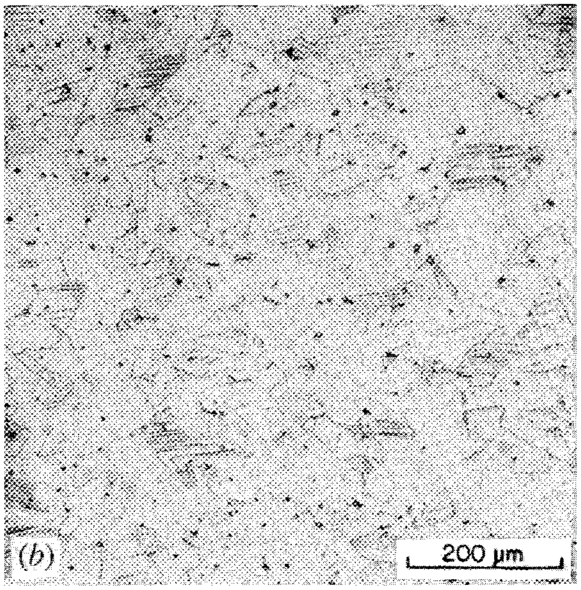


Y213850

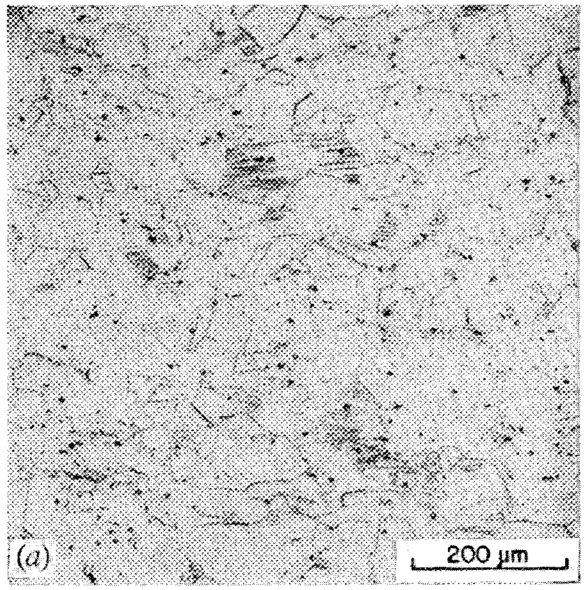


Y213852

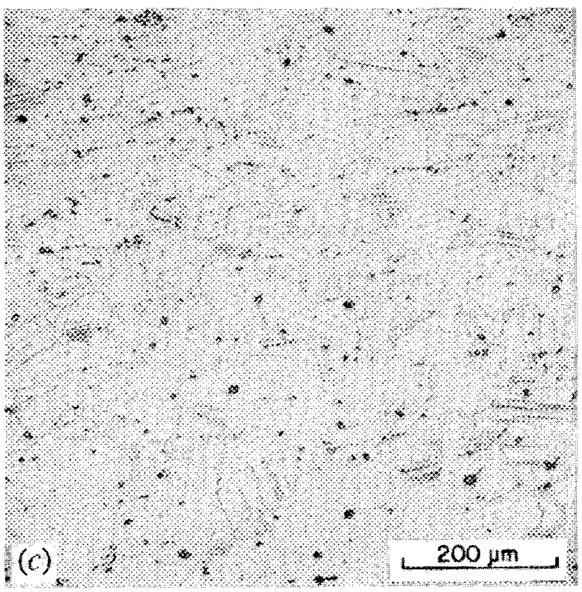


Y213851

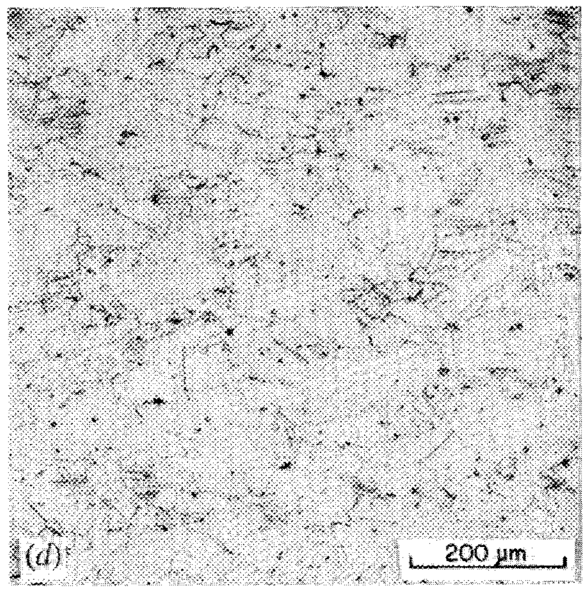


**Fig. A.4. Photomicrographs of the microstructures of the cold-rolled 6.3-mm plates of the MS series HT-UPS alloys: (*a*) MS1, (*b*) MS4, (*c*) MS5, and (*d*) MS6.**

Y216714

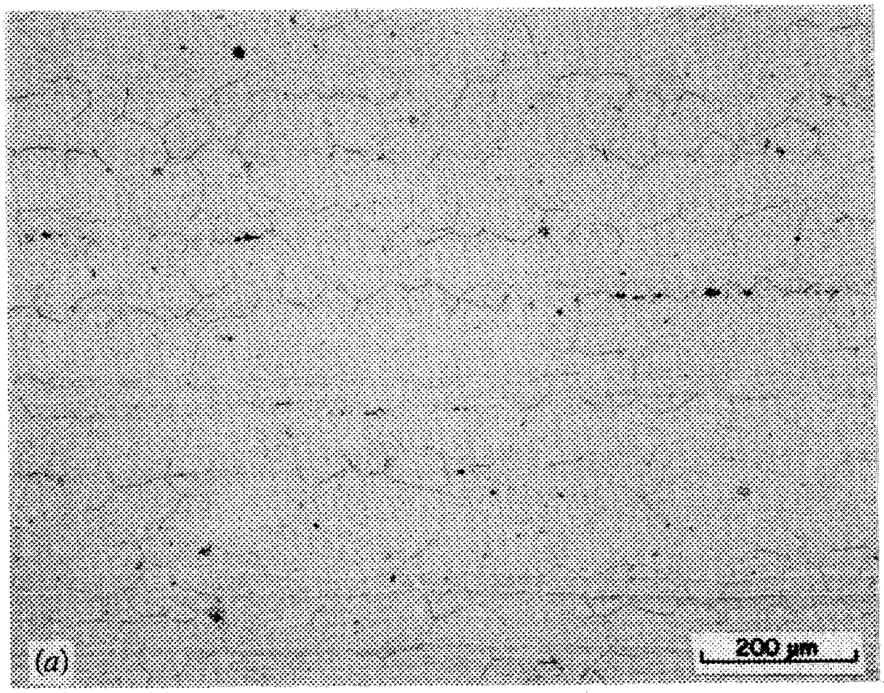


Y216713

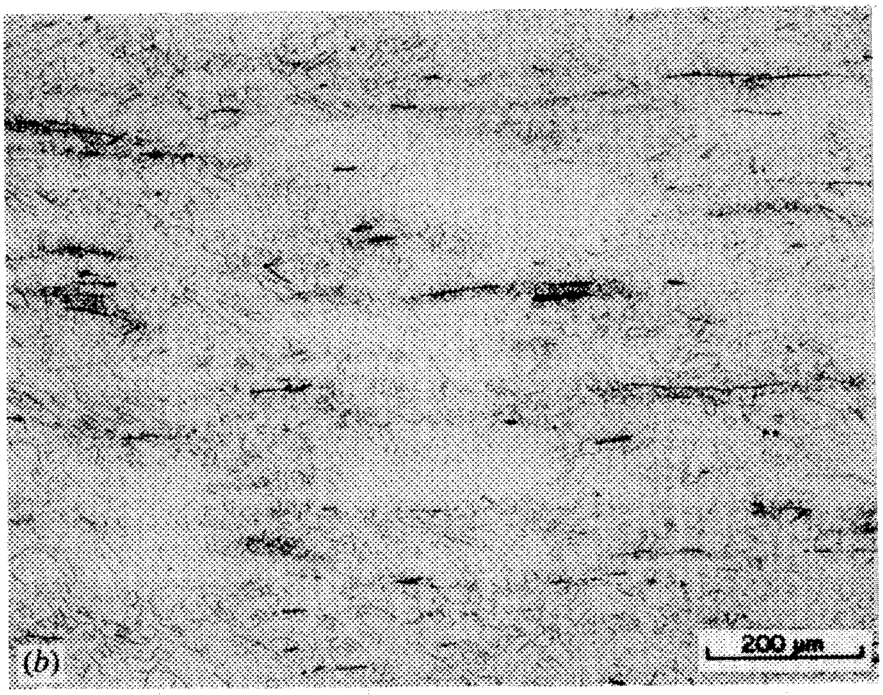


**Fig. A.5. Photomicrographs of the microstructures of (*a*) the BWT as-extruded tubing and (*b*) cold-pilgered and annealed CET tubing.**

# APPENDIX B

# TENSILE DATA FOR HT-UPS ALLOYS

## Table B1. Tensile data for MS alloys

| Test | Specimen | Condition | Temp (°C) | Rate (1/min) | Yield (MPa) | Ultimate (MPa) | UE (%) | Fracture (MPa) | Elong. (%) | RA (%) |
|---|---|---|---|---|---|---|---|---|---|---|
| 26698 | CE0-01 | 1115 | 700 | 0.05 | 157 | 358 | 16.5 | 225 | 44.10 | 60.96 |
| 26699 | CE0-05 | Mill | 25 | 0.05 | 395 | 615 | 24.7 | 419 | 48.20 | 75.85 |
| 26700 | CE0-08 | 1115 | 25 | 0.05 | 228 | 580 | 31.1 | 392 | 56.10 | 74.97 |
| 26701 | CE1-11 | 1200 | 700 | 0.005 | 123 | 359 | 25.4 | 187 | 26.30 | 45.76 |
| 26702 | CE1-13 | 1115 | 25 | 0.005 | 213 | 565 | 29.2 | 342 | 55.60 | 74.98 |
| 26703 | CE1-15 | Mill | 25 | 0.005 | 231 | 561 | 34.5 | 362 | 58.00 | 76.51 |
| 26704 | CE1-17 | Mill | 700 | 0.005 | 155 | 330 | 16.2 | 191 | 43.80 | 67.44 |
| 26705 | CE1-18 | 1200 | 25 | 0.005 | 175 | 551 | 54.9 | 366 | 72.30 | 75.06 |
| 26706 | CE2-01 | Mill | 700 | 0.005 | 246 | 350 | 10.6 | 211 | 42.00 | 64.47 |
| 26707 | CE2-04 | 1115 | 700 | 0.005 | 149 | 323 | 19.0 | 161 | 51.90 | 67.34 |
| 26708 | CE2-07 | 1200 | 700 | 0.005 | 120 | 345 | 24.8 | 211 | 38.20 | 42.96 |
| 26709 | CE2-08 | 1115 | 25 | 0.005 | 225 | 585 | 36.9 | 387 | 47.70 | 75.41 |
| 26710 | CE2-09 | Mill | 25 | 0.005 | 402 | 628 | 27.0 | 436 | 61.00 | 75.27 |
| 26711 | CE3-09 | 1115 | 25 | 0.005 | 222 | 567 | 32.6 | 365 | 55.10 | 73.98 |
| 26712 | CE3-13 | Mill | 25 | 0.005 | 392 | 592 | 26.4 | 368 | 47.10 | 77.11 |
| 26673 | CE3-28 | Mill | 700 | 0.05 | 292 | 414 | 15.4 | 276 | 66.60 | 38.20 |

## Table B2. Tensile data for MS alloys

| Test | Specimen | Condition | Temp (°C) | Rate (1/min) | Yield (MPa) | Ultimate (MPa) | UE (%) | Fracture (MPa) | Elong. (%) | RA (%) |
|---|---|---|---|---|---|---|---|---|---|---|
| 26890 | AX5-05 | Mill | 25 | 0.05 | 511 | 616 | 24.03 | 445 | 44.00 | 71.62 |
| 26891 | AX5-06 | Mill | 700 | 0.05 | 352 | 434 | | 269 | 25.40 | 62.40 |
| 26892 | AX5-33 | 760/24 h | 25 | 0.05 | 462 | 547 | 10.70 | 325 | 26.00 | 65.00 |
| 26893 | AX5-35 | 700/24 h | 25 | 0.05 | 577 | 729 | 15.00 | 503 | 21.80 | 60.00 |
| 26894 | AX5-36 | 730/24 h | 25 | 0.05 | 526 | 709 | 16.00 | 503 | 23.70 | 63.60 |
| 26895 | AX5-37 | Mill | 25 | 0.05 | 421 | 538 | 16.00 | 364 | 29.70 | 69.20 |
| 26896 | AX5-41 | 650/24 h | 25 | 0.05 | 513 | 679 | 20.00 | 519 | 27.50 | 60.70 |
| 26897 | AX6-05 | Mill | 25 | 0.05 | 457 | 609 | 30.25 | 432 | 51.00 | 72.84 |
| 26898 | AX6-06 | Mill | 700 | 0.05 | 316 | 432 | 14.00 | 279 | 30.70 | 62.08 |
| 26899 | AX7-05 | Mill | 25 | 0.05 | 467 | 607 | 24.02 | 431 | 37.58 | 73.42 |
| 26900 | AX7-06 | Mill | 700 | 0.05 | 319 | 431 | 13.97 | 299 | 30.00 | 56.36 |
| 25616 | AX7-08 | 650/20,000 h | 25 | 0.05 | 523 | 698 | 14.19 | 688 | 17.12 | 19.00 |
| 26901 | AX8-05 | Mill | 25 | 0.05 | 451 | 601 | 28.93 | 446 | 48.60 | 73.42 |
| 26902 | AX8-06 | Mill | 700 | 0.05 | 313 | 419 | 14.73 | 264 | 31.70 | 53.60 |

## Table B3. Tensile data for MS alloys

| Test | Specimen | Condition | Temp (°C) | Rate (1/min) | Yield (MPa) | Ultimate (MPa) | UE (%) | Fracture (MPa) | Elong. (%) | RA (%) |
|---|---|---|---|---|---|---|---|---|---|---|
| 25864 | MS1a-01 | Mill | 25 | 0.05 | 508 | 650 | 23.03 | 478 | 44.90 | 67.73 |
| 25865 | MS1a-02 | Mill | 600 | 0.05 | 366 | 541 | 21.47 | 227 | 51.67 | 62.40 |
| 25866 | MS1a-03 | Mill | 700 | 0.05 | 362 | 446 | 09.29 | 302 | 31.10 | 52.94 |
| 25862 | MS1b-01 | Mill | 25 | 0.05 | 675 | 752 | 11.43 | 553 | 19.00 | 60.38 |
| 25889 | MS1b-03 | 725/6 h | 25 | 0.05 | 700 | 812 | 12.17 | 599 | 19.30 | 52.26 |
| 25888 | MS1b-06 | Mill | 25 | 0.05 | 686 | 785 | 13.85 | 525 | 25.00 | |
| 25867 | MS4a-01 | Mill | 25 | 0.05 | 515 | 653 | 20.55 | 492 | 30.00 | 62.59 |
| 25868 | MS4a-02 | Mill | 600 | 0.05 | 381 | 530 | 17.36 | 485 | 27.30 | 49.30 |
| 25869 | MS4a-03 | Mill | 700 | 0.05 | 400 | 458 | 07.35 | 295 | 34.00 | 59.29 |
| 25863 | MS4b-01 | Mill | 25 | 0.05 | 690 | 758 | 09.79 | 525 | 21.24 | 55.55 |
| 25890 | MS4b-03 | 725/6 h | 25 | 0.05 | 719 | 838 | 13.39 | 636 | 21.21 | 57.12 |
| 25870 | MS5a-01 | Mill | 25 | 0.05 | 525 | 674 | 21.27 | 520 | 33.20 | 63.85 |
| 25871 | MS5a-02 | Mill | 600 | 0.05 | 394 | 567 | 20.04 | 481 | 31.60 | 43.99 |
| 25872 | MS5a-03 | Mill | 700 | 0.05 | 376 | 479 | 11.22 | 354 | 32.60 | 50.60 |
| 25915 | MS5a-05 | 725/6 h | 25 | 0.05 | 587 | 750 | 19.28 | 630 | 33.70 | 57.14 |
| 25916 | MS5a-06 | 725/6 h | 100 | 0.05 | 542 | 680 | 16.53 | 559 | 28.20 | 53.38 |
| 25917 | MS5a-07 | 725/6 h | 200 | 0.05 | 562 | 700 | 11.96 | 552 | 25.30 | 50.03 |
| 25918 | MS5a-08 | 725/6 h | 300 | 0.05 | 533 | 658 | 12.31 | 545 | 24.20 | 53.38 |
| 25919 | MS5a-09 | 725/6 h | 400 | 0.05 | 474 | 635 | 19.20 | 541 | 28.10 | 40.40 |
| 25920 | MS5a-10 | 725/6 h | 500 | 0.05 | 456 | 601 | 13.18 | 499 | 20.00 | 38.53 |
| 25921 | MS5a-11 | 725/6 h | 600 | 0.05 | 442 | 552 | 10.17 | 439 | 22.30 | 38.67 |
| 25922 | MS5a-12 | 725/6 h | 700 | 0.05 | 421 | 453 | 02.14 | 288 | 30.00 | 59.03 |
| 25876 | MS5b-01 | Mill | 25 | 0.05 | 730 | 791 | 12.77 | 553 | 23.93 | 55.55 |
| 25891 | MS5b-02 | 725/6 h | 25 | 0.05 | 735 | 835 | 13.07 | 664 | 21.54 | 54.49 |
| 25873 | MS6a-01 | Mill | 25 | 0.05 | 476 | 656 | 24.44 | 411 | 49.60 | 63.71 |
| 25874 | MS6a-02 | Mill | 600 | 0.05 | 358 | 551 | 18.81 | 454 | 31.60 | 50.71 |
| 25875 | MS6a-03 | Mill | 700 | 0.05 | 353 | 475 | 13.12 | 385 | 38.20 | 53.56 |
| 25877 | MS6b-01 | Mill | 25 | 0.05 | 007 | 753 | 09.17 | 534 | 17.52 | 68.19 |
| 25892 | MS6b-03 | 725/6 h | 25 | 0.05 | 708 | 791 | 09.45 | 636 | 15.73 | 59.38 |

## Table B4. Tensile data for MS alloys

| Test | Specimen | Condition | Temp (°C) | Rate (1/min) | Yield (MPA) | Ultimate (MPA) | UE (%) | Fracture (MPa) | Elong. (%) | RA (%) |
|---|---|---|---|---|---|---|---|---|---|---|
| 25991 | CET-01 | Mill | 25 | 0.05 | 293 | 606 | 32.7 | 419 | 33.42 | 78.45 |
| 25992 | CET-02 | Mill | 100 | 0.05 | 272 | 529 | 25.7 | 354 | 35.46 | 70.40 |
| 25993 | CET-03 | Mill | 200 | 0.05 | 223 | 457 | 25.0 | 343 | 31.37 | 66.93 |
| 25994 | CET-04 | Mill | 300 | 0.05 | 215 | 504 | 26.6 | 368 | 32.88 | 61.25 |
| 25995 | CET-05 | Mill | 400 | 0.05 | 202 | 534 | 38.5 | 421 | 44.70 | 55.91 |
| 25996 | CET-06 | Mill | 500 | 0.05 | 195 | 498 | 28.3 | 362 | 33.33 | 61.74 |
| 25997 | CET-07 | Mill | 600 | 0.05 | 185 | 469 | 24.2 | 341 | 33.15 | 60.55 |
| 25998 | CET-08 | Mill | 700 | 0.05 | 178 | 343 | 22.9 | 200 | 37.51 | 62.43 |

## Table B5. Tensile data for MS alloys

| Test | Specimen | Condition | Temp (°C) | Rate (1/min) | Yield (MPa) | Ultimate (MPa) | UE (%) | Fracture (MPa) | Elong. (%) | RA (%) |
|---|---|---|---|---|---|---|---|---|---|---|
| 26066 | BWT4-04 | Mill | 25 | 0.05 | 171 | 490 | 37.8 | 285 | 55.12 | 82.81 |
| 26067 | BWT4-05 | Mill | 100 | 0.05 | 150 | 457 | 30.4 | 250 | 50.15 | 85.14 |
| 26068 | BWT4-06 | Mill | 200 | 0.05 | 124 | 424 | 33.0 | 237 | 46.08 | 85.97 |
| 26069 | BWT4-07 | Mill | 300 | 0.05 | 118 | 432 | 37.3 | 273 | 48.64 | 78.95 |
| 26070 | BWT4-08 | Mill | 400 | 0.05 | 108 | 439 | 38.3 | 275 | 49.60 | 73.96 |
| 26071 | BWT4-09 | Mill | 500 | 0.05 | 103 | 421 | 41.9 | 277 | 50.87 | 69.26 |
| 26072 | BWT4-10 | Mill | 600 | 0.05 | 097 | 371 | 41.5 | 260 | 53.01 | 76.58 |
| 26073 | BWT4-11 | Mill | 700 | 0.05 | 090 | 355 | 29.4 | 203 | 45.83 | 72.71 |
| 26801 | BWT4-45 | 700/5000 | 25 | 0.05 | 275 | 539 | 28.1 | 446 | 43.00 | 60.50 |
| 26652 | CS5-06 | 5% Cold sunk | 25 | 0.05 | 483 | 577 | 13.5 | 319 | 38.10 | 80.40 |
| 26653 | CS5-07 | 5% Cold sunk | 700 | 0.05 | 337 | 408 | 08.5 | 212 | 21.50 | 78.10 |
| 26654 | CS10-03 | 10% Cold sunk | 25 | 0.05 | 667 | 713 | 02.4 | 393 | 25.50 | 78.28 |
| 26655 | CS10-07 | 10% Cold sunk | 700 | 0.05 | 486 | 508 | 01.0 | 247 | 25.00 | 69.88 |
| 26054 | BWT4-28 | Cold forged | 25 | 0.05 | 535 | 596 | 11.7 | 335 | 79.23 | 36.90 |
| 26055 | BWT4-29 | Cold forged | 500 | 0.05 | 313 | 467 | 23.6 | 319 | 34.00 | 70.38 |
| 26056 | BWT4-30 | Cold forged | 700 | 0.05 | 343 | 413 | 05.0 | 211 | 25.60 | 80.00 |
| 26273 | BWT2-01 | Mill | 25 | 0.05 | 209 | 496 | 40.9 | 288 | 57.80 | 82.61 |
| 26276 | BWT2-02 | Mill | 700 | 0.05 | 135 | 356 | 27.4 | 194 | 48.00 | 82.10 |

# Table B6. Tensile data for aged alloy CE1

| Specimen | Condition | Temp. (°C) | Aging time (h) | Yield strength (MPa) | Ultimate strength (MPa) | Uniform strain (%) | Elongation (%) |
|---|---|---|---|---|---|---|---|
| 28 | Annealed | 600 | 1 | 139 | 406 | 27.4 | 29.0 |
| 37 | Annealed | 600 | 1 | 147 | 425 | 30.3 | 33.1 |
| 16 | Annealed | 600 | 10 | 157 | 429 | 29.5 | 31.3 |
| 31 | Annealed | 600 | 1,000 | 224 | 406 | 17.1 | 19.1 |
| 13 | Annealed | 600 | 1,000 | 179 | 418 | 23.5 | 25.5 |
| 35 | Annealed | 600 | 10,000 | 259 | 415 | 11.4 | 12.8 |
| 26 | Annealed | 600 | 10,000 | 255 | 418 | 12.9 | 15.0 |
| 5 | Annealed | 700 | 1 | 141 | 356 | 21.5 | 24.0 |
| 27 | Annealed | 700 | 1 | 163 | 360 | 21.6 | 24.6 |
| 30 | Annealed | 700 | 10 | 165 | 361 | 20.5 | 24.8 |
| 51 | Annealed | 700 | 10 | 164 | 351 | 18.6 | 20.9 |
| 24 | Annealed | 700 | 1,000 | 232 | 316 | 08.4 | 11.4 |
| 47 | Annealed | 700 | 1,000 | 233 | 325 | 09.3 | 12.3 |
| 29 | Annealed | 700 | 10,000 | 224 | 325 | 07.6 | 14.3 |
| 25 | Annealed | 700 | 10,000 | 221 | 323 | 08.0 | 15.8 |
| 9 | Annealed | 800 | 1 | 173 | 215 | 07.0 | 15.0 |
| 19 | Annealed | 800 | 1 | 155 | 229 | 09.3 | 16.4 |
| 14 | Annealed | 800 | 10 | 184 | 214 | 05.0 | 14.5 |
| 50 | Annealed | 800 | 10 | 186 | 217 | 04.5 | 13.8 |
| 20 | Annealed | 800 | 1,000 | 153 | 180 | 05.6 | 18.8 |
| 23 | Annealed | 800 | 1,000 | 153 | 184 | 05.8 | 17.8 |
| 22 | Annealed | 800 | 10,000 | 143 | 178 | 06.8 | 22.8 |
| 4 | Annealed | 800 | 10,000 | 142 | 181 | 06.6 | 16.9 |
| 35 | 5% | 600 | 1 | 222 | 430 | 22.6 | 24.8 |
| 27 | 5% | 600 | 1 | 222 | 434 | 22.0 | 23.5 |
| 3 | 5% | 600 | 10 | 229 | 439 | 22.6 | 25.0 |
| 15 | 5% | 600 | 10 | 225 | 428 | 19.9 | 21.1 |
| 24 | 5% | 600 | 1,000 | 300 | 442 | 11.4 | 13.5 |
| 29 | 5% | 600 | 10,000 | 313 | 433 | 08.4 | 10.1 |
| 37 | 5% | 700 | 1 | 222 | 384 | 16.0 | 18.3 |
| 28 | 5% | 700 | 1 | 225 | 378 | 15.5 | 17.9 |
| 18 | 5% | 700 | 10 | 227 | 337 | 12.5 | 16.3 |
| 4 | 5% | 700 | 1,000 | 280 | 360 | 07.6 | 10.8 |
| 36 | 5% | 700 | 10,000 | 255 | 341 | 07.0 | 11.4 |
| 2 | 5% | 800 | 1 | 217 | 232 | 02.8 | 13.8 |
| 34 | 5% | 800 | 1 | 224 | 235 | 02.6 | 15.8 |
| 10 | 5% | 800 | 10 | 224 | 243 | 03.1 | 15.0 |
| 8 | 5% | 800 | 1,000 | 185 | 207 | 03.6 | 11.1 |
| 13 | 5% | 800 | 10,000 | 167 | 197 | 06.4 | 19.0 |
| 28 | 10% | 600 | 1 | 332 | 471 | 11.9 | 13.1 |
| 45 | 10% | 600 | 1 | 346 | 465 | 12.8 | 14.6 |
| 16 | 10% | 600 | 10 | 324 | 463 | 11.0 | 12.4 |
| 17 | 10% | 600 | 10 | 323 | 464 | 14.3 | 15.6 |
| 6 | 10% | 600 | 1,000 | 400 | 500 | 06.4 | 07.8 |
| 19 | 10% | 600 | 1,000 | 406 | 500 | 06.1 | 08.0 |
| 38 | 10% | 600 | 10,000 | 403 | 482 | 05.9 | 07.0 |
| 27 | 10% | 600 | 10,000 | 390 | 478 | 05.1 | 05.9 |
| 13 | 10% | 700 | 1 | 317 | 393 | 07.6 | 12.0 |
| 7 | 10% | 700 | 1 | 322 | 398 | 06.8 | 10.0 |
| 1 | 10% | 700 | 10 | 344 | 397 | 04.4 | 08.3 |
| 9 | 10% | 700 | 10 | 329 | 382 | 04.6 | 11.0 |
| 2 | 10% | 700 | 1,000 | 327 | 380 | 04.6 | 06.3 |
| 18 | 10% | 700 | 1,000 | 335 | 396 | 04.8 | 07.0 |
| 5 | 10% | 700 | 10,000 | 298 | 370 | 05.5 | 11.8 |
| 12 | 10% | 700 | 10,000 | 297 | 365 | 05.4 | 10.9 |
| 46 | 10% | 800 | 1 | 287 | 302 | 01.6 | 09.1 |
| 26 | 10% | 800 | 1 | 274 | 289 | 01.4 | 08.5 |
| 31 | 10% | 800 | 10 | 270 | 282 | 01.8 | 10.0 |
| 21 | 10% | 800 | 10 | 268 | 283 | 01.6 | 07.4 |
| 11 | 10% | 800 | 1,000 | 209 | 220 | 02.0 | 11.4 |
| 25 | 10% | 800 | 1,000 | 206 | 217 | 02.0 | 10.9 |
| 37 | 10% | 800 | 10,000 | 176 | 195 | 03.4 | 15.8 |
| 14 | 10% | 800 | 10,000 | 177 | 196 | 03.1 | 17.8 |

# APPENDIX C

# CREEP RUPTURE DATA FOR HT-UPS ALLOYS

# Table C1. Creep rupture data

| Test | Specimen | Condition | Temperature (°C) | Stress (MPa) | Minimum creep rate (%/h) | Time 1% (h) | Life (h) | In test (h) | Elongation (%) | RA (%) |
|---|---|---|---|---|---|---|---|---|---|---|
| 24740 | CE0-02 | 1115 | 700 | 170 | 1.80E-04 | 700 | | 553 | | |
| 24738 | CE0-03 | Hot rolled | 700 | 170 | 5.60E-05 | | | 691 | | |
| 24568 | CEO-04 | 1115 | 700 | 170 | 2.90E-04 | 4 | 238 | | 43.00 | 81.60 |
| 24575 | CEO-06 | 1115/5% cw/age | 700 | 181 | 1.34E-03 | 260 | 502 | | 35.50 | 74.70 |
| 24886 | CEO-07 | 1115/2% cw/age | 700 | 170 | 9.00E-03 | 7 | 189 | | 23.00 | 71.10 |
| 24569 | CEO-10 | 1115/5% cw | 700 | 179 | 3.00E-04 | 1,000 | 1519 | | 26.50 | 77.90 |
| 24908 | CEO-11 | 1200/5% cw | 700 | 170 | 6.50E-05 | 4,400 | 6981 | | 29.50 | 58.30 |
| 24579 | CEO-12 | 1115/2% cw | 700 | 170 | 1.00E-05 | 1,200 | 1722 | | 30.20 | 81.00 |
| 24900 | CEO-13 | Hot rolled | 700 | 170 | 1.00E-05 | 3,200 | 6174 | | 28.80 | 61.50 |
| 24876 | CEO-14 | 1200 | 700 | 170 | 1.40E-04 | 3,430 | 5098 | | 28.00 | 58.00 |
| 24720 | CE1-01 | Hot rolled | 700 | 100 | 3.20E-05 | | | 7,315 | | |
| 24725 | CE1-05 | 1115 | 700 | 100 | 1.55E-03 | 310 | | 2,662 | | |
| 24986 | CE1-08 | 1200/5% cw | 700 | 170 | 5.00E-05 | 3,100 | 5693 | | 23.60 | 56.50 |
| 24723 | CE1-09 | Hot rolled | 700 | 172 | 1.00E-04 | 730 | 1432 | | 40.10 | 71.30 |
| 24909 | CE1-12 | 1200 | 700 | 170 | 6.00E-05 | 2,350 | 3728 | | 35.30 | 63.80 |
| 24952 | CE2-02 | Hot rolled/aged | 700 | 170 | 1.00E-04 | 2,750 | 4136 | | 25.00 | 58.10 |
| 24918 | CE2-06 | 1200/aged | 700 | 170 | 7.20E-04 | 530 | 771 | | 34.50 | 73.10 |
| 24950 | CE2-10 | 1200/aged | 700 | 170 | 6.00E-04 | 200 | 464 | | 35.00 | 74.80 |
| 24903 | CE2-12 | 1200 | 700 | 170 | 1.40E-04 | 1,950 | 2713 | | 36.00 | 70.80 |
| 24739 | CE2-14 | 1115 | 700 | 170 | 1.60E-04 | 900 | 1415 | | 31.50 | 78.30 |
| 24738 | CE2-15 | Hot rolled | 700 | 170 | 1.10E-04 | 1,910 | 2365 | | 14.40 | 41.50 |
| 24735 | CE3-01 | Hot rolled | 700 | 170 | 6.00E-05 | 2,900 | 4941 | | 13.20 | 45.80 |
| 24776 | CE3-02 | Hot rolled/aged | 700 | 170 | 1.10E-04 | 2,200 | 3795 | | 23.00 | 53.00 |
| 24832 | CE3-03 | Hot rolled | 730 | 170 | 8.90E-04 | 960 | 1776 | | 17.50 | 54.00 |
| 24833 | CE3-04 | Hot rolled | 700 | 200 | 3.00E-04 | 1,240 | 1828 | | 26.80 | 70.40 |
| 24747 | CE3-05 | Hot rolled | 760 | 138 | 4.10E-04 | 950 | 1175 | | 13.60 | 41.60 |
| 24751 | CE3-06 | Hot rolled | 760 | 200 | 5.20E-03 | 40 | 53.8 | | 25.20 | 74.20 |
| 24773 | CE3-07 | 1115 | 700 | 100 | 1.80E-05 | 4,400 | 9392 | | 24.90 | 58.30 |
| 24944 | CE3-08 | 1115 | 760 | 140 | 4.00E-03 | 45 | 99.6 | | 54.40 | 75.40 |
| 24828 | CE3-10 | Hot rolled | 760 | 170 | 2.40E-03 | 122 | 229 | | 23.30 | 70.20 |
| 24825 | CE3-11 | Hot rolled | 700 | 100 | 8.00E-06 | | | 38,000 | | |
| 24775 | CE3-12 | 1115 | 700 | 170 | 2.90E-04 | 900 | 1391 | | 29.20 | 34.70 |
| 24838 | CE3-14 | Hot rolled | 700 | 140 | 3.70E-05 | 15,500 | 21204 | | 11.60 | 23.30 |
| 24946 | CE3-15 | Hot rolled | 760 | 170 | 6.00E-04 | 205 | | | | |
| | CE3-15 | Crept | 760 | 110 | 1.10E-04 | | | | | |
| | CE3-15 | Crept | 760 | 133 | 1.50E-03 | | | | | |
| | CE3-15 | Crept | 760 | 100 | 1.40E-04 | | | | | |
| | CE3-15 | Crept | 760 | 170 | | | 287 | | 19.10 | 60.40 |
| 24901 | CE3-16 | Hot rolled | 800 | 100 | 6.40E-04 | 925 | 1297 | | | |
| 24892 | CE3-17 | Hot rolled | 700 | 240 | 1.10E-03 | 375 | 630 | | 20.00 | 44.60 |
| 24902 | CE3-18 | 1200 | 700 | 170 | 1.40E-04 | 2,200 | 3309 | | 20.00 | 49.80 |
| 24884 | CE3-19 | Hot rolled | 700 | 120 | 1.80E-05 | | | 38,000 | | |
| 24891 | CE3-20 | Hot rolled | 760 | 100 | 1.70E-04 | 4,300 | 5313 | | | |
| 26672 | CE3-26 | Hot rolled | 650 | 300 | 5.00E-05 | 260 | 4045 | 3,500 | | |
| 26729 | CE3-27 | Hot rolled | 700 | 300 | 2.00E-03 | 2 | 317 | | 13.52 | 34.82 |
| 26676 | CE3-29 | Hot rolled | 675 | 300 | 6.00E-04 | 10 | 997 | | 13.12 | 29.80 |
| 25379 | CE3-21 | 1200 | 650 | 100 | 3.50E-06 | | | 25,000 | | |
| | CE3-21 | 1200/crept | 650 | 133 | 1.50E-05 | | | 22,000 | | |
| | CE3-21 | 1200/crept | 650 | 170 | 2.80E-04 | | | | | |
| 25416 | CE3-22 | Hot rolled | 700 | 100 | 1.00E-05 | | | 22,000 | | |
| 26035 | CE3-23 | 1200/9% cw | 650 | 200 | 1.00E-05 | | | 10,980 | | |
| | CE3-23 | Crept | 650 | 274 | 1.80E-02 | | | 20,493 | | |
| | CE3-23 | Crept | 650 | 235 | 7.00E-05 | | | | 24.00 | 29.16 |
| 25417 | CE3-24 | 1200 | 700 | 100 | 2.10E-05 | 12,000 | 20,493 | | 12.00 | 32.10 |
| 25861 | CE3-25 | Hot rolled | 650 | 100 | 4.00E-06 | | | | | |
| | CE3-25 | Crept | 650 | 133 | 6.00E-06 | | | | | |
| | CE3-25 | Crept | 650 | 170 | | | | 10,000 | | |
| 25385 | AX5-01 | 1200 | 700 | 170 | 1.10E-04 | 2,500 | 4,171 | | 33.90 | 61.60 |
| 25562 | AX5-02 | 1200/2% cw | 700 | 170 | 3.00E-05 | 2,700 | 4,692 | | 39.20 | 66.90 |
| 25572 | AX5-03 | 1200/2%/aged | 700 | 170 | 2.00E-01 | 1.8 | 94.2 | | 67.80 | 69.60 |
| 25355 | AX5-07 | Cold rolled | 700 | 170 | | | | 30,000 | | |
| 25665 | AX5-09 | 1200 | 600 | 350 | 1.40E-04 | 1,500 | 1,956 | | 45.00 | 5,936.00 |
| 25806 | AX5-12 | Cold rolled | 600 | 300 | 6.00E-06 | | | 11,300 | 16.00 | 62.00 |
| 25741 | AX5-14 | Cold rolled | 600 | 350 | 1.30E-05 | | | 20,000 | | |
| 25684 | AX5-20 | Cold rolled | 600 | 400 | 3.00E-04 | 2,400 | 2,830 | | 14.90 | 50.80 |
| 25685 | AX5-21 | Cold rolled | 600 | 375 | 1.70E-04 | 5,122 | 5,122 | | 15.40 | 39.10 |
| 25686 | AX5-22 | Cold rolled | 600 | 350 | 1.00E-05 | | | 20,000 | | |
| 25687 | AX5-23 | Cold rolled | 600 | 325 | | | | 20,000 | | |
| 25688 | AX5-24 | Cold rolled | 600 | 300 | | | | 4,250 | | |
| | AX5-24 | Crept | 600 | 375 | 3.60E-04 | | 1,436 | | | |

# Table C1. Creep rupture data (continued)

| Test | Specimen | Condition | Temperature (°C) | Stress (MPa) | Minimum creep rate (%/h) | Time 1% (h) | Life (h) | In test (h) | Elongation (%) | RA (%) |
|---|---|---|---|---|---|---|---|---|---|---|
| 25689 | AX5-25 | 600/1300 h aged | 600 | 350 | 5.00E-05 | 12,500 | 18,566 | | | |
| 25690 | AX5-26 | 600/2518 h aged | 600 | 350 | 1.60E-04 | 4,600 | 8,364 | | | |
| 25691 | AX5-27 | 600/4055 h aged | 600 | 450 | 5.00E-01 | 1.8 | 12.2 | | 18.70 | 42.10 |
| 25692 | AX5-28 | 600/4055 h aged | 600 | 400 | 5.00E-02 | 20 | 127 | | 20.20 | 51.30 |
| 25693 | AX5-29 | 600/4221 h aged | 600 | 350 | 2.50E-05 | 5,300 | 6,472 | | | |
| 26008 | AX5-30 | Cold rolled | 600 | 450 | | 785 | 802 | | | |
| 25391 | AX6-01 | 1200 | 700 | 170 | 1.20E-04 | 2,900 | 4,919 | | 38.60 | 62.30 |
| 25043 | AX6-07 | Cold rolled | 700 | 170 | 4.00E-05 | | 5,733 | | | |
| 25654 | AX6-13 | 1200 | 800 | 100 | 1.60E-02 | 26 | 127 | | 63.30 | 71.90 |
| 25745 | AX6-16 | Chromized | 700 | 120 | 2.00E-04 | 1,380 | 3,559 | | 26.70 | 42.10 |
| 25649 | AX6-17 | Chromized | 800 | 100 | 6.00E-02 | 10 | 47 | | 55.00 | 75.40 |
| 25650 | AX6-18 | Chromized | 700 | 170 | 6.20E-04 | 7 | 630 | | 19.90 | 60.30 |
| 25670 | AX6-19 | Chromized | 700 | 170 | 2.70E-03 | 1 | 521 | | 23.00 | 32.70 |
| 25390 | AX7-01 | 1200 | 700 | 170 | 1.00E-04 | 2,000 | 2,804 | | 32.70 | 63.60 |
| 25461 | AX7-02 | 1200 | 650 | 200 | 2.00E-05 | 20,600 | 25,891 | | 24.20 | 52.90 |
| 25492 | AX7-03 | 1200/2% cw | 700 | 170 | 1.50E-04 | 2,000 | 2,888 | | 33.30 | 69.60 |
| 25563 | AX7-04 | 1200/2% cw/aged | 700 | 170 | 3.00E-04 | 20 | 910 | | 36.20 | 65.10 |
| 25044 | AX7-07 | Cold rolled | 700 | 170 | 3.60E-05 | 6,500 | 6,695 | | 13.60 | 45.40 |
| 25616 | AX7-08 | Cold rolled | 650 | 240 | 2.00E-05 | | | 25,000 | | |
| 25592 | AX7-09 | 1200 | 675 | 200 | 1.50E-05 | 8,200 | 10,112 | | 28.60 | 50.00 |
| 25610 | AX7-10 | Cold rolled | 700 | 190 | 2.20E-05 | 4,400 | 4,599 | | 10.10 | 44.70 |
| 25609 | AX7-11 | Cold rolled | 700 | 140 | 1.50E-05 | | | 24,000 | | |
| 25611 | AX7-12 | Cold rolled | 650 | 200 | 4.00E-06 | | | 20,000 | | |
| | AX7-12 | Crept | 760 | 200 | 2.60E-03 | 130 | 174 | | 13.10 | 35.20 |
| 25605 | AX7-13 | 1200 | 700 | 200 | 1.50E-04 | 1,350 | 1,978 | | 26.80 | 61.60 |
| 25608 | AX7-14 | 1200 | 700 | 140 | 6.00E-05 | 2,500 | 5,186 | | 29.60 | 55.90 |
| 26457 | AX7-16 | Cold rolled/aged | 700 | 280 | 3.50E-03 | | 620 | | | 37.30 |
| 26730 | AX7-17 | Cold rolled | 760 | 170 | 2.60E-04 | 1,250 | 1,400 | | 20.80 | 57.80 |
| 26733 | AX7-18 | Cold rolled | 800 | 140 | 3.40E-04 | 610 | 678 | | 21.20 | 66.90 |
| 26736 | AX7-19 | Cold rolled | 650 | 300 | | | | 3,000 | | |
| 26739 | AX7-20 | Cold rolled | 700 | 240 | 1.30E-04 | | | 2,800 | | |
| 26737 | AX7-21 | Cold rolled | 650 | 350 | 1.40E-02 | 37 | 875 | | 17.60 | 39.20 |
| 26732 | AX7-22 | Cold rolled | 850 | 100 | 1.60E-03 | 208 | 230 | | 20.00 | 68.50 |
| 25396 | AX8-01 | 1200 | 700 | 170 | 5.00E-04 | 2,700 | 4,633 | | 26.20 | 68.40 |
| 25347 | AX8-07 | Cold rolled | 700 | 170 | 1.50E-05 | 18,000 | 18,745 | | 4.70 | 10.00 |
| 25800 | AX8-08 | Cold rolled | 700 | 200 | 6.00E-06 | | | 19,000 | | |
| 25813 | AX8-09 | Cold rolled | 730 | 170 | 2.00E-05 | 13,600 | 15,081 | | 15.00 | 36.00 |
| 25801 | AX8-11 | Cold rolled | 700 | 240 | 8.00E-05 | 2,800 | 3,198 | | 17.40 | 61.80 |
| 25887 | AX8-13 | Cold rolled | 760 | 140 | 1.00E-04 | 4,800 | 6,418 | | 12.10 | 31.50 |
| 26110 | CET-09 | 1120 | 700 | 140 | | 1,050 | 2,661 | | 31.40 | 73.90 |
| 26046 | CET-10 | 1120 | 700 | 200 | 1.50E-04 | 281 | 405 | | 13.40 | 71.30 |
| 26085 | CET-11 | 1120 | 700 | 170 | 8.00E-04 | 275 | 555 | | 29.00 | 68.70 |
| 26115 | CET-12 | 1120 | 650 | 240 | 1.80E-04 | 750 | 2,331 | | 23.30 | 75.60 |
| 26117 | CET-14 | 1120 | 650 | 275 | 2.80E-03 | 120 | 1,057 | | 20.50 | 73.50 |
| 26116 | CET-15 | 1120 | 650 | 200 | 5.30E-05 | 4,200 | 5,761 | | 29.90 | 63.80 |
| 26027 | BWT-01 | Extruded | 700 | 200 | 2.50E-03 | 170 | 320 | | 33.30 | 84.33 |
| 26031 | BWT-02 | Extruded | 700 | 170 | 6.00E-04 | 475 | 1,316 | | 30.60 | 75.40 |
| 26034 | BWT-03 | Extruded | 650 | 200 | 2.50E-05 | 9,200 | | 14,250 | | |
| 26086 | BWT-12 | Extruded | 650 | 170 | 1.30E-05 | 11,000 | | 13,000 | | |
| 26091 | BWT-13 | Extruded | 730 | 170 | 1.20E-02 | 0.8 | 77.6 | | 41.20 | 81.70 |
| 26092 | BWT-14 | Extruded | 700 | 104 | 3.00E-05 | | | 8,600 | | |
| | BWT-14 | Crept | 700 | 69 | 3.70E-06 | | | 5,000 | | |
| 26096 | BWT-15 | Extruded | 700 | 120 | 7.00E-05 | 5,300 | 9,148 | | 26.60 | 68.40 |
| 26100 | BWT-16 | Extruded | 600 | 400 | | | | | 45.90 | 73.40 |
| 26235 | BWT-17 | Extruded | 730 | 120 | 1.00E-03 | 320 | 834 | | 39.30 | 81.90 |
| 26091 | BWT-18 | Extruded | 600 | 350 | 2.00E-04 | 1,200 | 1,272 | | 37.30 | 74.90 |
| 26656 | BWT-19 | Extruded | 700 | 140 | 1.40E-04 | 2,700 | | 3,700 | | |
| 26788 | BWT-20 | Extruded | 730 | 170 | 1.20E-02 | 40 | 97.7 | | 43.00 | 69.30 |
| 26790 | BWT-21 | Extruded | 760 | 170 | 2.80E-01 | 1.4 | 9.9 | | 43.00 | 86.30 |
| 26791 | BWT-22 | Extruded | 800 | 70 | 1.30E-03 | 260 | 760.4 | | 32.60 | 76.70 |
| 26796 | BWT-23 | Extruded | 730 | 140 | 5.00E-03 | 80 | 278 | | 49.10 | 85.50 |
| 26254 | BWT-24 | Extruded | 760 | 100 | 3.00E-03 | 175 | 277.8 | | 34.60 | 83.40 |
| 26234 | BWT-38E | Extruded | 700 | 100 | 2.00E-05 | | | 5,100 | | |
| | BWT-38E | Crept | 700 | 133 | 5.90E-03 | | | 5,600 | | |
| 26026 | BWT-25 | Forged | 700 | 200 | 3.00E-05 | 11,200 | 12,723 | | 13.80 | 66.90 |
| 26028 | BWT-26 | Forged | 700 | 170 | 1.60E-05 | | | 210 | | |
| | BWT-26 | Crept | 730 | 170 | 1.00E-04 | | 3,685 | | | 66.70 |
| 26053 | BWT-27 | Forged | 650 | 200 | 4.00E-06 | | | 844 | | |
| | BWT-27 | Crept | 760 | 200 | 5.00E-04 | | 537 | | 17.90 | 82.90 |
| 26087 | BWT-31 | Forged | 650 | 170 | 1.00E-05 | | | 10,000 | | |
| | BWT-31 | Crept | 700 | 170 | | | | 500 | | |
| | BWT-31 | Crept | 730 | 170 | | | | 500 | | |
| | BWT-31 | Crept | 760 | 170 | 7.50E-05 | 950 | | | | |
| | BWT-31 | Crept | 730 | 170 | | | | | | |
| | BWT-31 | Crept | 700 | 170 | | | | | | |

# Table C1. Creep rupture data (continued)

| Test | Specimen | Condition | Temperature (°C) | Stress (MPa) | Minimum creep rate (%/h) | Time 1% (h) | Life (h) | In test (h) | Elongation (%) | RA (%) |
|---|---|---|---|---|---|---|---|---|---|---|
| 26093 | BWT-32 | Forged | 730 | 170 | 4.00E-05 | 6,200 | 6,650 | | 16.20 | 62.70 |
| 26285 | BWT-33 | Forged | 730 | 200 | 1.80E-04 | 2,350 | 2,577 | | 17.00 | 65.80 |
| 26797 | BWT-34 | Forged | 760 | 200 | 1.70E-03 | 235 | 257 | | 21.40 | 79.70 |
| 26798 | BWT-35 | Forged | 600 | 400 | | | | 1,630 | | |
| 26475 | CS5-01 | 5% Cold sunk | 700 | 240 | 1.40E-04 | 2,700 | 3,038 | | 16.00 | 71.10 |
| 26601 | CS5-02 | 5% Cold sunk | 700 | 170 | | | | 5,000 | | |
| 26607 | CS5-03 | 5% Cold sunk | 700 | 240 | 2.20E-04 | | | 835 | | |
| | CS5-03 | Crept | 730 | 240 | 4.80E-04 | | | 145 | | |
| | CS5-03 | Crept | 700 | 240 | | | | 611 | 25.60 | 82.00 |
| 26608 | CS5-04 | 5% Cold sunk | 760 | 170 | 6.00E-04 | 740 | 818 | | 20.20 | 81.20 |
| 26602 | CS10-01 | 10% Cold sunk | 700 | 170 | | | | 5,000 | | |
| 26901 | MS1-02b | Cold rolled | 650 | 350 | 2.00E-04 | 2,400 | 2,926 | | | 41.50 |
| 25906 | MS1-04b | 725/6 h aged | 650 | 350 | 2.00E-04 | 1,100 | 3,211 | | 8.20 | 43.60 |
| 25909 | MS1-05b | 725/6 h aged | 650 | 400 | 3.40E-03 | 200 | 480 | | 8.40 | 27.50 |
| 25910 | MS1-07b | Cold rolled | 650 | 400 | 1.20E-03 | 450 | 775 | | 9.50 | 37.20 |
| 26009 | MS1-08b | Cold rolled | 600 | 450 | | 1,070 | 1,078 | | | |
| 26010 | MS1-09b | Cold rolled | 600 | 400 | 1.00E-04 | 100 | 9,496 | | | |
| 25902 | MS4-02b | Cold rolled | 650 | 350 | 1.80E-04 | 2,500 | 3,613 | | 17.30 | 42.10 |
| 25906 | MS4-04b | 725/6 h aged | 650 | 350 | 2.00E-04 | 2,500 | 3,830 | | 19.20 | 37.80 |
| 25903 | MS5-02b | Cold rolled | 650 | 350 | 2.40E-04 | 2,600 | 3,156 | | 9.10 | 53.00 |
| 25907 | MS5-04b | 725/6 h aged | 650 | 350 | | 200 | 3,087 | | 9.50 | 30.40 |
| 26137 | MS6-06 | Cold rolled | 700 | 240 | 1.00E-04 | 2,700 | 3,024 | | 14.60 | 52.10 |
| 26283 | MS6-07 | Cold rolled | 760 | 140 | 6.00E-05 | 2,600 | 4,406 | | | |
| 26256 | MS6-08 | Cold rolled | 600 | 450 | 3.00E-04 | 600 | 651 | | 13.60 | 28.80 |
| 26464 | MS6-09 | Cold rolled | 760 | 200 | 6.00E-04 | 580 | 643 | | 17.00 | |
| 26258 | MS6-15 | Cold rolled | 650 | 350 | 1.00E-03 | 610 | 1,299 | | 12.60 | 46.90 |
| 26462 | MS6-18 | Cold rolled | 700 | 240 | 5.00E-05 | | | 4,000 | | |
| 26904 | MS6-02b | Cold rolled | 650 | 350 | 1.70E-04 | 2,050 | 4,382 | | | |
| 25908 | MS6-04b | 725/6 h aged | 650 | 350 | 1.30E-04 | 2,100 | 4,359 | | 10.60 | 40.60 |
| 26113 | MS6-08b | Cold rolled | 650 | 375 | 2.50E-04 | 1,520 | 1,520 | | 7.60 | 34.00 |
| 26114 | MS6-09b | Cold rolled | 650 | 325 | 1.00E-05 | 3,800 | 4,969 | | 6.60 | 31.00 |
| 26284 | MS6-15b | Cold rolled | 600 | 350 | | | | 5,200 | | |
| 26594 | MS6-20b | Cold rolled | 700 | 300 | 6.00E-04 | 730 | 813 | | 11.80 | 50.60 |

# APPENDIX D

# WELDMENT DATA FOR HT-UPS ALLOYS

## Table D1. Stress rupture data for weldments

| Test | Specimen | Filler metal | Temperature (°C) | Stress MPa | Life (h) | In test (h) | RA (%) | Failure location |
|---|---|---|---|---|---|---|---|---|
| 24916 | CE2W-01 | In 82 GTA | 700 | 170 | 771 | | 35.7 | Weld |
| 24937 | CE1W-01 | CuMo GTA | 700 | 170 | 834 | | 00.6 | Weld |
| 24936 | CE1W-02 | CuMo SMA | 700 | 170 | 1758 | | 40.0 | Base |
| 25564 | AX5W-03 | CuMo SMA | 700 | 170 | 2827 | | 00.4 | Weld |
| 27761 | AX5W-04 | CuMo SMA | 700 | 140 | 5945 | | 01.2 | Weld |
| 25573 | AX6W-03 | CuMo SMA | 700 | 170 | 2919 | | 04.2 | Weld |
| 25678 | AX6W-04 | CuMo SMA | 700 | 240 | 259 | | 09.0 | Weld |
| 25571 | AX7W-03 | CuMo SMA | 700 | 170 | 3645 | | 04.0 | Weld |
| 26847 | AX7W-04 | CuMo SMA | 760 | 200 | 122 | | 04.0 | Weld |
| 25575 | AX8W-03 | CuMo SMA | 700 | 170 | 2819 | | 04.0 | Weld |
| 26848 | AX8W-04 | CuMo SMA | 760 | 120 | 1343 | | 03.6 | Weld |
| 25554 | CuMo-03 | CuMo SMA | 700 | 170 | 1681 | | 25.3 | Base |
| 25623 | AXCR-03 | CRE 16-8-2 | 700 | 170 | 2332 | | 39.6 | Weld |
| 25666 | AXCR-04 | CRE 16-8-2 | 700 | 240 | 211 | | 23.4 | Weld |
| 25780 | AXCR-05 | CRE 16-8-2 | 730 | 170 | 282 | | 49.2 | Weld |
| 25805 | AXCR-06 | CRE 16-8-2 | 730 | 140 | 1885 | | 39.0 | Weld |
| 25794 | AXCR-07 | CRE 16-8-2 | 700 | 140 | 3323 | | 25.8 | Weld |
| 25789 | AXCR-08 | CRE 16-8-2 | 650 | 240 | 620 | | 13.2 | Weld |
| 25810 | AXCR-09 | CRE 16-8-2 | 650 | 200 | 4079 | | 22.0 | Weld |
| | AllCR-01 | CRE 16-8-2 | 650 | 172 | 5930 | | 61.9 | Weld |
| | AllCR-02 | CRE 16-8-2 | 650 | 193 | 1473 | | 68.6 | Weld |
| | AllCR-03 | CRE 16-8-2 | 650 | 207 | 553 | | 64.5 | Weld |
| | AllCr-04 | CRE 16-8-2 | 650 | 224 | 361 | | 62.8 | Weld |
| | AllCr-05 | CRE 16-8-2 | 650 | 234 | 105 | | 61.2 | Weld |
| | AllCR-06 | CRE 16-8-2 | 650 | 241 | 0 | | 54.9 | Weld |
| 25554 | CuMoW-03 | CuMo SMA | 700 | 170 | 1681 | | 25.3 | Base |
| 26922 | CE3W-03 | 556 GTA | 700 | 240 | 46 | | 54.2 | Weld |
| 26918 | CE3W-01 | 556 GTA | 800 | 120 | 759 | | | |
| 26923 | AX5W-06 | 556 GTA | 700 | 280 | 48 | | 44.9 | Weld |
| 26919 | AX5W-05 | 556 GTA | 800 | 140 | 416 | | 13.3 | Fusion |
| 26917 | AX7W-09 | 556 GTA | 700 | 280 | 60 | | 32.8 | Weld |
| 26916 | AX7W-07 | 556 GTA | 800 | 140 | 394 | | 24.4 | Weld |
| 26663 | CS5W-01 | CRE 16-8-2 | 700 | 140 | | 4500 | | |
| 26718 | CS5W-06 | CRE 16-8-2 | 730 | 120 | | 3800 | | |
| 26717 | CS5W-07 | CRE 16-8-2 | 650 | 170 | | 3900 | | |
| 26794 | CS10W-4 | CRE 16-8-2 | 600 | 300 | 441 | | 40.3 | Weld |
| 26903 | BWT4-W1 | CRE 16-8-2 | 700 | 140 | | 1200 | | |
| 26904 | BWT4-W2 | CRE 16-8-2 | 700 | 200 | 344 | | 23.1 | Weld |
| 26889 | BWT4-W3 | CRE 16-8-2 | 700 | 140 | | 1300 | | |

## Table D2. Tensile data for BWT2 weldments

| Test | Specimen | Filler | Condition | Temperature (°C) | Ultimate (ksi) | Fracture (ksi) | Elongation (%) | RA (%) | Failure Location |
|---|---|---|---|---|---|---|---|---|---|
| 26950 | CE2W-01 | alloy 82 | As welded | 25 | 86.11 | 55.90 | 55.00 | 72.52 | Base |
| 26951 | CE2W-03 | alloy 82 | As welded | 700 | 47.37 | 16.60 | 41.50 | 68.44 | Weld |
| 26952 | CE1W-07 | CuMo SS (GTA) | As welded | 25 | 74.37 | 60.60 | 15.00 | 32.83 | Weld |
| 26953 | CE1W-08 | CuMo SS (GTA) | As welded | 25 | 75.08 | 20.40 | 12.20 | 30.66 | Weld |
| 26954 | CE1W-05 | CuMo SS (GTA) | As welded | 700 | 48.00 | 30.77 | 11.20 | 22.56 | Weld |
| 26955 | CE1W-09 | CuMo SS | As welded | 700 | 49.39 | 29.35 | 40.10 | 72.71 | Base |
| 26956 | CE1W-12 | CuMo SS | As welded | 25 | 88.72 | 72.75 | 51.40 | 72.92 | Base |
| 26804 | CE1W-13 | CuMo SS (GTA) | 10,000 h/700°C | 25 | 62.40 | 57.39 | 2.90 | 15.54 | Weld |
| 26885 | CE1W-14 | CuMo SS | 10,000 h/700°C | 25 | 91.67 | 83.00 | 26.00 | 48.70 | Base |
| 26911 | CE3W-05 | alloy 556 | As welded | 25 | 89.84 | 64.68 | 45.90 | 70.84 | Base |
| 26912 | CE3W-06 | alloy 556 | As welded | 700 | 59.08 | 37.18 | 30.30 | 60.06 | Base |
| 26957 | AX5W-01 | CuMo SS | As welded | 25 | 92.48 | 73.30 | 35.70 | 66.12 | Base |
| 26958 | AX5W-02 | CuMo SS | As welded | 700 | 60.19 | 55.00 | 13.50 | 22.55 | Weld |
| 26907 | AX5W-07 | alloy 556 | As welded | 25 | 91.00 | 66.28 | 32.60 | 67.61 | Base |
| 26908 | AX5W-08 | alloy 556 | As welded | 700 | 60.64 | 46.02 | 16.00 | 57.32 | Base |
| 26959 | AX6W-01 | CuMo SS | As welded | 25 | 91.06 | 69.26 | 45.00 | 66.82 | Base |
| 26960 | AX6W-02 | CuMo SS | As welded | 700 | 61.11 | 55.00 | 14.70 | 31.44 | Base |
| 26961 | AX6W/CRE-01 | CRE 16-8-2 | As welded | 25 | 91.31 | 72.40 | 25.40 | 65.02 | Base |
| 26962 | AX6W/CRE-02 | CRE 16-8-2 | As welded | 700 | 52.73 | 31.40 | 20.20 | 54.75 | Weld |
| 26963 | AX7W-01 | CuMo SS | As welded | 25 | 89.58 | 54.00 | 23.20 | 55.55 | Fusion line |
| 26964 | AX7W-02 | CuMo SS | As welded | 700 | 58.67 | 48.90 | 13.20 | 17.55 | Fusion line |
| 26805 | AX7W-06 | CuMo SS | 10,000 h/700°C | 25 | 96.16 | 93.71 | 11.00 | 14.25 | Heat-affected zone |
| 26909 | AX7W-10 | alloy 556 | As welded | 25 | 89.59 | 61.36 | 33.70 | 72.40 | Base |
| 26910 | AX7W-08 | alloy 556 | As welded | 700 | 62.34 | 38.71 | 16.00 | 54.03 | Base |
| 26965 | AX8W-01 | CuMo SS | As welded | 25 | 90.94 | 70.70 | 47.20 | 67.99 | Weld |
| 26966 | AX8W-02 | CuMo SS | As welded | 700 | 60.09 | 56.00 | 14.40 | 26.03 | Weld |
| 26802 | AX8W-05 | CuMo SS | 10,000 h/700°C | 25 | 98.19 | 90.65 | 18.00 | 21.50 | Weld |
| 26275 | BWT2W-1 | CRE 16-8-2 | As welded | 25 | 75.74 | 21.04 | 61.80 | 58.49 | Base |
| 26276 | BWT2W-2 | CRE 16-8-2 | As welded | 700 | 46.71 | 27.35 | 36.40 | 98.49 | Heat-affected zone |
| 26528 | CS5%-w1 | CRE 16-8-2 | As welded | 25 | 82.51 | 49.44 | 37.40 | 77.09 | Heat-affected zone |
| 26529 | CS5%-w1 | CRE 16-8-2 | As welded | 700 | 46.67 | 26.85 | 28.60 | 62.03 | Weld |
| 26530 | CS10%-w1 | CRE 16-8-2 | As welded | 25 | 88.36 | 65.27 | 33.10 | 71.68 | Heat-affected zone |
| 26531 | CS10%-w2 | CRE 16-8-2 | As welded | 700 | 46.82 | 26.18 | 20.00 | 66.09 | Weld |
| 26920 | BWT4-W6 | CRE 16-8-2 | crept/700°C | 25 | 78.75 | 54.10 | 35.00 | 71.46 | Base |
| 26921 | BWT4-W4 | CRE 16-8-2 | crept/700°C | 700 | 39.66 | 19.46 | 39.10 | 60.04 | Base |
| 26967 | CuMoW-01 | CuMo SS | As welded | 25 | 82.40 | 63.10 | 51.00 | 69.52 | Base |
| 26968 | CuMoW-02 | CuMo SS | As welded | 700 | 48.79 | 34.60 | 50.00 | 52.66 | Base |
| 26887 | CuMoW-05 | CuMo SS | 10,000 h/700°C | 25 | 91.71 | 82.80 | 33.50 | 46.44 | Base |

ORNL-6629/P1

## INTERNAL DISTRIBUTION

1-2. Central Research Library
3. Document Reference Section
4-5. Laboratory Records Department
6. Laboratory Records, ORNL RC
7. ORNL Patent Section
8-10. M&C Records Office
11. D. J. Alexander
12. J. Bentley
13-17. E. Bolling
18. R. A. Bradley
19. D. N. Braski
20. C. R. Brinkman
21. P. T. Carlson
22. J. R. DiStefano
23. G. M. Goodwin
24. R. S. Holcomb
25. J. A. Horak
26. R. R. Judkins
27. J. R. Keiser
28. O. F. Kimball
29-33. J. F. King
34-38. P. J. Maziasz
39. H. E. McCoy
40. R. K. Nanstad
41. P. L. Rittenhouse
42. T. K. Roche
43. A. F. Rowcliffe
44. V. K. Sikka
45. G. M. Slaughter
46-50. R. W. Swindeman
51. P. F. Tortorelli
52. J. R. Weir, Jr.
53. D. F. Wilson
54. K. F. Wu
55. A. D. Brailsford (Consultant)
56. H. D. Brody (Consultant)
57. D. P. Pope (Consultant)
58. M. L. Savitz (Consultant)
59. E. R. Thompson (Consultant)
60. J. B. Wachtman (Consultant)

## EXTERNAL DISTRIBUTION

61-62. ARGONNE NATIONAL LABORATORY, 9700 S. Cass Avenue, Argonne, IL 60439

W. A. Ellingson
K. Natesan

63. BABCOCK & WILCOX, Fossil River Power Generation Division, 20 South Van Buren Avenue, Barberton, OH 44203

W. C. Mack

64. BABCOCK & WILCOX RESEARCH LABORATORY, 1562 Beeson Street, Alliance, OH 44601

M. J. Topolski

65. CABOT CORPORATION, Corrosion Resistant Alloys, 1020 West Park Avenue, Kokomo, IN 46901

A. I. Asphahani

66. CARPENTER TECHNOLOGY CORP., Steel Division, P.O. Box 662, Reading, PA 29603

    J. W. Martin

67. CHICAGO BRIDGE AND IRON COMPANY, 800 Jorie Blvd., Oak Brook, IL 60521

    E. Upitis

68. ROBERT L. CLOUD AND ASSOCIATES, 125 University Ave., Berkeley, CA 94710

    W. R. Mikesell

69-70. COMBUSTION ENGINEERING, INC., 911 W. Main Street, Chattanooga, TN 37402

    D. A. Canonico
    B. Roberts

71. COMMISSION OF THE EUROPEAN COMMUNITIES, Petten Establishment, Postbus 2, 1755 ZG Petten, The Netherlands

    Marcel Van de Voorde

72. CORNELL UNIVERSITY, Materials Sciences and Engineering Department, Bard Hall, Ithaca, NY 14853

    Che-Yu Li

73-76. ELECTRIC POWER RESEARCH INSTITUTE, 3412 Hillview Avenue, P.O. Box 10412, Palo Alto, CA 94303

    W. T. Bakker
    R. I. Jaffee
    J. Stringer
    R. Viswanathan

77. EXXON RESEARCH AND ENGINEERING CO., P.O. Box 101, Florham Park, NJ 07932

    M. J. Humphries

78. FOSTER WHEELER DEVELOPMENT CORPORATION, 12 Peach Tree Hill Road, Livingston, NJ 07039

    J. Blaugh

79. GA TECHNOLOGIES, INC., Reactor Structural Materials Branch, Fuels and Materials Division, P.O. Box 81608, San Diego, CA 92138

    D. I. Roberts

80. GENERAL ELECTRIC COMPANY, Turbine Materials Engineering, Building 41, Room 306, 1 River Road, Schenectady, NY 12345

    J. Pepe

82. GILBERT ASSOCIATES, INC., Morgantown Road, Green Hills, Reading, PA 19603

R. L. Dail

83. INCO ALLOYS INTERNATIONAL, INC., P.O. Box 1958, Huntington, WV 25720

T. H. Bassford

84. LUKENS STEEL COMPANY, R&D Center, Coatesville, PA 19320

J. Gulya

85. THE MATERIALS PROPERTIES COUNCIL, INC., United Engineering Center, 345 E. 47th Street, New York, NY 10017

M. Prager

86. NATIONAL MATERIALS ADVISORY BOARD, National Research Council, 2101 Constitution Avenue, Washington, DC 20418

K. M. Zwilsky

87. OFFICE OF NAVAL RESEARCH, Code 431, 800 N. Quincy Street, Arlington, VA 22217

S. G. Fishman

88. STANDARD OIL, INDIANA, P.O. Box 400 - MS B-8, Naperville, IL 60540

S. Ibarra

89. STONE AND WEBSTER ENGINEERING CORPORATION, 245 Summer Street, P.O. Box 2325, Boston, MA 02107

M. P. Berardi

90. SUPERIOR TUBE COMPANY, P.O. Box 191, Norristown, PA 19404

C. C. Mathews

91. TENNESSEE VALLEY AUTHORITY, Metallurgical & NDT Section, 820 Chestnut Street, Tower II, Chattanooga, TN 37401

S. O. Hilton

92. R. D. THOMAS AND COMPANY, INC., 103 Avon Road, Narberth, PA 19072

R. D. Thomas, Jr.

93-94. UNIVERSITY OF CALIFORNIA AT BERKELEY, Department of Materials Science and Mineral Engineering, Berkeley, CA 94720

E. R. Parker
R. O. Ritchie

95. UNIVERSITY OF ILLINOIS, Department of Mechanical and Industrial Engineering, 1206 W. Green Street, Urbana, IL 61801

    D. L. Marriott

96. UNIVERSITY OF MANCHESTER INSTITUTE OF SCIENCE AND TECHNOLOGY, P.O. Box 88, Manchester, M601QD, United Kingdom

    F. H. Stott

97. UNIVERSITY OF PITTSBURGH, Department of Metallurgical and Materials Engineering, 848 Benedum Hall, Pittsburgh, PA 15261

    G. H. Meier

98. UNIVERSITY OF TENNESSEE, Department of Materials Science, Knoxville, TN 37996

    C. D. Lundin

99. DOE, ENERGY CONVERSION AND UTILIZATION TECHNOLOGIES DIVISION, CE-14, 5E-091 Forrestal Building, Washington, DC 20585

    J. J. Eberhardt

100-101. DOE, OAK RIDGE OPERATIONS OFFICE, P.O. Box 2001, Oak Ridge, TN 37831

    Assistant Manager for Research and Development
    E. E. Hoffman

102. DOE, OFFICE OF BASIC ENERGY SCIENCES, Materials Sciences Division, ER-131, J314/GTN, Washington, DC 20585

    F. V. Nolfi, Jr.

103-104. DOE, OFFICE OF FOSSIL ENERGY, Washington, DC 20585

    J. P. Carr (FE-24, C179/GTN)
    R. E. Harrington (FE-20, C164/GTN)

105. DOE, OFFICE OF VEHICLE AND ENGINE R&D, CE-131, 5G-064 Forrestal Building, Washington, DC 20585

    R. B. Schultz

106-110. DOE, MORGANTOWN ENERGY TECHNOLOGY CENTER, P.O. Box 880, Morgantown, WV 26505

    J. W. Byam, Jr.
    D. Dubis
    V. P. Kothari
    J. E. Sholes
    J. S. Wilson

111-114. DOE, PITTSBURGH ENERGY TECHNOLOGY CENTER, P.O. Box 10940, Pittsburgh, PA 15236

| | |
|---|---|
| R. A. Carabetta | J. J. Joubert |
| S. W. Chun | F. W. Steffgen |

115-124. DOE, OFFICE OF SCIENTIFIC AND TECHNICAL INFORMATION, P.O. Box 62, Oak Ridge, TN 37831

For distribution by microfiche as shown in DOE/OSTI-4500, Distribution Categories UC-103 (Fluidized Bed Combustion) and UC-114 (Coal-Based Materials and Components).